

1996

Oxo and peroxo ligand transfer reactions involving methylrhenium trioxide

Mahdi Muhammad Abu-Omar
Iowa State University

Follow this and additional works at: <https://lib.dr.iastate.edu/rtd>

 Part of the [Inorganic Chemistry Commons](#)

Recommended Citation

Abu-Omar, Mahdi Muhammad, "Oxo and peroxo ligand transfer reactions involving methylrhenium trioxide " (1996). *Retrospective Theses and Dissertations*. 11356.
<https://lib.dr.iastate.edu/rtd/11356>

This Dissertation is brought to you for free and open access by the Iowa State University Capstones, Theses and Dissertations at Iowa State University Digital Repository. It has been accepted for inclusion in Retrospective Theses and Dissertations by an authorized administrator of Iowa State University Digital Repository. For more information, please contact digirep@iastate.edu.

INFORMATION TO USERS

This manuscript has been reproduced from the microfilm master. UMI films the text directly from the original or copy submitted. Thus, some thesis and dissertation copies are in typewriter face, while others may be from any type of computer printer.

The quality of this reproduction is dependent upon the quality of the copy submitted. Broken or indistinct print, colored or poor quality illustrations and photographs, print bleedthrough, substandard margins, and improper alignment can adversely affect reproduction.

In the unlikely event that the author did not send UMI a complete manuscript and there are missing pages, these will be noted. Also, if unauthorized copyright material had to be removed, a note will indicate the deletion.

Oversize materials (e.g., maps, drawings, charts) are reproduced by sectioning the original, beginning at the upper left-hand corner and continuing from left to right in equal sections with small overlaps. Each original is also photographed in one exposure and is included in reduced form at the back of the book.

Photographs included in the original manuscript have been reproduced xerographically in this copy. Higher quality 6" x 9" black and white photographic prints are available for any photographs or illustrations appearing in this copy for an additional charge. Contact UMI directly to order.

UMI

A Bell & Howell Information Company
300 North Zeeb Road, Ann Arbor, MI 48106-1346 USA
313/761-4700 800/521-0600



Oxo and peroxy ligand transfer reactions involving methylrhenium trioxide

by

Mahdi Muhammad Abu-Omar

**A dissertation submitted to the graduate faculty
in partial fulfillment of the requirements for the degree of
DOCTOR OF PHILOSOPHY**

Department : Chemistry

Major: Inorganic Chemistry

Major Professor: James H. Espenson

Iowa State University

Ames, Iowa

1996

UMI Number: 9635305

**UMI Microform 9635305
Copyright 1996, by UMI Company. All rights reserved.**

**This microform edition is protected against unauthorized
copying under Title 17, United States Code.**

UMI
300 North Zeeb Road
Ann Arbor, MI 48103

**Graduate College
Iowa State University**

**This is to certify that the doctoral dissertation of
Mahdi Muhammad Abu-Omar
has met the dissertation requirements of Iowa State University**

Signature was redacted for privacy.

Major Professor

Signature was redacted for privacy.

For the Major Department

Signature was redacted for privacy.

For the Graduate College

TABLE OF CONTENTS

	<u>Page</u>
GENERAL INTRODUCTION	1
Introduction	1
The Rhenium Catalyst	1
Oxo transfer reactions of MTO	3
Catalytic peroxy transfer reactions	5
Dissertation Organization	10
References	10
CHAPTER I. OXYGEN TRANSFER REACTIONS OF METHYLRHENIUM OXIDES	13
Abstract	13
Introduction	14
Experimental Section	16
Materials	16
Kinetic studies	16
Product analysis	18
Results	18
Reaction of MTO and H ₃ PO ₂	18
Oligomerization	20
The reduction of anions by MDO	23
Kinetic plateaus	27
Reactions with oxo metal complexes	31
Organic oxo substrates	32

Discussion	33
The H ₃ PO ₂ reaction	33
Mechanism of O-Atom Transfer to MDO	35
Reaction thermodynamics	37
Acknowledgments	41
References	43
CHAPTER II. OXIDATIONS OF CYCLIC β-DIKETONES CATALYZED BY METHYLRHENIUM TRIOXIDE	47
Abstract	47
Introduction	48
Experimental Section	50
Materials	50
Kinetic studies	50
Synthetic procedure	51
Results	53
General observations	53
Kinetics	54
Detection of an intermediate	60
Monochlorodione	62
Aliphatic β-diketones	64
Discussion	65
Acknowledgments	68
References	68

CHAPTER III. DEACTIVATION OF METHYLRHENTIUM TRIOXIDE-PEROXIDE CATALYST BY DIVERSE AND COMPETING PATHWAYS	71
Abstract	71
Introduction	72
Experimental Section	74
Materials	74
Instrumentation	74
Results	75
Identification of A by NMR	75
Is water coordinated to A and B?	77
Catalyst deactivation-general observations	79
Catalyst decomposition-kinetics	80
Catalyst decomposition-pH profile	87
Labeling studies	89
The decomposition of MTO itself	91
Equilibrium constants for peroxide coordination	92
Discussion	94
Neglected reactions	98
Oxygen evolution from B	101
Methanol formation	102
Methane formation	105
Formation of A and B	105
Summary	106
Acknowledgment	107
References	108

CHAPTER IV. OXIDATIONS OF ER₃ (E = P, As, or Sb) BY HYDROGEN PEROXIDE: METHYLRHENTIUM TRIOXIDE AS CATALYST	110
Abstract	110
Introduction	111
Experimental Section	112
Materials	112
Product Analysis	113
Kinetic Studies	113
Equilibrium Studies	115
Results	117
Equilibrium Constants	117
Oxygen transfer from CH₃ReO₃	119
The uncatalyzed oxidations	119
Catalysis with CH₃ReO₃: An Overview	119
Kinetics at high [PPh₃]	123
Kinetics at variable [ER₃]: Initial-rate method	123
Catalysis with CH₃ReO₃: Determination of <i>k</i>₃ for all substrates	127
Catalysis with CH₃ReO₃: The role of B	128
The case of PTA: competition kinetics	131
The integrity of the catalyst	135
Discussion	136
Conclusion	143
Acknowledgment	144
References	145

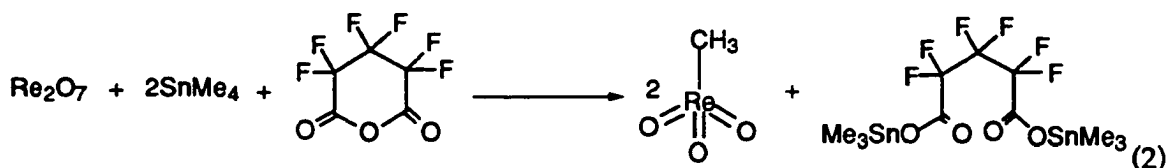
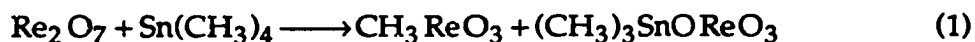
GENERAL CONCLUSIONS	148
----------------------------	------------

ACKNOWLEDGMENTS	151
------------------------	------------

GENERAL INTRODUCTION

Introduction

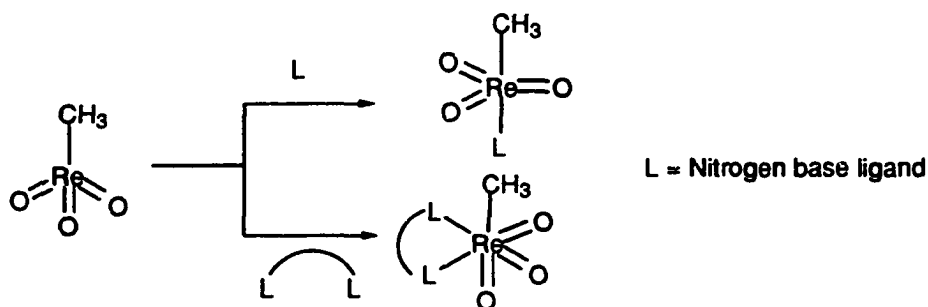
The Rhenium Catalyst. The chemistry and reactivities of transition metal oxo complexes have attracted extensive attention in the past decade due to their application in catalysis.¹ Methylrhenium trioxide, or MTO for short, was initially prepared by Beattie and Jones in 1979,² from residues of $(\text{CH}_3)_3\text{ReO}_2$ left open to the atmosphere. The synthesis was later improved by employing dirhenium heptoxide and tetramethyl tin as the starting reagent, eq 1.³ The procedure was yet further refined by the incorporation of perfluoroglutaric anhydride, eq 2.⁴



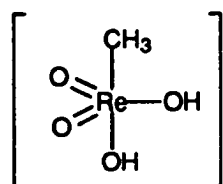
The spectroscopic features of MTO are summarized in Table 1. With only 14 valence electrons, at least in the formal sense, it comes as no surprise that MTO acts as a Lewis acid towards monodentate and bidentate nitrogen bases, such as aniline, ammonia, pyridine, and bipyridine.⁵ With monodentate ligands, MTO forms a trigonal bipyramidal adduct with the nitrogen base *trans* to the methyl. Bidentate ligands coordinate to MTO to give an octahedral complex with the bidentate ligand *trans* to two oxo ligands leaving the third oxo ligand *trans* to the methyl group. These coordination features of MTO are summarized in Scheme 1.

Table 1. Spectroscopic features of MTO.

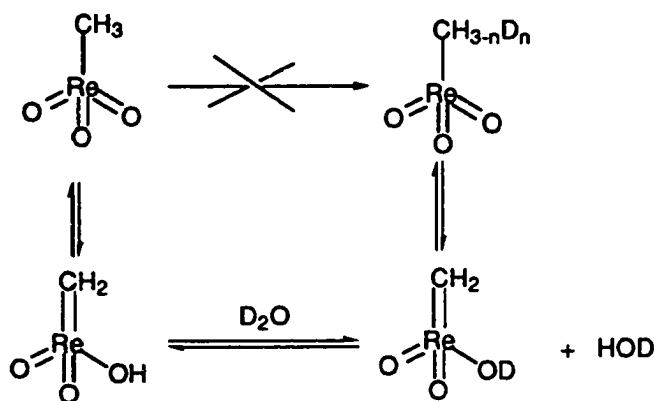
Spectroscopy	Signals
IR in CH ₂ Cl ₂	1000(w), 967 cm ⁻¹ (vs)
¹ H NMR in CDCl ₃	2.63 ppm (s, CH ₃)
¹³ C NMR in CDCl ₃	19.03 ppm (q, ² J(C,H) = 138 Hz)
UV-vis in H ₂ O	239 nm (ε 1900 L mol ⁻¹ cm ⁻¹) 270 nm (sh, ε 1300 L mol ⁻¹ cm ⁻¹)

**Scheme 1. Coordination Chemistry of MTO.**

One of the most intriguing features of MTO is its ability to exchange its oxo ligands with those of water. ¹⁷O NMR experiments have shown that the oxo ligands of MTO are exchanged easily with ¹⁷O-labeled water.⁶ The exchange was also verified by dissolving MTO in ¹⁸O-labeled water and then measuring the mass spectrum of MTO.^{7,8} It is worth noting here that although this exchange must occur through water coordination to the metal center, no water coordination has been observed by NMR, indicating great lability of the coordinated water molecules. A reasonable intermediate by which this ligand exchange may be accomplished is shown below. Supporting such a proposed intermediate is the fact that MTO displays different chemical shifts in different solvents in the ¹H and ¹⁷O NMR. For example, δ(¹⁷O) in CHCl₃ is 829, but 861 in CH₃OH.



Since MTO features a short Re-C bond distance of 2.060(9) Å,⁹ the possibility of a carbene-type [or enol, CH₂ReO₂(OH)] structure was considered. However, the lack of hydrogen exchange for deuterium in D₂O, Scheme 2,⁸ deems such an intermediate structure as nonexistent.

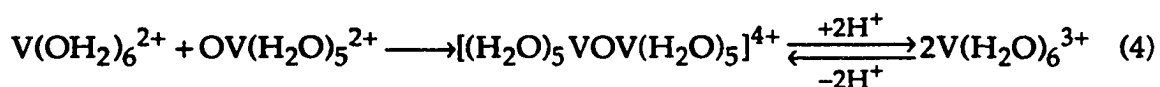
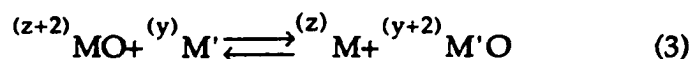
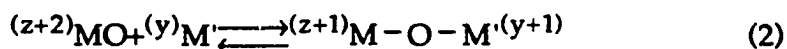


Scheme 2

MTO has been studied extensively for its catalytic ability with H₂O₂.¹⁰⁻¹³ The peroxide chemistry of MTO will be described later in the introduction. Attractive features of MTO include its ease of synthesis and purification, its stability in air, its solubility in water and all organic solvents, its effectiveness as either a homogeneous or a heterogeneous catalyst.

Oxo transfer reactions of MTO. Metal-centered oxygen atom transfer reactions are interesting because of their relevance to hydroxylase enzymes in biological systems and their potential in catalytic oxidation processes.¹⁴⁻¹⁷ Nitrate, for instance, serves in biological systems as an oxidant via the molybdenum-containing enzyme nitrate reductase.¹⁶ The three most common oxygen transfer

reactions involving transition metal complexes are summarized in eqs 3-5, where X/XO is a generalized oxygen atom acceptor/donor. Eq 5 is a special case of the generalized oxygen transfer reaction in eq 3 where the oxygen donor/acceptor is another metal complex. The incomplete oxygen transfer process is presented in eq 4 where a μ -oxo binuclear complex is formed. A typical example of this incomplete oxygen transfer process is the reaction of V^{2+} and VO^{2+} to give the intensely colored $[VOV]^{4+}$ complex, eq 6.¹⁸

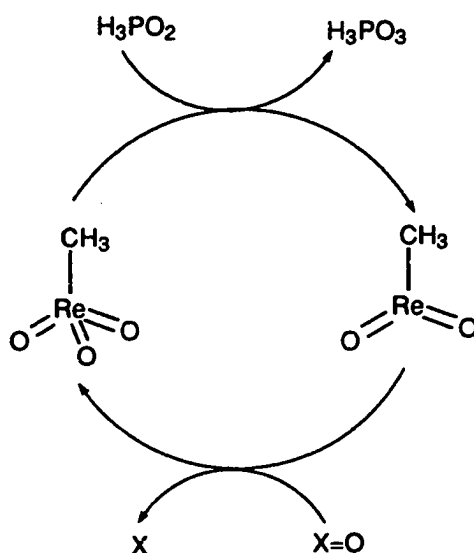


Inorganic oxoanions such as perchlorate are strong oxidants thermodynamically; however, kinetically they are sufficiently unreactive that they are used as "inert" electrolytes and counterions in syntheses of coordination metal complexes. The utilization of inorganic anions in organic oxidations has attracted much attention recently. A Mn(III) porphyrin complex has been used in photocatalytic oxidations of hydrocarbons by ClO_4^- and IO_4^- as oxidants.¹⁹ The oxidation of bromide by ClO_3^- catalyzed by a Mo(V) oxide has recently been realized.²⁰

The oxygen transfer reactions involving MTO are described in Chapter I and summarized in Scheme 3 below. The reactive reductant, methylrhenium dioxide (or MDO for short), is prepared in aqueous solution from the reaction of MTO and

hypophosphorous acid;²¹ the oxidation product from hypophosphorous acid is phosphorous acid. In organic solvents MDO may be prepared by the reaction of MTO and triphenylphosphine.^{22,23} Sn(II) in aqueous medium is also capable of reducing MTO to give the Re(V) complex. XO in Scheme 3 represents a wide range of substrates that include inorganic oxoanions, sulfoxides, pyridine N-oxides, triphenylarsine oxide, triphenylstibine oxide, and even a few metal oxides. The rate constants for these oxygen transfer reactions are reported in Chapter I. The kinetic parameters as well as the mechanistic aspects of these oxygen atom transfer reactions are the principal issues.

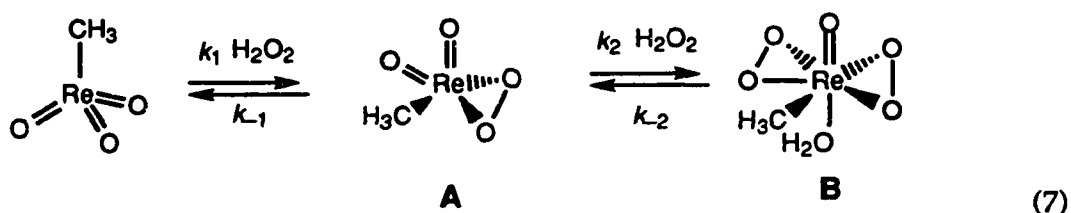
The transformations presented in Scheme 3 formulate a complete catalytic cycle in which MTO is an oxygen atom transfer catalyst facilitating oxygen atom transfer from XO reagents to hypophosphorous acid. In most instances these oxygen transfer reactions although favored thermodynamically do not occur at all under ambient conditions.



Scheme 3. Oxygen transfer reactions involving MTO.

Catalytic peroxo transfer reactions. The potential of MTO in catalysis was initially realized by Herrmann and coworkers.^{10,24} Methylrhenium trioxide reacts

with hydrogen peroxide to form mono and diperoxo rhenium complexes, **A** and **B**, respectively, eq 7.^{10,13} **A** and **B** are formed in equilibrium reactions ($K_1 = 16 \text{ L mol}^{-1}$ and $K_2 = 132 \text{ L mol}^{-1}$ at $25 \text{ }^\circ\text{C}$ and $\mu = 2.0 \text{ M}$ in aqueous solution).⁸ These peroxo complexes are the active forms of the catalyst in oxidation reactions with H_2O_2 . In the absence of an oxidizable substrate, the catalyst undergoes decomposition over a period of few hours depending on the $[\text{H}_2\text{O}_2]$ and the pH.⁸ The final products from deactivation are methanol and perrhenate. The full spectroscopic characterizations of **A** and **B** as well as the different and diverse competing pathways that lead to catalyst's deactivation are described in Chapter III.



The deactivation reactions in the MTO- H_2O_2 system are of interest in their own right, independent from their implications for catalyst stability. These reactions speak to the different modes by which peroxo-metal complexes can react, a subject that has commanded considerable independent interest.^{25,26} Since the decomposition of the MTO- H_2O_2 catalyst involves methanol formation and hence cleavage of the Me-Re bond, the reaction that lead to methanol formation are therefore greatly relevant to alkyl activation by metal oxides, an area of research that had attracted a great deal of interest in an effort to understand and improve organic oxidations with metal oxo complexes (*vide infra*).⁶

In addition to MTO, many high-valent metal oxides such as molybdates, tungstates, chromates, vanadates, among others, form peroxo complexes as well. Their abilities in catalysis have been reviewed recently.²⁷ The MTO catalyst does, however, offer the advantage of being suitable for both aqueous and organic

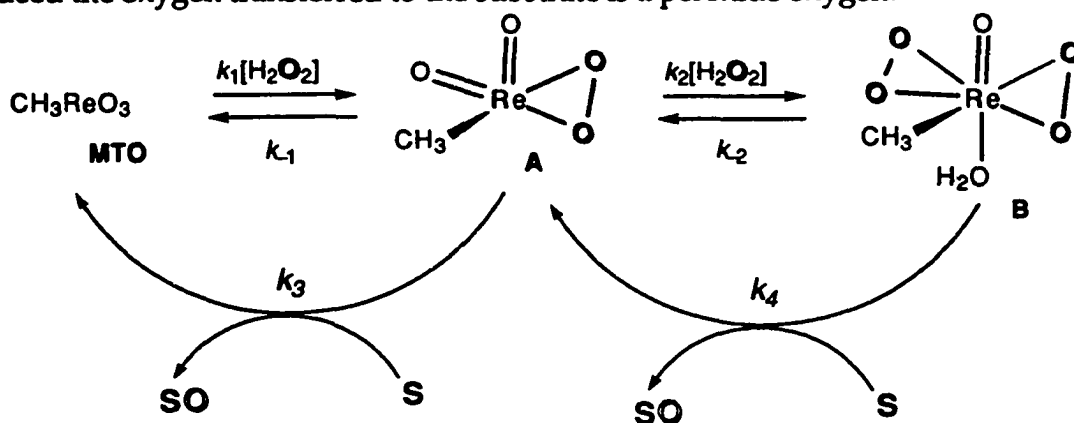
environments, and it does not feature pH dependent equilibria and oligomers formation that tend to complicate quantitative kinetic and mechanistic studies.

Other organometallic Re(VII) oxides that are analogous to MTO are known with a wide range of different R-groups in place of the methyl.⁶ These include ethyl, isopropyl, t-butyl, n-butyl, cyclopropyl, and pentamethyl cyclopentadienyl (Cp*) rhenium trioxide. With the exception of the cyclopropyl rhenium trioxide, these compounds are not very stable due to the presence of an easily accessible β -hydrogen, and they don't exhibit any catalytic activity that is comparable to that of MTO.²⁴ Even the cyclopropylrhenium trioxide, which is reactive catalytically with hydrogen peroxide, exhibits somewhat lower levels of reactivities in comparison to MTO. Cp*ReO₃ does not bind hydrogen peroxide; this could be understood in light of coordinative saturation of this complex, since Cp* is equivalent to three ligands.

It is worth noting here that ReO₄⁻ does not bind hydrogen peroxide, nor does it feature the catalytic chemistry observed for MTO. Therefore, this new catalytic chemistry of a Re(VII) oxide was the result of a subtle change in one ligand, namely, oxo to methyl; perhaps the major effect is the change from a negatively charged species, ReO₄⁻, to a neutral one, CH₃ReO₃, not to mention of course that changing an oxo ligand to a methyl group diversifies the catalytic chemistry of MTO by extending it to organic media as well as water.

MTO catalyzes oxygen atom transfer from hydrogen peroxide (but not from alkyl hydroperoxides or oxygen) to many nucleophilic acceptors. These include phosphines,¹² triphenylarsine,¹² triphenylstibine,¹² sulfides,⁷ amines,²⁸ halide ions,²⁹ and alkenes.^{10,11,24,30} The kinetic data in each of these instances point to a mechanism in which the peroxide ligands of A and B act as electrophiles. Therefore, catalysis with MTO proceeds *via* electrophilic activation of hydrogen peroxide through binding to the oxophilic rhenium center. Since MTO is a strong Lewis acid, electron

density is depleted from the peroxide upon binding to rhenium. The catalytic transformations with MTO- H_2O_2 are illustrated in Scheme 4, where S represents a generic nucleophilic substrate. It has been established by ^{18}O labeling, as shown in Scheme 4, that the peroxo ligands of compounds A and B come from H_2O_2 and indeed the oxygen transferred to the substrate is a peroxide oxygen.^{7,31}

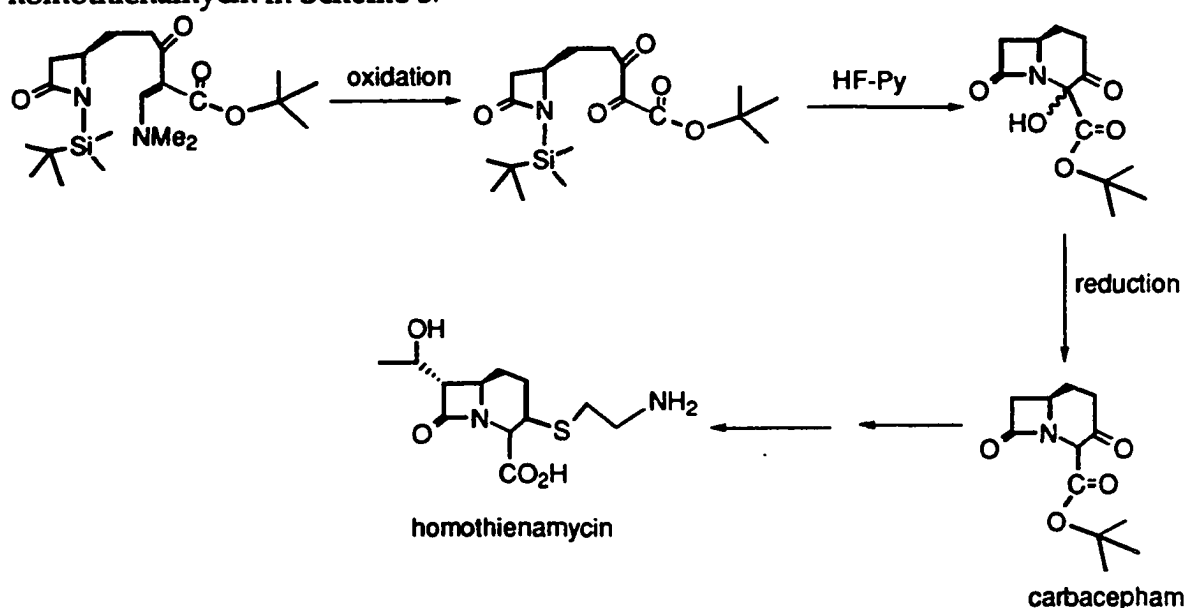


Scheme 4. A general catalytic cycle for MTO- H_2O_2 system.

In chapter IV the catalytic oxidations of a large family of phosphine, triphenylarsine, and triphenylstibine are described. Systematic changes in the substituents on the phosphorous were made to vary the nucleophilicity of the phosphine and its cone angles. The kinetic effects due to these changes were determined in order to understand and obtain support for the mechanism of oxygen transfer from A and B.

Although the peroxo ligands of A and B behave in most instances as electrophiles (*vide infra*), peroxide systems, however, do have open to them just the opposite possibility:^{32,33} that peroxide will react as a nucleophile toward substrates that are sufficiently electron poor. Instances in which the alternative is operative are poorly documented for A and B. MTO has been reported as an effective catalyst for the Baeyer-Villiger oxidations of cyclic ketones to give the corresponding lactones.³⁴ The catalytic reactions of MTO- H_2O_2 , therefore, have been extended to β -diketones.

The catalytic oxidations of β -diketones by hydrogen peroxide is described in Chapter II. The β -diketones studied in Chapter II are present mainly in the enolic form which is electron deficient owing to the conjugation of the double bond with the electron-withdrawing carbonyl group. Another interest in oxidations of β -diketones stems from their use in the synthesis of natural products,³⁵ such as naturally occurring antibiotics.³⁶ An example is illustrated for the synthesis of homothienamycin in Scheme 5.³⁶



Scheme 5

Catalytic oxidations of β -diketones with MTO- H_2O_2 result in cleavage products, carboxylic acids, *via* an intermediate that could be detected by NMR in some instances. The intermediate resulting from the initial oxidation of the enol is then cleaved through oxygen insertion into C-C bond. This latter oxidation step is analogous to Baeyer-Villiger oxidations where A and B may act as nucleophiles rather than their customary electrophilic behavior. These catalytic oxidations show that MTO can change mechanisms according to substrate demand.

Dissertation Organization

The dissertation consists of four chapters. Chapter I corresponds to a manuscript to be submitted to *Inorganic Chemistry*. Chapter II is in press in *Organometallics*. Chapters III and IV have been published in the *Journal of the American Chemical Society*. Each chapter is self-contained with its own equations, figures, tables, and references. Following the last manuscript is general conclusions. With the exception of the O₂ measurements (Chapter III) which were collected by Professor Peter J. Hansen and the preparation of perbromic acid (Chapter I) which was done by Dr. Evan H. Appleman, all the work in this dissertation was performed by the author of this thesis, Mahdi M. Abu-Omar.

References

- (1) Casey, C. P. *Science* **1993**, *259*, 1552.
- (2) Beattie, I. R.; Jones, P. J. *Inorg. Chem.* **1979**, *18*, 2318.
- (3) Herrmann, W. A.; Ramao, C. C.; Kiprof, P.; Behm, J.; Cook, M. R.; Taillefer, J. *J. Organomet. Chem.* **1991**, *413*, 11.
- (4) Herrmann, W. A.; Kuhn, F. E.; Fischer, R. W.; Thiel, W. R.; Ramao, C. C. *Inorg. Chem.* **1992**, *31*, 4431.
- (5) Herrmann, W. A.; Kuchler, J. G.; Weichselbaumer, G.; Herdtweck, E.; Kiprof, P. *J. Organomet. Chem.* **1989**, *372*, 351.
- (6) Herrmann, W. A. *Angew. Chem. Int. Ed. Engl.* **1988**, *27*, 1297.
- (7) Vassell, K. A.; Espenson, J. H. *Inorg. Chem.* **1994**, *33*, 5491.
- (8) Abu-Omar, M. M.; Hansen, P. J.; Espenson, J. H. *J. Am. Chem. Soc.* **1996**, *118*, in press.
- (9) Herrmann, W. A.; Kiprof, P.; Rydpal, K.; Tremmel, J.; Blom, R.; Alberto, R.; Behm, J.; Albach, R. W.; Bock, H.; Solouki, B.; Mink, J.; Lichtenberger, D.; Gruhn, N. *J. Am. Chem. Soc.* **1991**, *113*, 6527.

- (10) Herrmann, W. A.; Fischer, R. W.; Marz, D. W. *Angew. Chem. Int. Ed. Engl.* **1991**, *30*, 1638.
- (11) Herrmann, W. A.; Fischer, R. W.; Schere, W.; Rauch, M. U. *Angew. Chem. Int. Ed. Engl.* **1993**, *32*, 1157.
- (12) Abu-Omar, M. M.; Espenson, J. H. *J. Am. Chem. Soc.* **1995**, *117*, 272.
- (13) Yamazaki, S.; Espenson, J. H.; Huston, P. *Inorg. Chem.* **1993**, *32*, 4683.
- (14) Chinn, L. J. *Selection of Oxidants in Synthesis*; Marcel Dekker: New York, 1971.
- (15) Smith, G. F. *The Wet Chemical Oxidation of Organic Compositions Employing Perchloric Acid*; G. F. Smith Chemical Co.: Columbus, Ohio, 1965.
- (16) M. P. Conghlan, Ed.; *Molybdenum and Molybdenum-containing Enzymes*; Pergamon: New York, 1980.
- (17) Spence, J. T. In ; H. Sigel, Ed.; Marcel Dekker: New York, 1976.
- (18) Newton, T. W.; Baker, F. B. *Inorg. Chem.* **1964**, *3*, 569.
- (19) Suslick, K. S.; Acholla, F. V.; Cook, B. R. *J. Am. Chem. Soc.* **1987**, *109*, 2818.
- (20) Villata, L. S.; Martire, D. O.; Capparelli, A. L. *J. Mol. Catal.* **1995**, *99*, 143.
- (21) Abu-Omar, M. M.; Espenson, J. H. **1995**,
- (22) Zhu, Z.; Espenson, J. H. *J. Mol. Catal.* **1995**, *103*, 87.
- (23) Herrmann, W. A.; Roesky, P. W.; Wang, M.; Scherer, W. *Organomet.* **1994**, *13*, 4531.
- (24) Herrmann, W. A.; Fischer, R. W.; Rauch, M. U.; Scherer, W. *J. Mol. Catal.* **1994**, *86*, 243.
- (25) Brown, S. N.; Mayer, J. M. *Inorg. Chem.* **1992**, *31*, 4091.
- (26) Ledon, H.; Bonnet, M.; Lallemand, J.-Y. *J. Chem. Soc., Chem. Comm.* **1979**, 702.
- (27) Strukul, G. *Catalytic Oxidations with Hydrogen Peroxide as Oxidant*; Kluwer Academic Publishers: Dordrecht, 1992.
- (28) Zhu, Z.; Espenson, J. H. *J. Org. Chem.* **1995**, *60*, 1326.

- (29) Espenson, J. H.; Pestovsky, O.; Huston, P.; Staudt, S. *J. Am. Chem. Soc.* **1994**, *116*, 2869.
- (30) Al-Ajlouni, A. M.; Espenson, J. H. *J. Am. Chem. Soc.* **1995**, *117*, 9243.
- (31) Pestovsky, O.; Eldik, R. v.; Huston, P.; Espenson, J. H. *J. Chem. Soc. Dalton Trans.* **1995**, 133.
- (32) Gusso, A.; Baccin, C.; Strukul, G. *Organomet.* **1994**, *13*, 3442.
- (33) Payne, G. B. *J. Org. Chem.* **1961**, *26*, 4793.
- (34) Herrmann, W. A.; Fischer, R. W.; Correia, J. D. G. *J. Mol. Catal.* **1994**, *94*, 213.
- (35) Salzmann, T. N.; Ratcliffe, R. W.; Christensen, B. G. *Tet. Lett.* **1980**, *21*, 1193.
- (36) Wasserman, H. H.; Han, W. T. *Tet. Lett.* **1984**, *25*, 3743.

CHAPTER I

OXYGEN TRANSFER REACTIONS OF METHYLRHENIUM OXIDES

A paper submitted to *Inorganic Chemistry*

Mahdi M. Abu-Omar, Evan H. Appelman, and James H. Espenson

Abstract

Methylrhenium dioxide, CH_3ReO_2 (or MDO), is produced from methylrhenium trioxide, CH_3ReO_3 (or MTO) and hypophosphorous acid in acidic aqueous medium. Its mechanism is discussed in light of MTO's coordination ability and the inverse k_{ie} : $\text{H}_2\text{P}(\text{O})\text{OH}$, $k = 0.028 \text{ L mol}^{-1} \text{ s}^{-1}$; $\text{D}_2\text{P}(\text{O})\text{OH}$, $k = 0.039 \text{ L mol}^{-1} \text{ s}^{-1}$. The Re(V) complex, MDO, reduces perchlorate and other inorganic oxoanions (XO_n^- , where $\text{X} = \text{Cl}, \text{Br}, \text{or I}$ and $n = 4$ or 3). The rate is controlled by the first oxygen abstraction from perchlorate to give chlorate, with a second-order rate constant at pH 0 and 25 °C of $7.3 \text{ L mol}^{-1} \text{ s}^{-1}$. Organic oxygen-donors such as sulfoxides and pyridine N-oxides oxidize MDO to MTO as do metal oxo complexes: $\text{VO}_{\text{aq}}^{2+}$, $\text{VO}_{2\text{aq}}^+$, $\text{HOMoO}_{2\text{aq}}^+$, and MnO_4^- . The reaction between $\text{V}_{\text{aq}}^{2+}$ with MTO and the reduction of VO^{2+} with MDO made it possible to determine the free energy for MDO/MTO. Oxygen-atom transfer from oxygen donors to MDO involves nucleophilic attack of $\text{X}=\text{O}$ on the electrophilic Re(V) center of MDO; the reaction proceeds via $[\text{MDO}\cdot\text{XO}]$ adduct, which is supported by the saturation kinetics observed for some of the anions. The kinetic parameters that control and facilitate such oxygen transfer processes are suggested.

Introduction

Our subject is the kinetics and thermodynamics of transfer of an oxygen atom from a donor to an acceptor and the correlation of kinetic data for a family of such reactions in terms of their mechanism. The mobility of oxygen atoms among rhenium compounds in particular has been reviewed, and thermodynamic data for many such reactions have been described.¹ These issues arose in our research into certain catalytic reactions of methylrhenium trioxide (CH_3ReO_3 , abbreviated as MTO), where it became apparent that a reduced species $\text{CH}_3\text{ReO}_2 \cdot \text{L}_n$ (L = solvent, ligand) could be generated.^{2,3} In aprotic solvents (toluene, benzene, chloroform) triphenyl phosphine proved to be a suitable acceptor. In water hypophosphorous acid serves quite well. The unknown degree of hydration of CH_3ReO_2 aside for now, the equation for its formation is:



Methylrhenium dioxide (MDO) is a strong 2e reducing agent able to abstract an oxygen atom from many substrates. Suitable partners are oxoanions (XO_n^- , including even the notoriously nonreactive ClO_4^- , as presented in a previous communication,⁴ organic oxides (amine oxides, sulfoxides, epoxides, etc.) and certain oxo-metal species such as VO^{2+} . Our goal has been to provide data for these reactions and their kinetics and thermodynamics. We have also defined structural and electronic factors that control the reactivity. To no surprise, the reaction rates could not be successfully correlated in a Marcus sense with the overall driving force, presumably because the overall driving force so poorly represents the species that emerge from the transition state. Also, the intrinsic O-transfer rates (self-exchange) are in general not known. On the other hand, we have been able to some extent to relate the kinetic data to the element-oxygen force constants.

MDO is without doubt oxidized, but the term electron transfer will be avoided. It is used in the literature both to designate redox processes in general and to specify a particular mechanism. There is also no call at this stage to identify a perhaps problematic (but perhaps valid) relation between our subject and certain other oxidation-reduction reactions that proceed by an inner-sphere mechanism said to involve atom-transfer. The large majority lead to a single unit of oxidation state change, which is not the case here. In a quite different chemical context this distinction has been addressed very thoughtfully in the literature.⁵

Since oxygen-transfer processes are important industrially and biologically, many catalytically-active transition metal complexes have been studied, including molybdenum(V) and (IV),^{6,7} ruthenium(V) and (IV),^{8,9} rhenium(V),^{10,11} and ruthenium(II).^{12,13} The literature also includes examples of the transfer of oxo ligands in oxometalloporphyrins systems: Mo^{VI}(TPP)(O)₂,¹⁴ Fe^{IV}(TPP)(O),¹⁵ and Ru^{VI}(TMP)(O)₂¹⁶ [TPP = 5,10,15,20-tetraphenylporphyrinato; and TMP = 5,10,15,20-tetramesitylporphyrinato]. In recent developments, the photocatalytic oxidation of hydrocarbons by a Mn(III) porphyrin complex utilizes ClO₄⁻ and IO₄⁻ as oxidants,¹⁷ and bromide ions are oxidized by ClO₃⁻, when catalyzed by a Mo(V) oxo complex.¹⁸

Oxides of early transition metals have attracted attention.¹⁹⁻²⁵ MTO in particular has a notable ability to catalyze reactions of hydrogen peroxide,²⁶⁻³³ which it activates by coordination to the high-valent rhenium.^{31,34,35} More recently the ability of MTO to catalytically transfer "nitrene" and "carbene" moieties has been realized.³⁶ Reactions involving oxygen atom transfer between rhenium (MDO and MTO) and a substrate (XO and X) can be explored in considerable detail, since the species involved are stable in aqueous, semi-aqueous, and organic media.

Experimental Section

Materials. High-purity water was obtained by passing laboratory distilled water through a Millipore-Q water purification system. Perbromic acid was prepared from the fluorine oxidation of bromate.³⁷ Solutions of VO^{2+} in triflate medium were obtained by adsorbing vanadyl ion from a solution of the vanadyl sulfate (Alfa) onto a column of Dowex 50W-X8 cation exchange resin, rinsing it free of sulfate ions and eluting with 1.0 M HOTf. Solutions of V^{2+} were prepared by reduction of VO^{2+} with amalgamated zinc. $\text{HOMo}(\text{O})_2^+(\text{aq})$ was prepared from dissolving Na_2MoO_4 (J. T. Baker) in HOTf medium. Triphenylstibine oxide was prepared from the oxidation of triphenylstibine by H_2O_2 catalyzed by MTO.²⁹ $\text{VO}_2^+(\text{aq})$ was prepared by dissolving V_2O_5 (J. T. Baker) in aq. HOTf. Most other chemicals were reagent grade and obtained commercially: MTO (Aldrich), hypophosphorous acid (J. T. Baker, 50% solutions in water), sodium hypophosphite (J. T. Baker), deuterated hypophosphorous acid (Aldrich, 50% solutions in D_2O), phosphorous acid (Aldrich), nitric acid (Fischer), sodium nitrite (Fischer), sodium chlorate (Fischer), perchloric acid (Fischer), sodium bromate (Fischer), sodium iodate (Fischer), potassium permanganate (Fischer), dimethyl sulfoxide (Fischer), phenylmethyl sulfoxide (Aldrich), *p*-tolylmethyl sulfoxide (Aldrich), phenylvinyl sulfoxide (Aldrich), all pyridine N-oxides (Aldrich), and triphenylarsine oxide (Aldrich). Solutions of trifluoromethane sulfonic acid (triflic acid, HOTf) were obtained by carefully diluting the pure commercial material (Aldrich).

Kinetic studies were performed in aqueous solutions for the most part; the aryl,alkyl sulfoxides and $\text{Ph}_3\text{E}=\text{O}$ (E = As, Sb) were studied in acetonitrile-water (1:1 or 3:1 v/v, as needed). All of these solutions contained 1.0 M HOTf to maintain a constant electrolyte medium and to stabilize MTO and MDO against polymerization in aqueous medium.^{22,23} Kinetic data were collected at 25.0 ± 0.2 °C with Shimadzu

UV-2101PC and UV-3101PC spectrophotometers and with an Applied Photophysics Sequential DS-17MV stopped-flow spectrometer. The buildup of MTO was followed at 270 nm (ϵ 1300 L mol⁻¹ cm⁻¹).

The oxygen-donating agent was usually taken in large excess over MDO and the reactions followed pseudo-first-order kinetics according to eq 2. When comparable concentrations of the two were taken, the data were fit to eq 3 for mixed-second-order kinetics.

$$\text{Abs}_t = \text{Abs}_\infty + \{\text{Abs}_0 - \text{Abs}_\infty\} \times e^{-k_\psi t} \quad (2)$$

$$\text{Abs}_t = \text{Abs}_\infty + \frac{\{\text{Abs}_0 - \text{Abs}_\infty\} \times \{[B]_0 - m[A]_0\} \times e^{-k_\psi t}}{[B]_0 - m[A]_0 e^{-k_\psi t}} \quad (3)$$

where $[B]_0$ and $[A]_0$ are the initial concentrations, with $[B]_0$ the larger, and k_ψ represents $\{[B]_0 - [A]_0\}k$ in eq 2 and the nearly-equivalent quantity $\{[B]_0 - [A]_0/2\}k$ in eq 3, where k is the bimolecular rate constant between a given oxygen donor XO and MDO. The value of m in eq 3 is the stoichiometric consumption ratio of A to B in the overall equation, which is not necessarily unity should subsequent O-atom abstractions be much more rapid than the first.

Several reagents had large UV absorptions that masked that of MTO. Their rate constants were determined by competition experiments that used two substrates, one with a known rate constant. Product concentrations were determined from their integrated ¹H NMR signals during the initial stages (< 10%) of the reaction. Equimolar amounts of the two competing reagents (~0.1 M) were mixed with ~0.1 M H₃PO₂ and ~0.01 M MTO. After one catalytic cycle (~20 min.) the ¹H spectrum was recorded and integrated. As an example, one such substrate is PhS(O)Me. We paired it with Me₂SO. The ratio of the products in comparison with their starting concentrations allows the calculation of the missing value:

$$k_{\text{PhS(O)Me}} = \frac{[\text{PhSMe}]_t}{[\text{Me}_2\text{S}]_t} \times k_{\text{Me}_2\text{SO}} \times \frac{[\text{Me}_2\text{S}]_0}{[\text{PhSMe}]_0} \quad (4)$$

Product analysis was carried out with ^1H NMR for the organic substrates and MTO; the reformation of MTO from the reaction of MDO and oxoanions was verified by the UV-vis and ^1H spectra of MTO. Chloride ions from the reduction of perchlorate were determined quantitatively by ion chromatography.³⁸ The formation of phosphorous acid in eq 1 was verified in aqueous and organic media by ^1H and ^{31}P NMR.

Results

Reaction of MTO and H_3PO_2 . Repetitive scans for the progress of reaction 1 are shown in Figure 1, corresponding to the formation of MDO and H_3PO_3 . Similar conditions were used for kinetics: 5.0×10^{-4} M MTO, 0.10–0.70 M H_3PO_2 , and 1.0 M HOTf. The data were fitted to a biexponential equation to allow for intrusion of a slower second stage, discussed in the next section. The rate constant for reaction 1 is $(2.8 \pm 0.2) \times 10^{-2} \text{ L mol}^{-1} \text{ s}^{-1}$.

The kinetic isotope effect (k_{ie}) was investigated by using D_3PO_2 in D_2O . A similar analysis gave $k_{\text{D}} = (3.9 \pm 0.2) \times 10^{-2} \text{ L mol}^{-1} \text{ s}^{-1}$. To confirm that the inverse k_{ie} arises from the P–H/P–D bond, and not from the solvent or OH group, an experiment was conducted with H_3PO_2 in D_2O under conditions where the MTO reaction occurs more rapidly than P–H exchange with the solvent.³⁹ The rate constant was the same as in H_2O .

The activation parameters were determined from the values of k over the range 5–48 °C. Least-squares fitting to the transition state theory expression (eq 5) resulted in these values: $\Delta\text{H}^\ddagger = 12 \pm 1 \text{ kcal mol}^{-1}$, $\Delta\text{S}^\ddagger = -27 \pm 2 \text{ cal mol}^{-1} \text{ K}^{-1}$.

$$k = \frac{k_{\text{B}}T}{h} \times e^{-\Delta\text{H}^\ddagger/RT} \times e^{\Delta\text{S}^\ddagger/R} \quad (5)$$

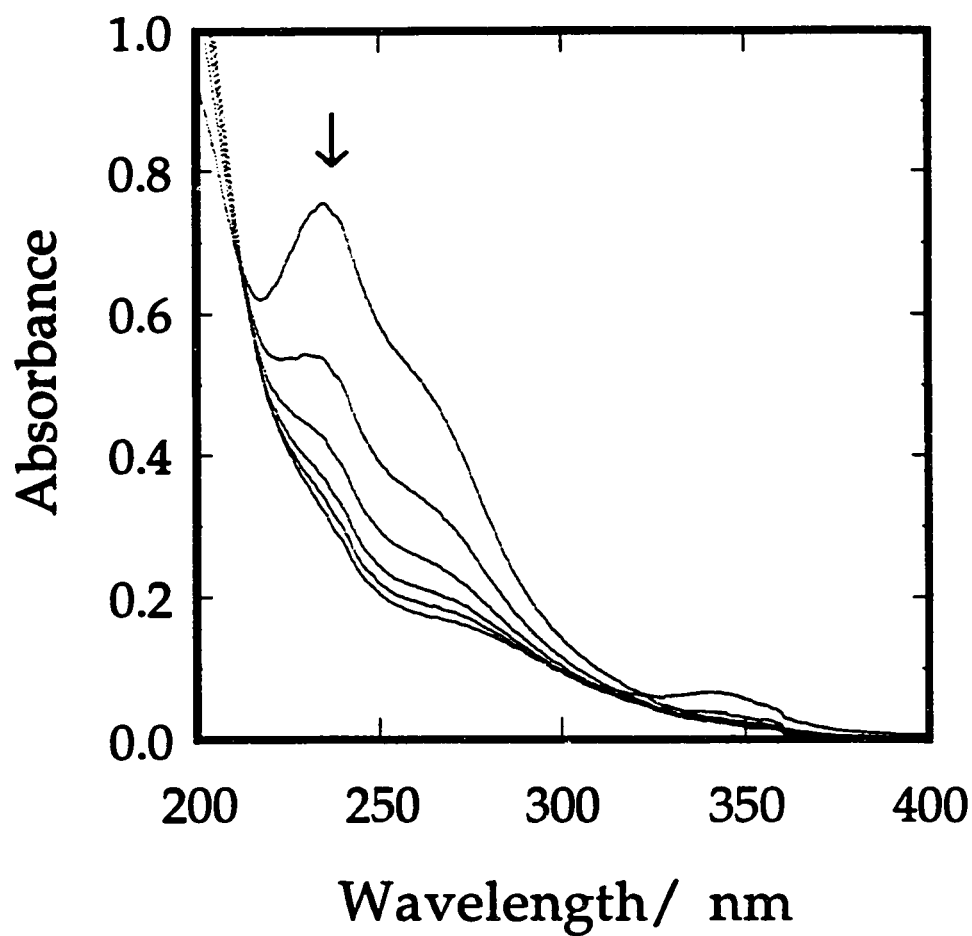
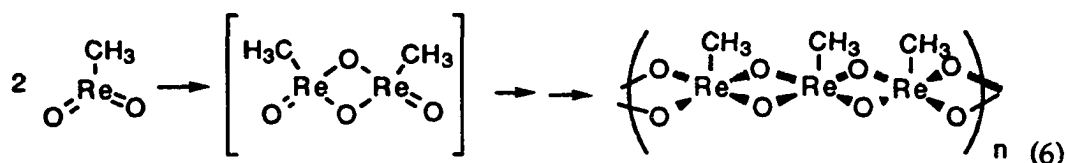


Figure 1. Spectral changes depicting the formation of MDO from the reaction between MTO and H_3PO_2 . Conditions: $[\text{MTO}] = 2.0 \times 10^{-4} \text{ M}$, $[\text{H}_3\text{PO}_2] = 0.19 \text{ M}$, $[\text{HOTf}] = 1.0 \text{ M}$, temp. = $25 \text{ }^\circ\text{C}$, optical path length = 2.00 cm , and time-interval = 2 mins .

Oligomerization. At longer times during the reaction between MTO and excess H_3PO_2 , a blue color was formed and then a black precipitate was deposited. The spectral changes during that stage are shown in Figure 2. Its rate does not depend on the concentrations of H_3PO_3 or H_3PO_2 , only on the total rhenium concentration. We therefore attribute the second stage to the dimerization and oligomerization of MDO, eq 6. Analogous oligomerization and polymerization reactions have been observed for MTO in more concentrated aqueous solutions.^{22,23}



The sensitivity of the second stage to the total rhenium concentration is illustrated in Figure 3. Two absorbance-time recordings are displayed, one with rhenium taken at half the amount of the other. The concentration reduction greatly lowers the amount of $(\text{MDO})_n$ formed. To avoid significant oligomer formation, $[\text{Re}]_T$ was kept in the range $1.0\text{--}2.5 \times 10^{-4}$ M for the kinetic studies.

MDO has also been prepared from MTO and PPh_3 in organic media, producing a species with coordinated phosphine or phosphine oxide.^{2,40} In the present case we presume one or more water molecules is coordinated to MDO, since H_2PO_2^- and H_2PO_3^- are so weakly coordinating and the solutions were maintained at pH 0 and their ^{31}P chemical shifts were unaltered. To confirm that MDO is formed in eq 1, the reaction was run in acetonitrile and MDO trapped by 1,2-bipyridine and by phenyl acetylene, Scheme 1. The adducts were characterized by ^1H NMR and by IR, Table 1; the spectroscopic data agree with literature values.⁴⁰

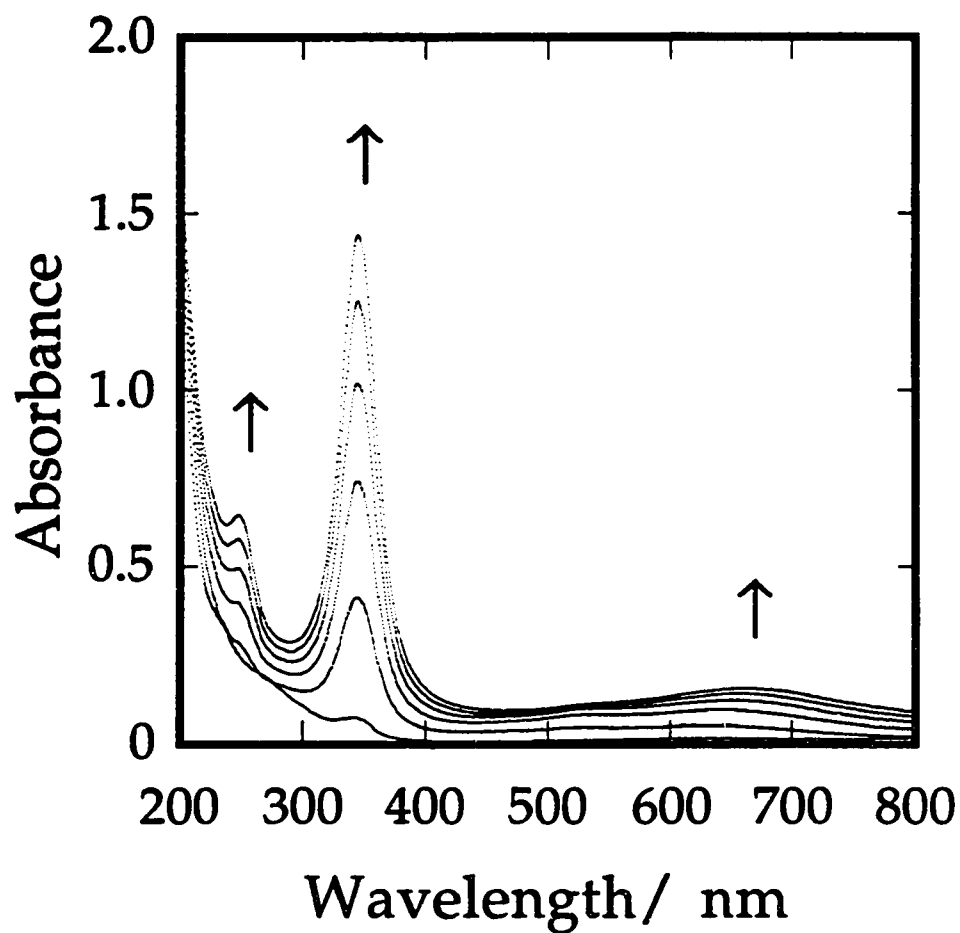


Figure 2. Changes in the UV-vis due to dimerization and oligomerization of MDO following its formation from MTO and H_3PO_2 . Conditions: $[\text{MTO}] = 5.0 \times 10^{-4}$ M, $[\text{H}_3\text{PO}_2] = 0.70$ M, $[\text{HOTf}] = 1.0$ M, temp. = 25 °C, and time-interval = 12 mins.

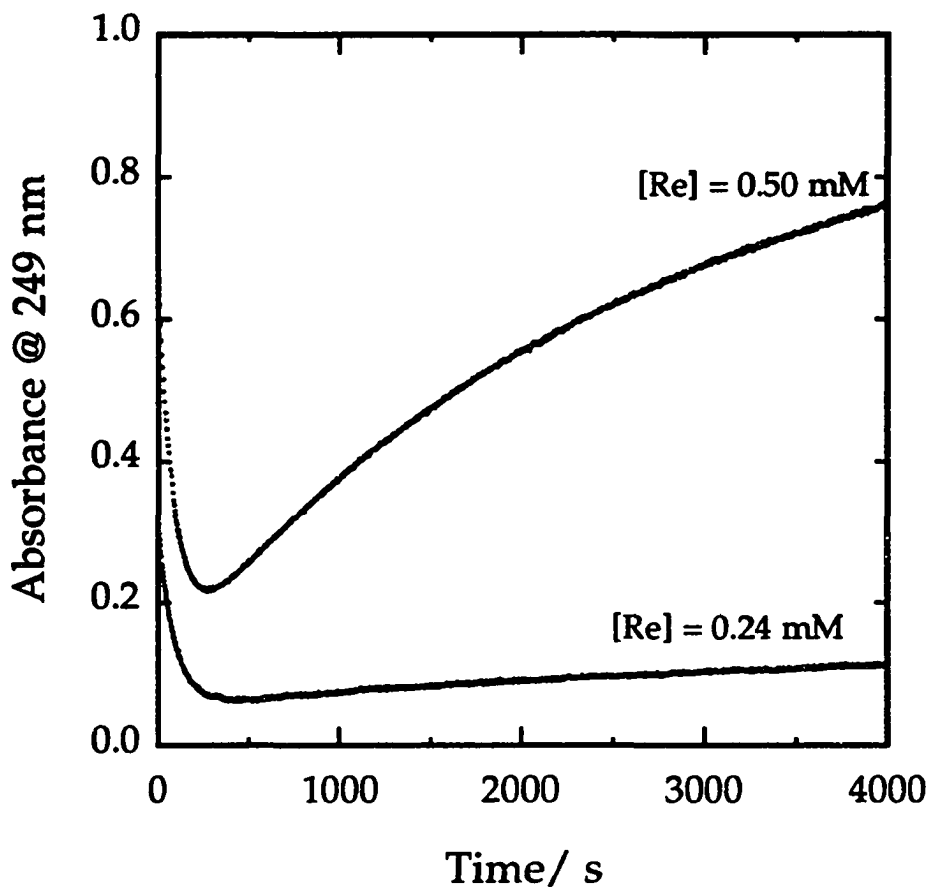
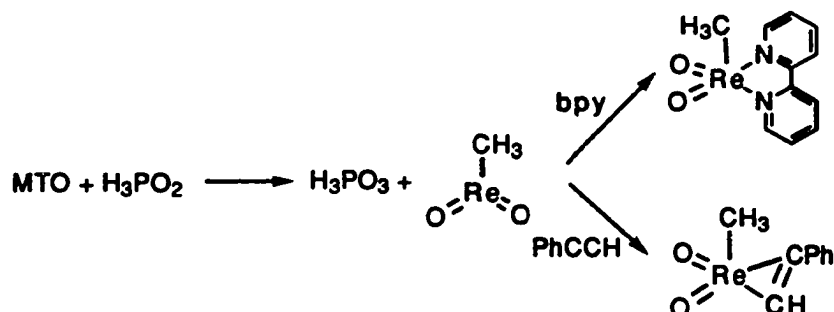


Figure 3. Time-profiles for the reaction of MTO and H_3PO_2 at two different rhenium concentrations illustrating the sensitivity of the second-stage involving oligomerization of the reduced rhenium oxide (MDO) to the $[\text{Re}]$. Conditions: $[\text{MTO}] = 5.0 \times 10^{-4} \text{ M}$ or $2.4 \times 10^{-4} \text{ M}$, $[\text{H}_3\text{PO}_2] = 0.50 \text{ M}$, and $[\text{HOTf}] = 1.0 \text{ M}$ at $25.0 \pm 0.2 \text{ }^\circ\text{C}$.

Scheme 1

Table 1. ^1H NMR and IR data for MDO derivatives

Compound	^1H NMR (CDCl_3), δ/ppm	IR, ν/cm^{-1}
	0.98 (s, Re- CH_3)	936 (s)
	7.36 (t, <i>meta</i> -2H)	910 (vs)
	7.88 (t, <i>para</i> -2H)	
	8.37 (d, <i>meta</i> -2H)	
	8.75 (d, <i>ortho</i> -2H)	
	2.78 (s, Re- CH_3)	
	9.37 (s, HCCPh)	
	7.53 (m, HCCPh)	
	7.82 (m, HCCPh)	

The reduction of anions by MDO. After the generation of ca. 2×10^{-4} M MDO from MTO (2×10^{-4} M) and 0.1–0.2 M H_3PO_2 , and prior to $(\text{MDO})_n$ formation, the desired oxoanion XO_n^- was added. The ensuing reaction, eq 7a, restores the UV

spectrum of MTO. Figure 4 depicts the initial formation of MDO and the quantitative restoration of MTO upon perchloric acid addition.



$$v = mk[\text{MDO}][\text{XO}_n^-] \quad (7b)$$

The stoichiometric consumption of XO_n^- per MDO was investigated by spectrophotometric titrations and by a kinetic method. The latter entails assuming a plausible value of m in eq 3 (for example, for the reaction between ClO_4^- and MDO, m might be 4 or 1). Only one of the values gave a proper kinetic fit in a given case, and in that way m , thus the reaction stoichiometry, could be determined. The reduction of the oxoanions by H_3PO_2 is entirely negligible on the time scale of their reduction by MDO, and much longer than that. The rate law for the oxoanions is given in eq 7b. Values of k and m are listed in Table 2.

The reduction of nitrate ions by MDO produces nitrous acid, characterized by its distinctive UV-vis spectrum. Since H_3PO_2 and NO_3^- were present at concentrations much higher than that of MTO, the rhenium complex is in effect a catalyst for oxygen transfer from NO_3^- to H_3PO_2 . That is, reactions 1 and 7a occurring in sequence amount to Re-catalyzed O atom transfer, not just for nitrate ions, but for all of the participating oxoanions.

In the particular case of NO_3^- , the situation changes after many cycles, as the accumulating nitrous acid, now more concentrated, begins to undergo decomposition, eq 8.⁴¹



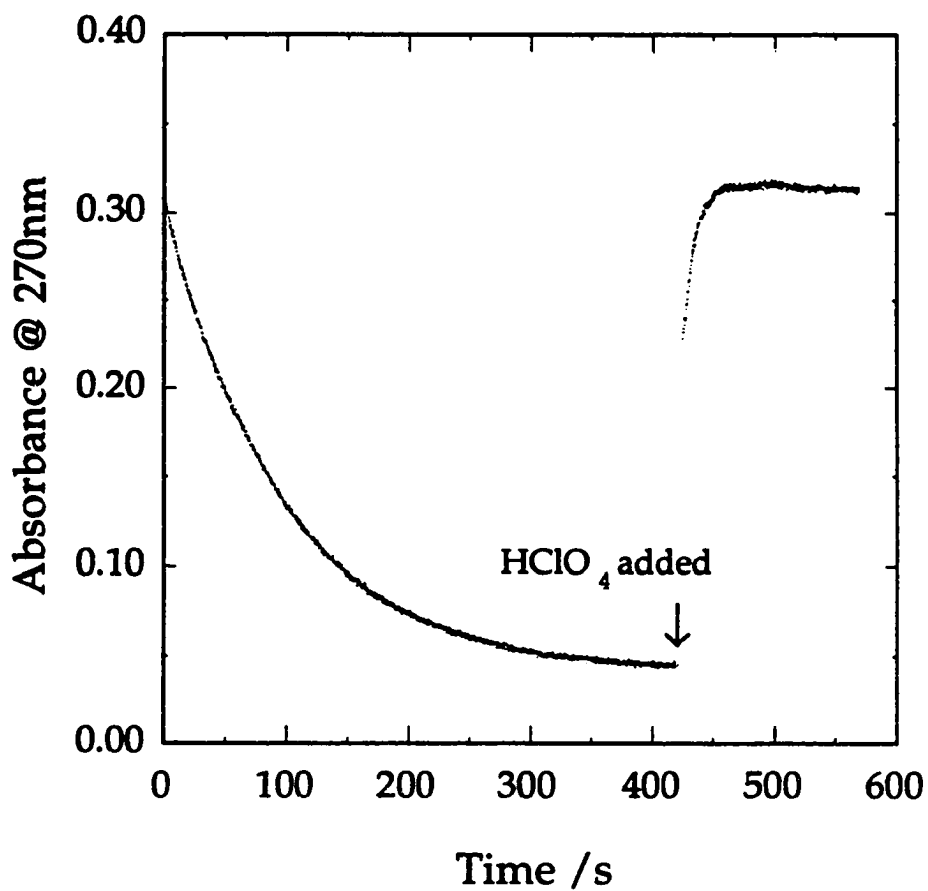


Figure 4. A kinetic time-profile depicting initially the formation of MDO and then the regeneration of MTO after HClO_4 is added. Conditions: $[\text{MTO}] = 2.1 \times 10^{-4} \text{ M}$, $[\text{H}_3\text{PO}_2] = 0.40 \text{ M}$, and $[\text{HOTf}] = 1.0 \text{ M}$ at $25.0 \pm 0.2 \text{ }^\circ\text{C}$; at the arrow mark $4.0 \times 10^{-3} \text{ M HClO}_4$ is added.

Table 2. Rate constants for the reaction of methylrhenium dioxide (MDO) with oxoanions and oxometal complexes at pH 0 and 25.0 °C

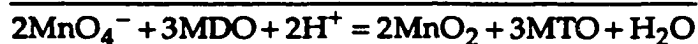
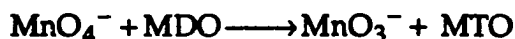
Oxoanion	$k_1/\text{L mol}^{-1} \text{s}^{-1}$	Stoichiometry MDO: XO_n^-	FC $\times 10^8/\text{g cm}^{-2}$ ^a
ClO_4^-	7.3 ± 0.2	4:1	5.08
ClO_3^-	$(3.8 \pm 0.2) \times 10^4$	3:1	4.44
BrO_4^-	$(2.6 \pm 0.2) \times 10^5$	1:1	4.10
BrO_3^-	$(2.0 \pm 0.2) \times 10^5$	3:1	3.80
IO_3^-	$(1.2 \pm 0.1) \times 10^5$	3:1	3.33
NO_3^-	$(4.4 \pm 0.2) \times 10^1$	1:1	5.69
MnO_4^-	1.0×10^6	3:2	3.96
HONO	$(4.41 \pm 0.30) \times 10^2$	1:1	4.61
VO^{2+}	$(1.93 \pm 0.05) \times 10^2$	1:1	4.62
VO_2^+	$(9.9 \pm 0.3) \times 10^5$	1:1	—
HOMoO_2^+	$(6.0 \pm 0.4) \times 10^4$	1:1	3.91

^a FC = Apparent force constant, calculated from v_{asym} for X=O bonds and reduced mass assuming a diatomic model.

Nitrous acid itself reacts with MDO. The kinetic study used a relatively low $[\text{HONO}] = 5\text{--}20 \text{ mM}$ to avoid its self-decomposition. MTO was formed and (we presume) hyponitrous acid, a *trans* dimer of "HON",⁴² the likely initial product, given the way this reaction follows the pattern observed for other oxoanions. Since $k(\text{HONO}) \sim 10 \times k(\text{NO}_3^-)$, the HONO formed from NO_3^- did not compete or interfere with the kinetic data for the nitrate reduction stage when a $>10\times$ excess of NO_3^- was used.

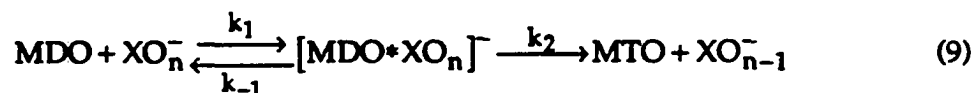
The reaction with permanganate is much like the others, except faster. Steps after the first are involved, and we show a plausible sequence in Scheme 2, formulated from these observations and literature data.⁴³

Scheme 2



Kinetic plateaus. For many of the reactions, when higher $[\text{XO}_n^-]$ were used, the pseudo-first-order rate constants were no longer directly proportional to $[\text{XO}_n^-]$. As displayed in Figure 5, plots of k_ψ versus $[\text{XO}_n^-]$ attained a plateau at a high enough concentration of the anion. The curvature for perchlorate and nitrate ions occurs only at high concentration, and might arise from a medium effect, in that neither anion is a perfect substitute for triflate ion in terms of activities even at constant ionic strength. The curvature for chlorate and perbromate ions, however, sets in at a low concentration of the anion, and clearly cannot arise from a medium effect. Only for bromate ions did the plot of k_ψ versus $[\text{BrO}_3^-]$ remain linear throughout; here, however, the upper limit of rate constants by the stopped-flow

technique limited the accessible concentration range. Thus the curvature represents an authentic and general kinetic phenomenon, which can be interpreted in terms of a presumably oxygen-bridged intermediate:



The steady-state expression clearly does not apply, since it would not result in the reaction rate plateauing at high concentration. But a prior-equilibrium (pe) expression, eq 10 with $K = k_1/k_{-1}$, would do so, as would the even more general improved-steady-state expression (imp),⁴⁴ eq 11, which does not require the first step be rapidly equilibrated prior to the second.

$$k_{\Psi}^{\text{pe}} = \frac{Kk_2[\text{XO}_n^-]}{1 + K[\text{XO}_n^-]} \quad (10)$$

$$k_{\Psi}^{\text{imp}} = \frac{k_1k_2[\text{XO}_n^-]}{k_{-1} + k_2 + k_1[\text{XO}_n^-]} \quad (11)$$

At the plateau both expressions lead to a limiting rate constant of k_2 , because the rate saturates as adduct formation shifts toward the right. When two substrates were used together, in an effort to validate this proposal further, a situation was created in which a pair of such intermediates would be involved. The formation of both would jointly lower the reagent pool shared by each, giving rise to a significant and predictable rate retardation for the two together. The rates for mixed substrates are indeed slower than the sum of rates of the independent reactions, supporting adduct formation. Efforts to make this a more quantitative treatment were frustrated, however, by all of the rates becoming so high that they pushed the reliable detection limit of the instrumentation.

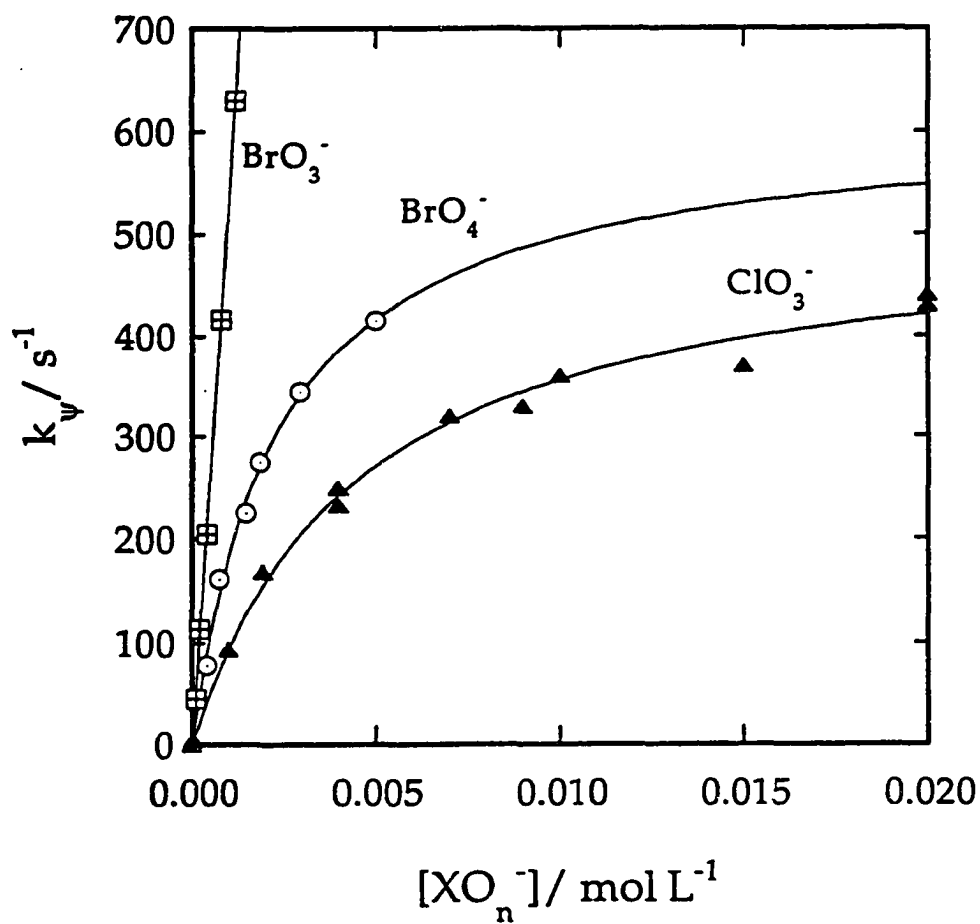


Figure 5. A group of k_{Ψ} versus $[\text{XO}_n^-]$ plots to illustrate the observed saturation kinetics in the oxidation of MDO to MTO by these oxy anions.

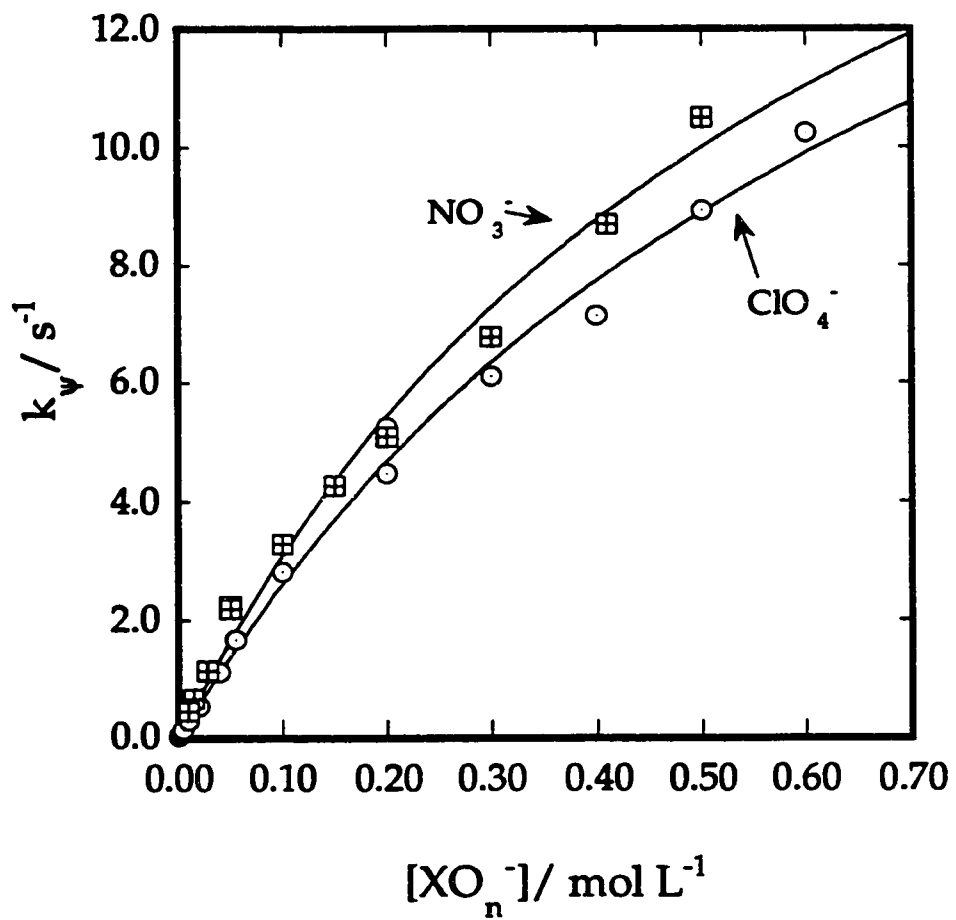
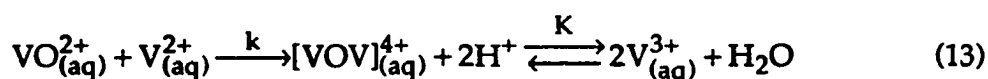
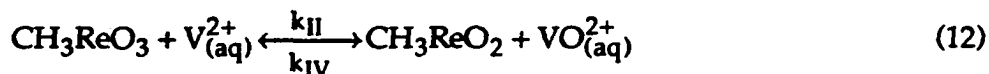


Figure 5. (Continued)

Reactions with oxo metal complexes. MTO and $V(H_2O)_6^{2+}$ react by O-atom transfer, and the process in fact is a reversible one, eq 12. The absorption at 270 nm fades initially corresponding to the reduction of MTO to MDO and then rises in a second stage; concurrent with the latter stage is a new peak at 425 nm, which is due to the formation of $[V-O-V]_{aq}^{4+}$ from V^{2+} and VO^{2+} , eq 13.⁴⁵



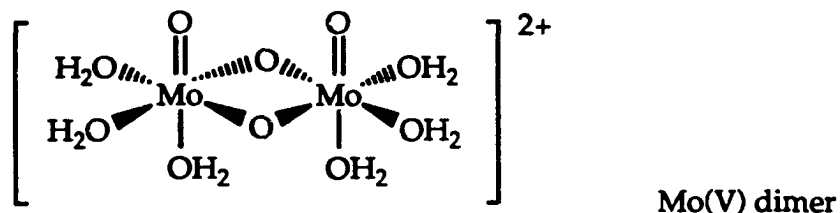
The stopped-flow technique was used to study the kinetics under argon, since V^{2+} is air sensitive. The conditions were 0.15 mM MTO, 1.8~24 mM V^{2+} , pH 0 at 25.0 °C. The two stage kinetic profiles were fitted to a biexponential function; the first-stage value of k_{ψ} was directly proportional to $[V^{2+}]$, giving $k_{II} = 68 \pm 1 \text{ L mol}^{-1} \text{ s}^{-1}$. The reverse reaction was studied by using H_3PO_2 to generate MDO; H_3PO_2 and VO^{2+} do not react. The rate constant so obtained is $k_{IV} = 193 \pm 5 \text{ L mol}^{-1} \text{ s}^{-1}$. The quotient affords the equilibrium constant $K_{12} = 0.35 \pm 0.01$.

Although V_{aq}^{3+} is not oxidized by MTO, VO_2^+ transfers an oxygen to MDO. Stopped-flow kinetics were followed at λ 315 nm with these concentrations: 0.25 mM MDO, 1.5~3.0 mM VO_2^+ . The value of k_V (eq 14) is $(9.9 \pm 0.3) \times 10^5 \text{ L mol}^{-1} \text{ s}^{-1}$. The known reactions between V^{3+} and VO_2^+ and between H_3PO_2 and VO_2^+ were negligible on this time scale.



At pH <1 molybdenum(VI) is present primarily as the octahedral species $[HOMoO_2(OH_2)_3]^+$,⁴⁶ and molybdenum(V) as the dimer shown, having two

bridging oxo groups and characterized by its distinctive absorption spectrum, λ_{\max} 297 nm ($\epsilon 8 \times 10^3 \text{ L mol}^{-1} \text{ cm}^{-1}$), 384 nm ($1.6 \times 10^2 \text{ L mol}^{-1} \text{ cm}^{-1}$).⁴⁷



The reaction of MDO with Mo(VI) to produce MTO and the Mo(V) dimer was followed at 297 nm. One set of conditions was these: 0.10 mM MDO, 0.8~1.5 mM Mo(VI), the other with excess MDO, 0.2~0.4 mM, and 0.02 mM Mo(VI), both with 1.0 M HOTf at 25.0 °C. Both sets of data fit first-order kinetics precisely. The second-order rate constants are $(6.4 \pm 0.3) \times 10^4$ and $(5.7 \pm 0.4) \times 10^4 \text{ L mol}^{-1} \text{ s}^{-1}$ for the two, the same within the experimental error, in keeping with the implied stoichiometry, $2\text{Mo}^{\text{VI}} + 2 \text{MDO} = 2 \text{MTO} + [\text{Mo}^{\text{V}}]_2$.

We are inclined to discount direct formation of Mo(V) as the route to the dimer in this case, since in no other cases was there any indication whatever of single electron transfer steps. More likely, this reaction like the others starts with O atom transfer, forming oxomolybdenum(IV), previously recognized as a reactive transient.⁴⁷ Oxomolybdenum(IV) then either reacts with molecular oxygen or disproportionates to yield the final Mo(V) dimer.^{47,48} The latter appears more likely than the involvement of molecular oxygen, this system being indifferent to its presence or exclusion.

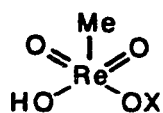
Organic oxo substrates. MDO was studied with sulfoxides, pyridine N-oxides, Ph_3AsO and Ph_3SbO . The pyridine N-oxides and DMSO are sufficiently soluble to allow the use of water as the solvent. The others are not, however, and mixed acetonitrile-water media were used.

Since DMSO lacks a significant UV absorption, the buildup of MTO was recorded. Both MTO and Me₂S were shown to be the products by their ¹H NMR spectra. For kinetics, these concentrations were used: 0.1 mM MDO, 16~700 mM DMSO, and both optical determinations and ¹H measurements are in agreement. These data and others are summarized in Table 3. Many of the listed substrates were studied by competition experiments, as presented in the Experimental Section. They relied on the thoroughly-studied DMSO as the reference compound.

Discussion

The H₃PO₂ reaction. Tautomerization of H₂P(O)OH to HP(OH)₂ is the initial step in several oxidation reactions, as with Br₂, I₂, and H₂O₂, for example.³⁹ The rate of the H₃PO₂-MTO reaction is higher than that of the tautomerization, however, eliminating that possibility.

Since this reaction displays an inverse k_{ie} , $k_H/k_D = 0.72$, rate-controlling hydride abstraction cannot be a valid mechanism. Instead, the k_{ie} reflects a P-H bond being weaker than an O-H bond, allowing us to speculate that O-H bond making is coincident with P-H bond breaking. An interpretation of the mechanism is found in the intermediates inferred during the exchange of oxygen atoms between MTO and water,^{20,49} the initial step in the binding of hydrogen peroxide,³⁵ and the dehydration of alcohols,⁵⁰ as depicted here, next to which is a depiction of the mechanism we have recognized in this case:



X = H, OH, R

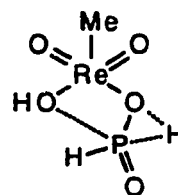


Table 3. Kinetic results for organo oxo compounds that react with MDO

Substrate, XO	σ_p	$[XO]_0 /$ mM ^a	Solvent, pH ^b	k/ L mol ⁻¹ s ⁻¹	FC $\times 10^8 /$ g cm ⁻² c	Method ^d
Me ₂ SO		16-700	100, 0	15.2 \pm 0.1	4.91	α
PhS(O)Me		1-3	50, 0	17 \pm 1	5.10	β
PhS(O)Me		100, 200	50, 1.24	17 \pm 1	5.10	χ
MeC ₆ H ₄ S(O)Me		100	50, 1.24	21	—	χ
PhS(O)CH=CH ₂		100	50, 1.24	11	—	χ
Ph ₃ AsO		50	50 or 25, 1.24	40	4.04	χ
Ph ₃ SbO		20	50, 0 or 1.24	55	4.60	χ
4-MeOC ₅ H ₄ NO	-0.27	50, 100	100, 1.24	7.80 $\times 10^3$	4.17	χ
4-MeC ₅ H ₄ NO	-0.17	50, 100	100, 1.24	7.10 $\times 10^3$	4.32	χ
C ₅ H ₅ NO	0.00	100-200	100, 1.24	4.60 $\times 10^3$	4.60	χ
4-ClC ₅ H ₄ NO	+0.23	150	100, 1.24	2.67 $\times 10^3$	4.25	χ
4-NCC ₅ H ₄ NO	+0.66	200	100, 1.24	6.5 $\times 10^2$	4.83	χ

^a XO taken in large excess; [MDO]₀ was typically 0.05-0.2 mM.

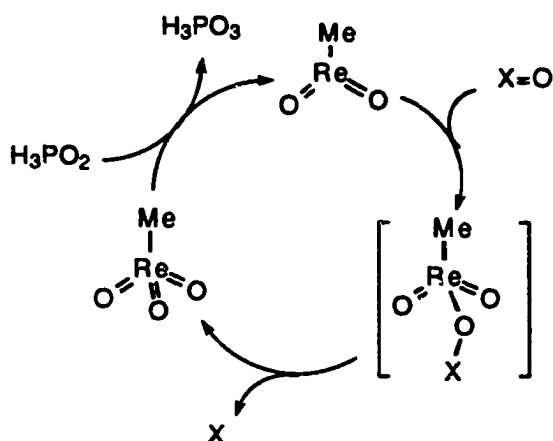
^b Water vol-% in CH₃CN-H₂O

^c FC = Apparent force constant, calculated from v_{asym} for X=O bonds and reduced mass assuming a diatomic model.

^d Methods: α = MTO buildup at 270 nm; β = Sulfide buildup at 250 nm; χ = with NMR and chemical competition as in eq 4.

Mechanism of O-Atom Transfer to MDO. The saturation kinetics for several of the oxoanions give direct evidence of adduct formation on the path for oxo transfer. The formation of Lewis acid-base adducts between MTO and organic oxygen donors such as sulfoxides³ lends credence to the notion that MDO forms such an adduct prior to oxygen transfer. Adduct formation has been detected for reactions of organic oxygen donors to Mo(IV) and Re(V) complexes.^{6,10} In this instance the evidence was kinetic not spectroscopic, signaling that the MDO intermediates are highly reactive in comparison with the others. These reactions can be carried out in a catalytic manner, as illustrated in Scheme 3.

Scheme 3



Further insight into the nature of the structure at the transition state was obtained from structure-reactivity correlations.^{51,52} The rate constants for the pyridine N-oxides are correlated with the substituent constants σ , Table 3. Figure 6 shows a plot of $\log(k_X/k_H)$ against σ_X , the slope of which gives the reaction constant: $\rho = -1.18$. The linear correlation shows the mechanism is common to all; the negative sign of ρ agrees with the assigned mechanism in which the nucleophilic pyridine N-oxides attack the electropositive rhenium center. Similar but perhaps less pronounced trends were found for the sulfoxides, Table 3.

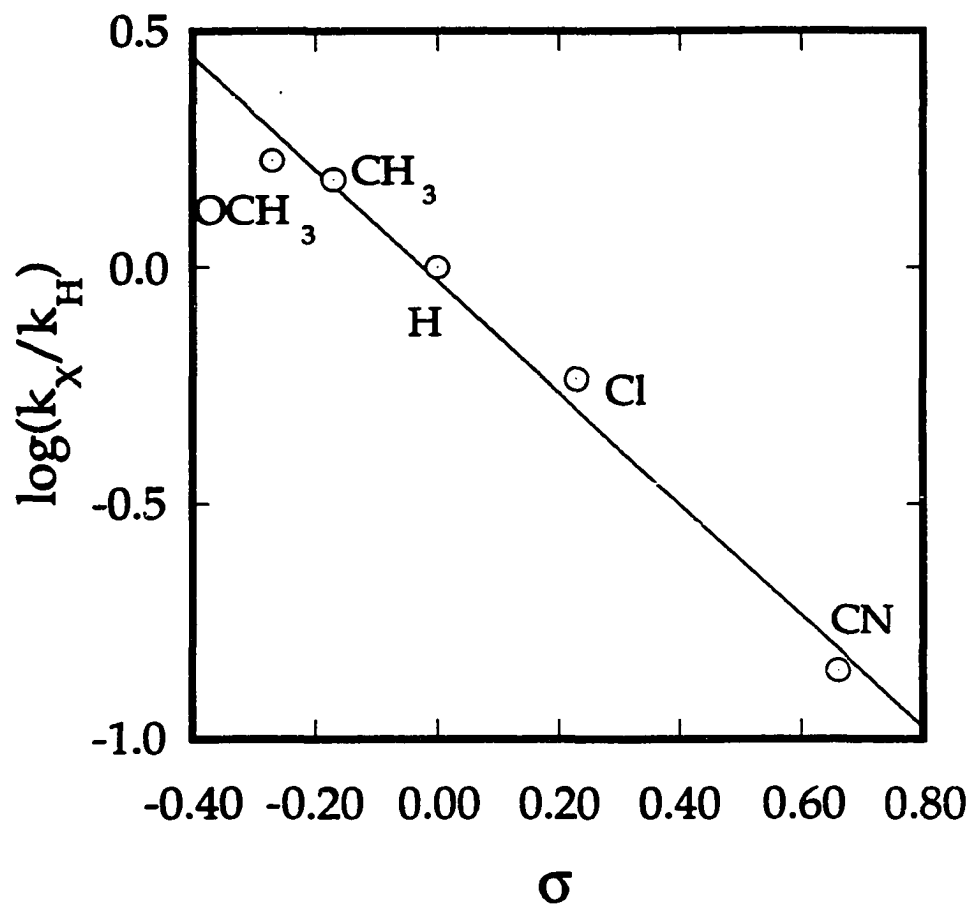


Figure 6. The Hammett correlation between the rate constants for the reactions of substituted pyridine N-oxides with MDO. The linear fit yields the reaction constant ρ of -1.18 ± 0.08 .

Reaction thermodynamics. One can express Gibbs free energy changes in one of three equivalent ways: from E° data for the 2e half-reaction (eq 15a), for O-atom release (eq 15b), and for release of molecular oxygen (eq 15c). We illustrate this with the data for the perchlorate/chlorate reaction:

Reaction	Symbol	$\Delta G^\circ/\text{kcal mol}^{-1}$		
		ClO_4^-	MTO	
$\text{XO} + 2\text{e}^- + 2\text{H}^+ = \text{X} + \text{H}_2\text{O}$	$\Delta G^\circ_{\text{E}}$	-55	-2	(15a)
$\text{XO} = \text{X} + \text{O}(\text{g})$	$\Delta G^\circ_{\text{O}}$	57	111	(15b)
$\text{XO} = \text{X} + 1/2 \text{O}_2(\text{g})$	$\Delta G^\circ_{\text{ox}}$	2	56	(15c)

The interconversion of the three is done with routine thermodynamic functions, and given one of the values from the literature^{1,53,54} the others are immediately available. Since the reaction between V^{2+} , VO^{2+} , MTO and MDO comes to a finite equilibrium, the value of its equilibrium constant allows the calculation of the same three values for MTO. They are shown in the list alongside the perchlorate ion entries.

Indeed, the vanadium-rhenium reaction provides a useful illustration. Whereas MDO reacts with DMSO and other O-atom donors fairly rapidly, V^{2+} is nonreactive, despite equivalent thermodynamics. Likewise the reactions with perchlorate ion differ greatly as to rate: $k = 7.3 \text{ L mol}^{-1} \text{ s}^{-1}$ for MDO and $2.2 \times 10^{-5} \text{ L mol}^{-1} \text{ s}^{-1}$ for V^{2+} .⁵⁵ The reactivity towards O-donors is not entirely thermodynamic in origin.

Nonetheless it is instructive to explore a possible correlation between rate constants and driving force within the series of MDO reactions. The rate constants are given in Tables 2 and 3, and the values of ΔG° were obtained as the difference between MTO/MDO and the given substrate. Figure 7 illustrates the general failure

of such correlations, even within homologous sub-series of the whole. It seems to us the problems are these: (1) Driving force is but one of the involved parameters; in the sense of Marcus-Hush theory one needs to consider the intrinsic rates of O-atom exchange, such as the ClO_4^- - ClO_3^- interconversion; since they have not been determined we set this approach aside. (2) The thermodynamic data accurately reflect the overall reaction, but not necessarily the species to emerge from the transition state. Consider, for example, ClO_4^- vs. VO^{2+} . The former, having transferred an O atom to MDO, emerges as ClO_3^- , at most with distorted angles and distances. On the other hand, O-atom abstraction from $(\text{H}_2\text{O})_5\text{VO}^{2+}$ leaves, one presumes, $(\text{H}_2\text{O})_5\text{V}^{2+}$. Its Gibbs free energy differs from that of the hexaaquavanadium(II) ground state by a considerable but unknown amount.

In a general sense the high reactivity of MDO can be traced to the oxophilicity of high-valent rhenium, the considerable stability of MTO, and the relatively low coordination numbers of MDO.

We then made an attempt to correlate the rate constants with the force constants for the X=O bonds of the various substrates, determined from the frequencies for the asymmetric vibration. The first method, recorded in Figure 8, was simply to calculate a force constant from the vibrational frequency and the reduced masses by a diatomic approximation. This cannot be rigorously correct, of course,^{56,57} but the results in a qualitative sense are nonetheless suggestive. The correlation is by no means exact, but certainly better than that provided by the thermodynamics of the overall reactions, no doubt because the force constant is a better measure of the activation barriers involved.

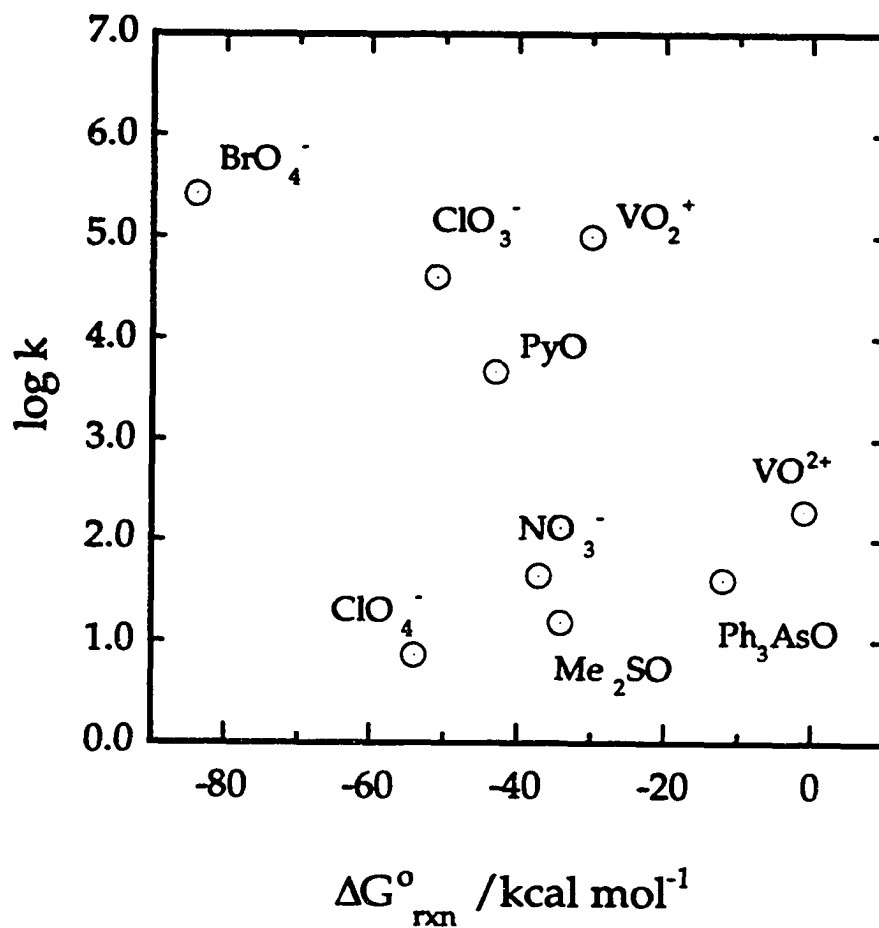


Figure 7. A plot of $\log k$ for the reactions of MDO/XO versus $\Delta G^\circ_{\text{rxn}}$ for a representative group of oxygen donors.

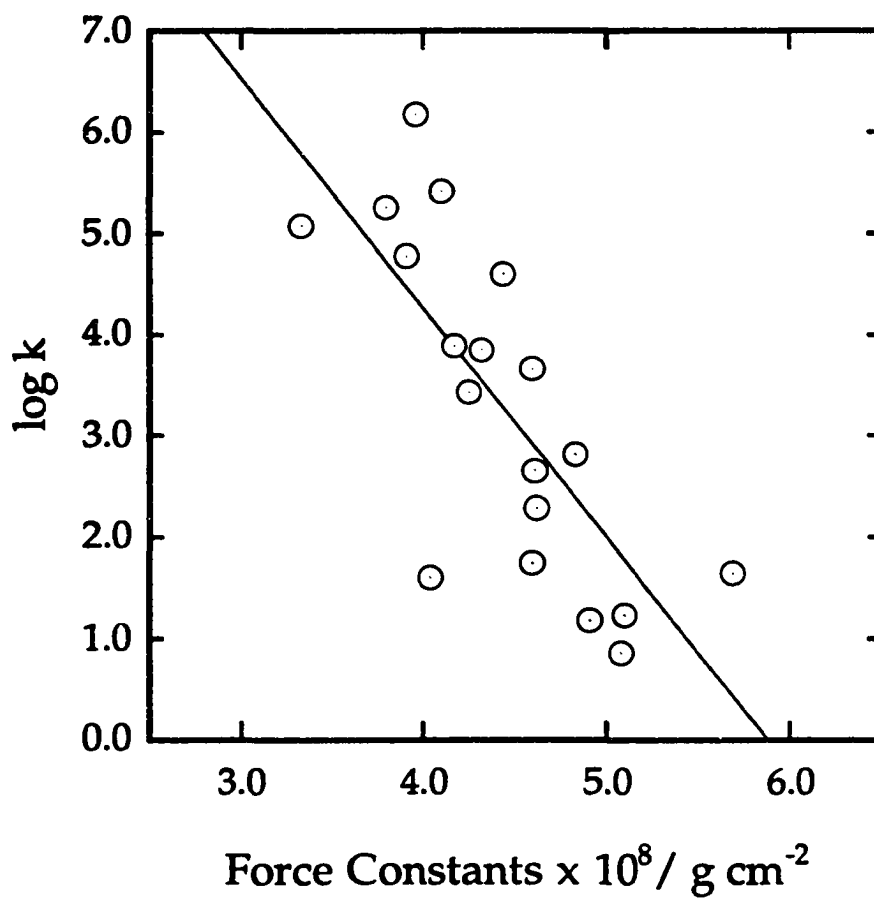


Figure 8. Log k for the reactions of MDO versus force constants for the asymmetric stretch of X=O bonds calculated from the vibrational frequencies and reduced masses assuming a diatomic model.

To pursue this, one really needs the force constant of an X=O bond obtained from a rigorous normal coordinate analysis.^{56,57} This complex procedure has been carried out previously on a number of our substrates,⁵⁸⁻⁶⁰ enough to attempt an analysis, as shown in **Figure 9**. The force constants were obtained by applying the commonly used force field known as general valence force field (GVFF).⁶⁰ It seems that the compounds divide into natural classes by formula, within each of which there is a close conformity to the model, but not overall. We shall leave the matter at this point for now, having noted some possibilities for future development of the subject.

Acknowledgments. We are grateful to Ms. Jie Li for the determinations by ion chromatography. This research was supported by the U.S. National Science Foundation and by a U.S. Department of Education Fellowship awarded to M.M.A-O.

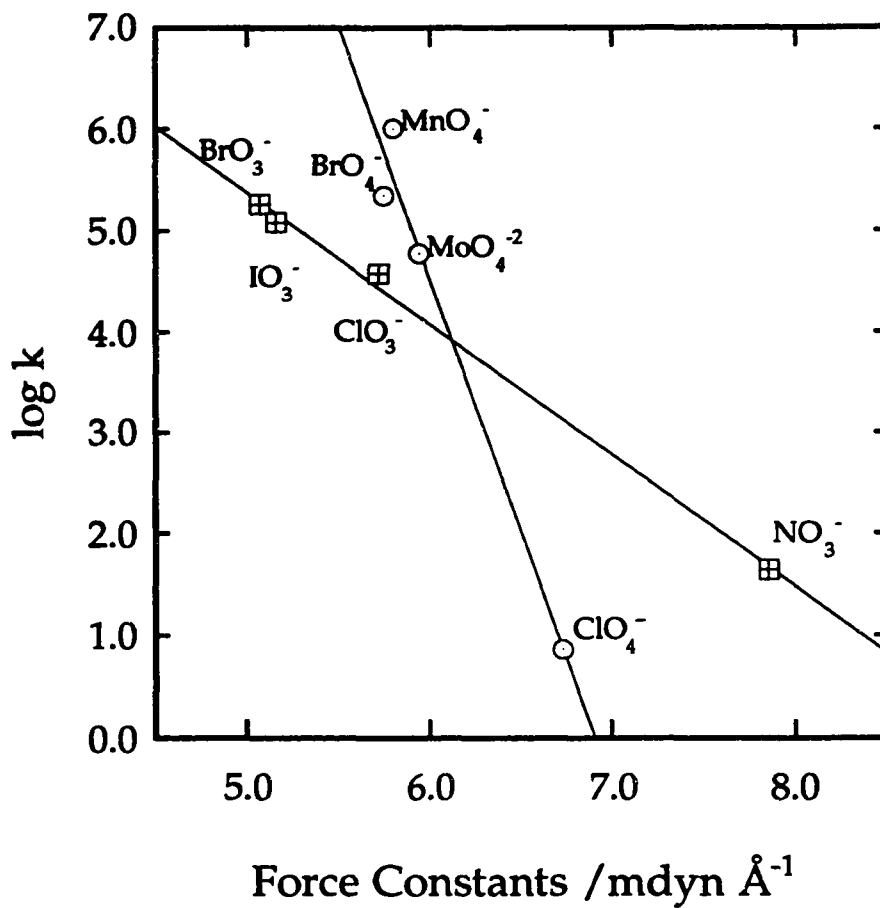


Figure 9. A plot of $\log k$ for MDO reactions with anions versus the force constants of X=O bonds from normal coordinate analysis applying GVFF.

References

- (1) Holm, R. H.; Donahue, J. P. *Polyhedron* **1993**, *12*, 571.
- (2) Herrmann, W. A.; Roesky, P. W.; Wang, M.; Scherer, W. *Organometallics* **1994**, *13*, 4531.
- (3) Zhu, Z.; Espenson, J. H. *J. Mol. Catal.* **1995**, *103*, 87.
- (4) Abu-Omar, M. M.; Espenson, J. H. *Inorg. Chem.* **1995**, *34*, 6239.
- (5) Schwarz, C. L.; Bullock, R.; Morris, R.; Creutz, C. J. *Am. Chem. Soc.* **1991**, *113*, 1225.
- (6) Caradonna, J. P.; Reddy, P. R.; Holm, R. H. *J. Am. Chem. Soc.* **1988**, *110*, 2139.
- (7) Schultz, B. E.; Gheller, S. F.; Muetterties, M. C.; Scott, M. J.; Holm, R. H. *J. Am. Chem. Soc.* **1993**, *115*, 2714.
- (8) Moyer, B. A.; Sipe, B. K.; Meyer, T. J. *Inorg. Chem.* **1981**, *20*, 1475.
- (9) Kahn, M. T.; Rao, A. P.; Samad, S. A.; Chatterjee, D.; Bhatt, S. D.; Merchant, R. *R. Proc. Indian Acad. Sci.* **1990**, *102*, 231.
- (10) DuMez, D. D.; Mayer, J. M. *Inorg. Chem.* **1995**, *34*, 6396.
- (11) Rybak, W. K.; Zagicek, A. J. *Coord. Chem.* **1992**, *26*, 79.
- (12) Durham, B.; Wilso, S. R.; Hodgson, D. J.; Meyer, T. J. *J. Am. Chem. Soc.* **1980**, *102*, 600.
- (13) Moyer, B. A.; Meyer, T. J. *J. Am. Chem. Soc.* **1979**, *101*, 1326.
- (14) Ledon, H.; Bonnet, M. J. *Mol. Catal.* **1980**, *7*, 309.
- (15) Chin, D. H.; Mar, G. N. L.; Balch, A. L. *J. Am. Chem. Soc.* **1980**, *102*, 5945.
- (16) Groves, J. T.; Quinn, R. *Inorg. Chem.* **1984**, *23*, 3844.
- (17) Suslick, K. S.; Acholla, F. V.; Cook, B. R. *J. Am. Chem. Soc.* **1987**, *109*, 2818.
- (18) Villata, L. S.; Martire, D. O.; Capparelli, A. L. *J. Mol. Catal.* **1995**, *99*, 143.
- (19) Herrmann, W. A.; Okuda, J. *J. Mol. Catal.* **1987**, *41*, 109.
- (20) Herrmann, W. A. *Angew. Chem. Int. Ed. Engl.* **1988**, *27*, 1297.

- (21) Herrmann, W. A. *J. Organomet. Chem.* **1990**, *382*, 1.
- (22) Herrmann, W. A.; Fischer, R. W.; Scherer, W. *Adv. Mater.* **1992**, *4*, 653.
- (23) Herrmann, W. A.; Fischer, R. W. *J. Am. Chem. Soc.* **1995**, *117*, 3223.
- (24) Casey, C. P. *Science* **1993**, *259*, 1552.
- (25) Edwards, P.; Wilkinson, G. *J. Chem. Soc. Dalton Trans.* **1984**, 2695.
- (26) Espenson, J. H.; Pestovsky, O.; Huston, P.; Staudt, S. *J. Am. Chem. Soc.* **1994**, *116*, 2869.
- (27) Vassell, K. A.; Espenson, J. H. *Inorg. Chem.* **1994**, *33*, 5491.
- (28) Zhu, Z.; Espenson, J. H. *J. Org. Chem.* **1995**, *60*, 1326.
- (29) Abu-Omar, M. M.; Espenson, J. H. *J. Am. Chem. Soc.* **1995**, *117*, 272.
- (30) Al-Ajlouni, A. M.; Espenson, J. H. *J. Am. Chem. Soc.* **1995**, *117*, 9243.
- (31) Herrmann, W. A.; Fischer, R. W.; Marz, D. W. *Angew. Chem. Int. Ed. Engl.* **1991**, *30*, 1638.
- (32) Herrmann, W. A.; Fischer, R. W.; Schere, W.; Rauch, M. U. *Angew. Chem. Int. Ed. Engl.* **1993**, *32*, 1157.
- (33) Kholopov, A. B.; Nikitin, A. V.; Rubailo, V. L. *Kinetics and Catalysis* **1995**, *36*, 101.
- (34) Yamazaki, S.; Espenson, J. H.; Huston, P. *Inorg. Chem.* **1993**, *32*, 4683.
- (35) Pestovsky, O.; Eldik, R. v.; Huston, P.; Espenson, J. H. *J. Chem. Soc. Dalton Trans.* **1995**, 133.
- (36) Zhu, Z.; Espenson, J. H. *J. Org. Chem.* **1995**, *60*, 7090.
- (37) Appleman, E. H. *Inorg. Chem.* **1969**, *8*, 223.
- (38) Barron, R. E.; Fritz, J. S. *J. Chromatography* **1984**, *316*, 201.
- (39) Jenkins, W. A.; Yost, D. M. *J. Inorg. Nucl. Chem.* **1959**, *11*, 297.
- (40) Felixberger, J. K.; Kuchler, J. G.; Herdtweck, E.; Paciello, R. A.; Herrmann, W. A. *Angew. Chem. Int. Ed. Engl.* **1988**, *27*, 946.

- (41) Bonner, F. T.; Donald, C. E.; Hughes, M. N. *J. Chem. Soc. Dalton Trans.* 1989, 527.
- (42) Akhtar, M. J.; Bonner, F. T.; Hughes, M. N. *Inorg. Chem.* 1985, 24, 1934.
- (43) Mehrotra, R. N. *J. Chem. Soc. Dalton Trans.* 1984, 1531.
- (44) Espenson, J. H. *Chemical Kinetics and Reaction Mechanisms*; 2nd ed.; McGraw-Hill, Inc.: New York, 1995.
- (45) Newton, T. W.; Baker, F. B. *Inorg. Chem.* 1964, 3, 569.
- (46) Cruywagen, J. J.; Heyns, J. B. B.; Rohwer, E. F. C. H. *J. Inorg. Nucl. Chem.* 1978, 40, 53.
- (47) Richens, D. T.; Sykes, A. G. *Comments Inorg. Chem.* 1983, 1, 141.
- (48) Sasaki, Y.; Sykes, A. G. *J. Chem. Soc. Chem. Commun.* 1973, 767.
- (49) Abu-Omar, M. M.; Hansen, P. J.; Espenson, J. H. *J. Am. Chem. Soc.* 1996, 118, in press.
- (50) Zhu, Z.; Espenson, J. H. *J. Org. Chem.* 1996, 61, 324.
- (51) Hammett, L. P. *Chem. Rev.* 1935, 17, 125.
- (52) Hammett, L. P. *Physical Organic Chemistry*; McGraw-Hill Book Co.: London, 1970.
- (53) Latimer, W. M. *The Oxidation states of the Elements and their Potentials in Aqueous Solutions*; 2nd ed.; Prentice-Hall: New York, 1952.
- (54) Bard, A. J. In *Standard Potentials in Aqueous Solution*; A. J. Bard, R. Parsons and J. Jordan, Ed.; M. Dekker: New York, 1985.
- (55) King, W. R.; Garner, C. S. *J. Phys. Chem.* 1954, 58, 29.
- (56) Nakamoto, K. *Infrared and Raman Spectra of Inorganic and Coordination Compounds*; 3rd ed.; John Wiley & Sons: New York, 1978.
- (57) Drago, R. S. *Physical Methods for Chemists*; 2nd ed.; Saunders College Publishing: New York, 1992, pp 150-156.

- (58) Thirugnanasambandam, P.; Srinivasan, G. J. *J. Chem. Phys.* **1969**, *50*, 2467.
- (59) Gardiner, D. J.; Girling, R. B.; Hester, R. E. *J. Mol. Struct.* **1972**, *13*, 105.
- (60) Basile, L. J.; Ferraro, J. R.; Labonville, P.; Wall, M. C. *Coord. Chem. Rev.* **1973**, *11*, 21.

CHAPTER II

OXIDATIONS OF CYCLIC β -DIKETONES CATALYZED
BY METHYLRHENIUM TRIOXIDE

A paper accepted by *Organometallics*

Mahdi M. Abu-Omar and James H. Espenson

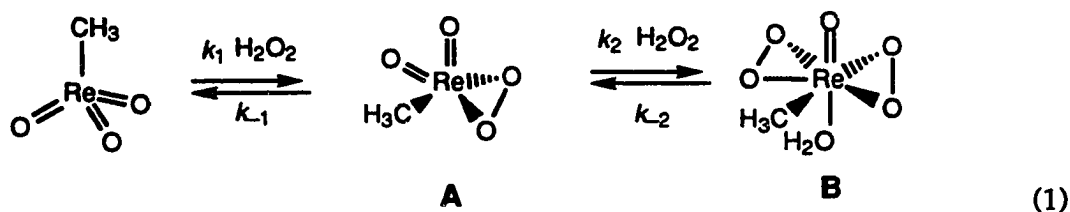
Abstract

Methylrhenium trioxide (CH_3ReO_3 or MTO) catalyzes the oxidation of β -diketones by hydrogen peroxide. The kinetics of the initial oxidation step have been investigated in $\text{CH}_3\text{CN}/\text{H}_2\text{O}$ (1:1 v/v) at 25 °C for a group of cyclic β -diketones. The initial oxidation step features the enol form, the majority species, as the reactant. Its rate responds to substituents in the "normal" manner: electron donating groups accelerate the reaction. We suggest that the double bond of the enol attacks a peroxo oxygen of a peroxorhenium complex **A** = $\text{CH}_3\text{Re}(\text{O})_2(\text{O}_2)$ or **B** = $\text{CH}_3\text{Re}(\text{O})(\text{O}_2)_2(\text{H}_2\text{O})$. This reaction affords a 2-hydroxy-1,3-dicarbonyl intermediate, which in some instances was detected by ^1H NMR. This hydroxy intermediate is susceptible to cleavage via a Baeyer-Villiger oxidation to yield carboxylic acids as final products. In contrast to the first reaction, this step may feature the peroxorhenium complexes **A** and **B** as nucleophiles rather than their customary electrophilic behavior; perhaps the trend is reversed by substrate binding to rhenium. Time profiles for the different stages of the reaction were also determined. The mechanistic aspects of these multi-step catalytic oxidations are discussed in terms of the electronic nature of the activated rhenium-bound peroxo ligands.

Introduction

Selective oxidations with hydrogen peroxide offer the potential for reducing wastes and by-products as compared to metal-based reagents such as permanganate and chromate, in that only water is produced.¹⁻³ Hydrogen peroxide, however, suffers from its kinetic inertness and from the involvement of radical pathways that lead to mixtures of products. The desirable reactions of hydrogen peroxide are those in which an oxygen atom from peroxide is transferred to the substrate. An efficient catalyst for hydrogen peroxide reactions can both overcome the kinetic barriers thus reducing the tendency for multiple reaction pathways.

Methylrhenium trioxide (CH_3ReO_3 or MTO) was first prepared in 1979,⁴ but only much later did Herrmann and co-workers recognized its potential in catalysis.⁵⁻⁷ MTO has been shown to be a catalyst for certain types of peroxide reactions. This catalyst possesses other desirable characteristics such as stability towards air and acid, and solubility in both organic and aqueous media. MTO catalysis involves in the first instance reactions with hydrogen peroxide to form monoperoxo and diperoxo rhenium complexes, A and B, respectively. They are formed in equilibrium reactions ($K_1 = 13 \text{ L mol}^{-1}$ and $K_2 = 132 \text{ L mol}^{-1}$ at 25°C and $\mu = 0.10 \text{ M}$ in $\text{CH}_3\text{CN}/\text{H}_2\text{O}$ 1:1 v/v solution),⁸⁻¹⁰ but the equilibria are not instantaneously established. Thus, in some instances, the steps in eq 1 participate as a part of the overall kinetic scheme in the catalyzed reactions.



Principally, although not exclusively, MTO catalyzes oxygen atom transfer from hydrogen peroxide (but not from alkyl hydroperoxides or oxygen) to certain

acceptors. They are often nucleophiles that can accept an oxygen atom: phosphines,⁸ sulfides,¹¹ amines,¹² halide ions,^{13,14} etc., or other electron-rich centers such as alkenes that are catalytically converted to epoxides.^{6,10}

The kinetic data in each of these instances point to a mechanism in which the nucleophile attacks a peroxide atom of **A** or **B**, this having been electrophilically activated by coordination to rhenium(VII), a strong Lewis acid. Indeed, certain predictions that follow from this mechanism have been verified: electron-donating substituents on a given substrate increase the reaction rate, and isotopic labeling showed that PhSCH₃ reacts with H₂¹⁶O₂ in the presence of MeRe¹⁸O₃ in H₂¹⁸O to yield only PhS(¹⁶O)CH₃.⁸ The nucleophilic step leads to the regeneration of MTO, which then recycles as in eq 1.

It is appreciated, however,¹⁵⁻¹⁸ that peroxide systems have open to them just the opposite possibility: that peroxide will react as a nucleophile toward substrates that are sufficiently electron poor. Instances in which the alternative is operative are, however, poorly documented for MTO-A-B systems. In this research, the catalytic reactions of the MTO-H₂O₂ system have been extended to β-dicarbonyl compounds. The β-diketones investigated in this study are present mainly in the enolic form which is electron-deficient owing to the conjugation of the double bond with the electron-withdrawing carbonyl group.¹⁹ Therefore, β-diketones can be used to examine the ability of **A** and **B** to oxidize electron-deficient substrates by a mechanism different from that which has been recognized for more electron-rich systems. Further interest in the oxidations of β-diketones stems from their use in the synthesis of natural products,²⁰ such as naturally-occurring antibiotics.²¹

Data will be presented to show that β-diketones are slowly cleaved with MTO-H₂O₂, in some instances via an intermediate that could be detected directly in the ¹H NMR spectrum, prior to further oxidation to a carboxylic acid. We have

found that the enol initially gives rise to an intermediate that is susceptible to cleavage via a Baeyer-Villiger oxidation in which the peroxorhenium complexes **A** and **B** may act as nucleophiles rather than their already-recognized electrophilic behavior. MTO has been reported as an effective catalyst for the Baeyer-Villiger oxidations of cyclic ketone to give the corresponding lactones.^{22,23} These catalytic oxidations show that MTO can change mechanisms according to substrate demand. Kinetic studies were completed for the initial step of oxidation of β -diketones, and time-resolved concentration profiles were obtained for the different stages of the reactions.

Experimental Section

Materials. HPLC grade acetonitrile (Fisher) was used, and high purity water was obtained by passing laboratory distilled water through a Millipore-Q water purification system. Hydrogen peroxide (30%, Fisher) was used to prepare peroxide solutions. Methylrhenium trioxide and the diketones (Aldrich) were reagent grade chemicals. The purity of the starting reagents was checked by ^1H NMR. Stock solutions of MTO were prepared in water, protected from light, stored at $-5\text{ }^\circ\text{C}$, used within few days, and standardized spectrophotometrically before each use.^{9,24} The reaction products were characterized by ^1H and ^{13}C NMR. The spectra matched those of authentic samples purchased from Aldrich.

Kinetic studies were performed at $25.0 \pm 0.2\text{ }^\circ\text{C}$ in 1:1 (v/v) $\text{CH}_3\text{CN-H}_2\text{O}$, containing 0.10 M perchloric acid. The acid was added to stabilize the MTO- H_2O_2 system against decomposition.²⁵ All manipulations were performed without exclusion of air, since the same results were obtained regardless. Conventional spectrophotometry (Shimadzu UV-2101PC or UV-3101PC) was used to monitor the kinetics. The temperature was maintained by a thermostated water-filled cuvette holder. The absorbance loss of the enolic tautomer of the β -diketones was recorded.

The enolic form of a β -diketone absorbs intensely in the near UV region (230-290 nm) with an extinction coefficient ca. $10^4 \text{ L mol}^{-1} \text{ cm}^{-1}$.¹⁹ Quartz cuvettes with short optical paths (0.10-0.01 cm) were used. Figure 1 displays a typical kinetic trace for the reaction of 2-chloro-5,5-dimethyl-1,3-cyclohexanedione (monochlorodimedone or MCD, for short).

With the exception of one substrate, MCD, the reactions followed first-order kinetics under these conditions. The pseudo-first-order rate constants (k_{ψ}) were evaluated by nonlinear fitting of the absorbance-time profiles to a single-exponential rate equation

$$\text{Abs}_t = \text{Abs}_{\infty} + (\text{Abs}_0 - \text{Abs}_{\infty}) \times \exp(-k_{\psi}t).$$

The MCD reaction required the use of the method of initial rates, however, owing to the involvement of chloride ions, a by-product, later in the reaction cycle, as described subsequently. The absorbance change over the initial 5% of the reaction was used to evaluate the initial rate.

Synthetic procedure. The MTO-catalyzed oxidation of 5,5-dimethyl-1,3-cyclohexanedione (dimedone) by H_2O_2 was also be carried out on a larger scale. We give the results of a typical experiment, to illustrate both the practicalities of the matter and the identification of the products. Dimedone (0.94 g, 6.74 mmol) in 150 mL of acetonitrile was treated with 30% H_2O_2 (2.70 mL, 27 mmol) and then MTO (57 mg, 0.23 mmol). The mixture was allowed to stir at room temperature for approximately 4.5 h. The reaction mixture was tested for formic acid with $\text{Ag}(\text{NH}_3)_4^+$, Tollen's reagent.^{26,27} Formation of a silver mirror indicated the presence of HCO_2H in the products. The mixture was then concentrated by rotary evaporation, and extracted with diethyl ether. The organic layer was dried over magnesium sulfate, filtered, and finally evaporated to give 3,3-dimethyl-glutaric

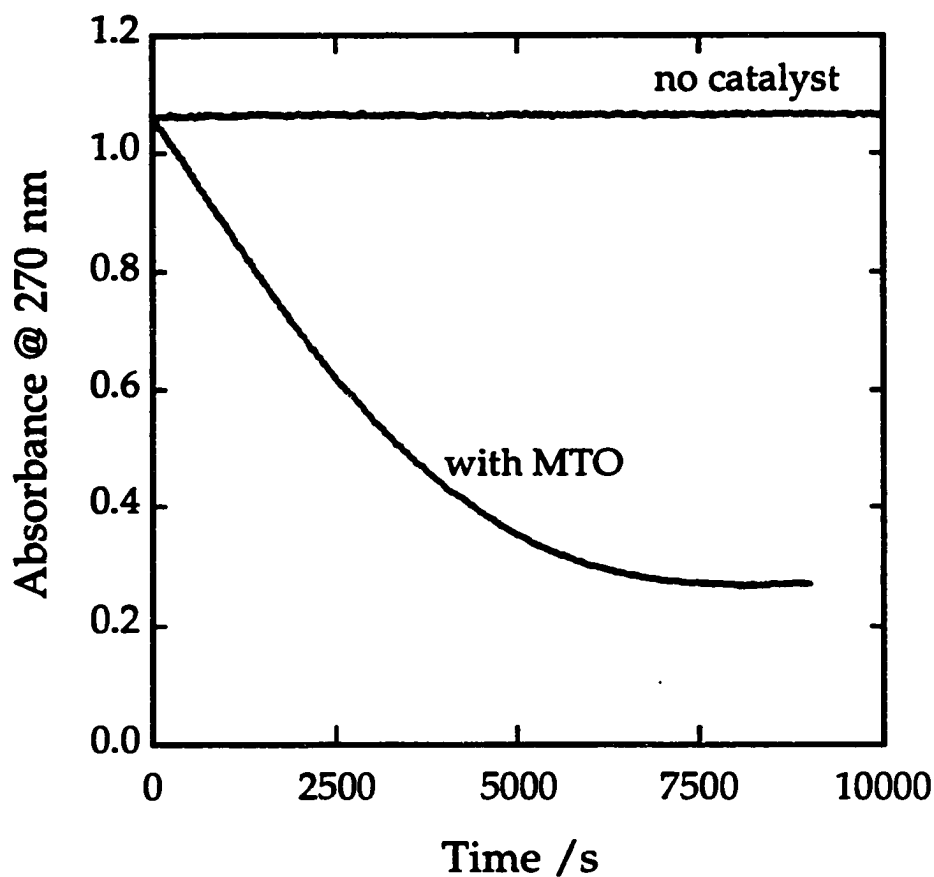
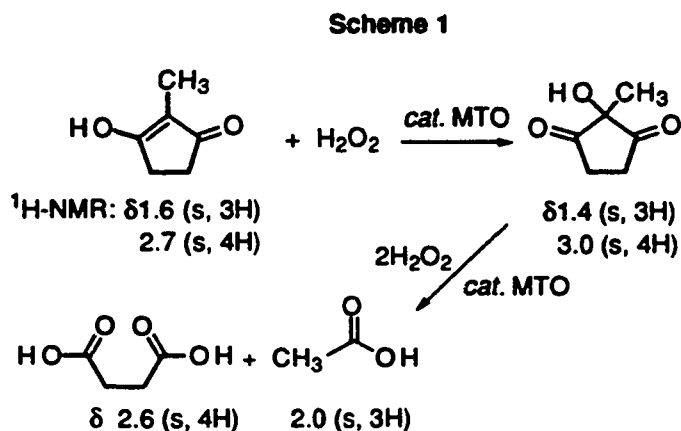


Figure 1. The MTO catalyzed oxidation of monochlorodimedone (MCD) compared to the uncatalyzed reaction. The enolic form (major species in solution, >95%) was monitored spectrophotometrically at 270 nm (optical path, 0.010 cm). Conditions: 5.5 mM MCD, 1.0 M H_2O_2 , and 0.10 M HClO_4 in $\text{CH}_3\text{CN}-\text{H}_2\text{O}$ (1:1 v/v) at 25 °C with 9.0 or 0 mM MTO.

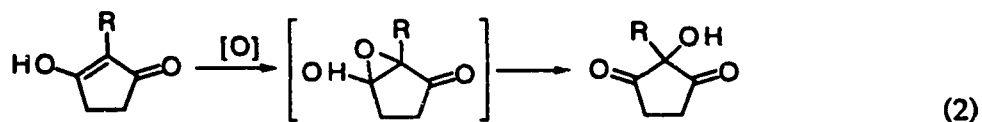
acid as a white solid (0.70 g, 4.4 mmol, 65% yield). This product had ^1H and ^{13}C NMR spectra and a melting point that matched those of the authentic compound.

Results

General observations. β -Diketones react slowly with $\text{MTO-H}_2\text{O}_2$. The initial oxidation step affords a 2-hydroxy-1,3-dicarbonyl intermediate, which could be detected in the ^1H NMR for the 2-methyl substituted dicarbonyls. This intermediate is then oxidized further to yield the final products which are the corresponding organic acids. These general observations are summarized in Scheme 1 for 2-methyl-1,3-cyclopentanedione.



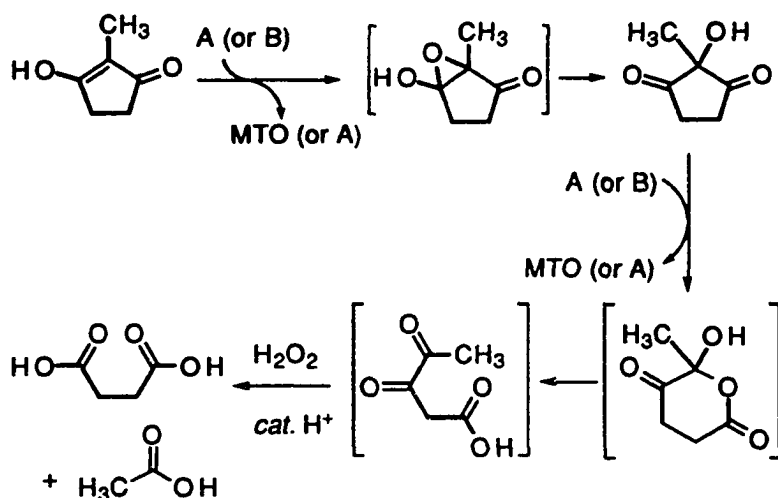
The β -diketones investigated in this study were present to more than 95% in the enolic form in solution. The 2-hydroxy-1,3-diketone intermediate arises from the rearrangement of the product of an initial epoxidation step:



The next step involves oxidative cleavage of the C-C bond, possibly via a Baeyer-Villiger mechanism. MTO is a known catalyst for the Baeyer-Villiger oxidations of cyclic ketones to the corresponding lactones.^{22,23} Also, 2-hydroxy-1,3-diketones

easily undergo cleavage with oxidizing agents such as IO_4^- and HOO^- .^{28,29} The lactone in this case rearranges due to the hydroxyl group on C-2. This affords an α -diketone intermediate (not observed) that is easily oxidized further by hydrogen peroxide to yield the final products, which are the carboxylic acids. α -Diketones are oxidized by hydrogen peroxide to organic acids, catalyzed by both acid and base.^{15,29} Therefore, we propose this sequence: epoxidation of the enolic tautomer (major species in solution) initially, followed by oxygen insertion into C-C bond, and finally rupture of the α -di-keto intermediate to afford organic acids. This mechanism is illustrated for the case of 2-methyl-1,3-cyclopentanedione in Scheme 2. The different β -diketones that we investigated are listed in Table 1 alongside the final products and yields obtained from catalytic oxidations with MTO- H_2O_2 system.

Scheme 2



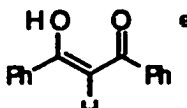
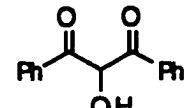
Kinetics. The strong UV absorption of the enols was used to follow their reactions with A and B, the rhenium-peroxides. The initial epoxidation of the enol destroys the conjugation responsible for the intense UV absorption of these species.

Therefore, spectrophotometric techniques enabled us to study the kinetics of the initial oxidation step only. Figure 1 displays a typical kinetic trace for the MTO-catalyzed reaction of MCD with H_2O_2 ; the results from a control experiment lacking MTO are also shown; clearly, the uncatalyzed reaction is insignificant.

Table 1. Products and yields from the MTO-catalyzed oxidations of β -diketones by hydrogen peroxide^a

Compound	Products	% Conversion ^b	% Yield ^c
	 	66	100
	 	95	74, 26
	 	85	100
	 	95	100
	 	100	100
	 	95	100
	 	90	100

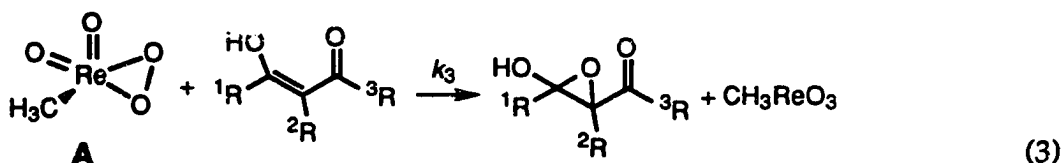
Table 1.
(continued)

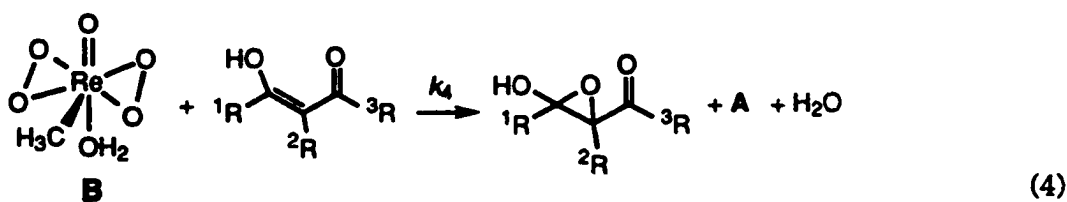
Compound	Products	% Conversion ^b	% Yield ^c
		62	85

^a Conditions: MTO: β -diketone:H₂O₂ = 1:12:70 at 25 °C, in 1:1 CD₃CN/D₂O and pD 1. ^b Based on starting material. ^c By NMR based on conversion. ^d In CD₃CN at 25 °C. ^e In CDCl₃ at 25 °C, MTO: β -diketone:H₂O₂ = 1:10:50.

The solvent used for these studies was 1:1 acetonitrile–water (v/v). This was chosen in light of the lack of solubility of most of the cyclic diketones in organic solvents and the fact that the rates of formation of **A** and **B** are much faster in semi-aqueous media than in dry organic solvents.^{8,10,25} This latter fact simplifies the kinetic treatment since the peroxide reactions of MTO can be regarded as rapid prior equilibria. An aqueous or semi-aqueous medium, however, necessitates the addition of acid for catalyst stability.²⁵ Although acid alone catalyzes the oxidation of β -diketones by hydrogen peroxide without MTO, this effect is not appreciable; the MTO-catalyzed oxidations have been found in all instances to be much faster than those of acid alone.

The different reactions involved in the catalytic cycle are described in eq 1, 3 and 4.





The complete form of the steady-state rate law is shown in eq 5, in which $[\beta]$ is an abbreviation for $[\beta\text{-Diketone}]$ and v symbolizes its consumption rate. This equation results from the application of the steady state approximation to the entire reaction scheme.

$$-\frac{d[\beta]}{dt} = v = \frac{k_1 k_3 [\text{Re}]_T [\text{H}_2\text{O}_2] [\beta] + \frac{k_1 k_2 k_4 [\text{Re}]_T [\beta] [\text{H}_2\text{O}_2]^2}{k_4 [\beta] + k_{-2}}}{k_{-1} + k_3 [\beta] + k_1 [\text{H}_2\text{O}_2] + \frac{k_1 k_2 [\text{H}_2\text{O}_2]^2}{k_4 [\beta] + k_{-2}}} \quad (5)$$

Depending on the concentrations and values of k_3 and k_4 , the interplay of eq 1, 3, and 4 in defining the experimental kinetics will differ. For example, one set of conditions under which the MTO-peroxide reactions of eq 1 are rapid with respect to the oxidation steps (eq 3-4) are as follows: $[\beta\text{-Diketone}] = [\text{MTO}] = 5 \times 10^{-4} \text{ M}$, and $0.006\text{-}0.10 \text{ M H}_2\text{O}_2$. Since the equilibria in eq 1 are established much faster than the oxidation of β -diketones at these higher peroxide levels, the concentrations of **A** and **B** remain constant throughout the reaction in these circumstances. In that case, the complex form of eq 5 reduces to a simpler form, eq 6, with the concentrations of **A** and **B** given by the values at equilibrium in eq 1.

$$v = k_\psi [\beta] = k_3 [\beta] [\text{A}] + k_4 [\beta] [\text{B}] \quad (6)$$

Both eq 5 and 6 were applied to the case of 2-methyl-1,3-cyclopentanedione. The results are shown in Figures 2a and b, respectively. Both fits yield the same values for k_3 and k_4 , in each case with the use of values of the rate constants k_1 , k_{-1} , k_2 , and k_{-2} for eq 1 that had been determined previously.⁸⁻¹⁰ The second-order rate constants for the reactions of cyclic β -diketones with A (k_3) and B (k_4) are shown in Table 2.

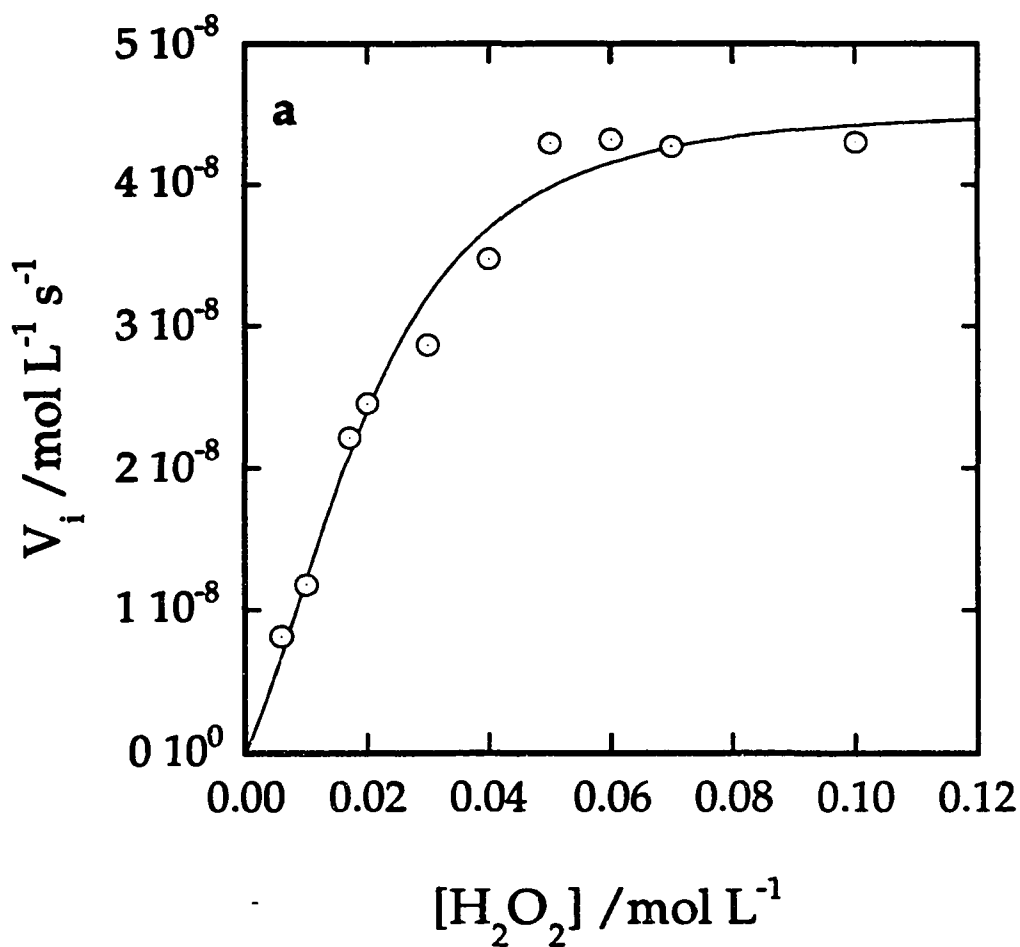


Figure 2. Kinetic data for the oxidation of 2-methyl-1,3-cyclopentanedione fitted to (a) eq 5 and (b) eq 6. Conditions: 0.60 mM 2-Me-1,3-cyclopentanedione, 0.50 mM MTO and 0.006-0.10 M H_2O_2 in $\text{CH}_3\text{CN}-\text{H}_2\text{O}$ (1:1 v/v) containing 0.10 M HClO_4 at 25 °C.

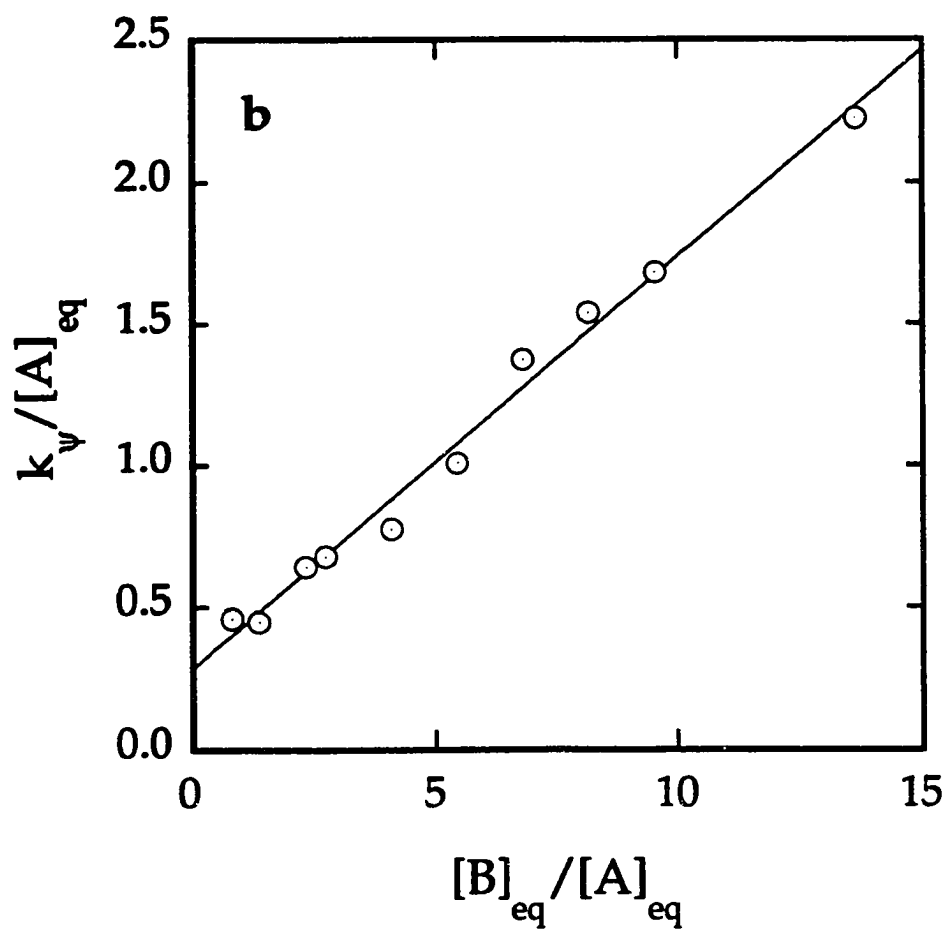
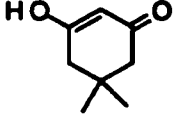
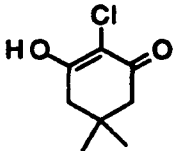
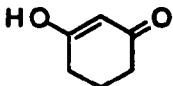
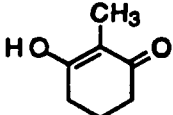
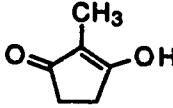
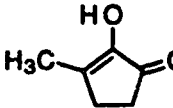


Figure 2b.

Table 2. Rate constants for the oxidation of cyclic β -diketones by the rhenium peroxides A and B.^a

Compound	$k_3/\text{L mol}^{-1} \text{s}^{-1}$	$k_4/\text{L mol}^{-1} \text{s}^{-1}$
	0.19 ± 0.03	0.11 ± 0.01
	—	0.018 ± 0.001
	0.28 ± 0.06	0.11 ± 0.01
	0.86 ± 0.02	0.17 ± 0.02
	0.28 ± 0.04	0.15 ± 0.01
	—	0.12 ± 0.01

^a At 25 °C in $\text{CH}_3\text{CN-H}_2\text{O}$ (1:1 v/v) containing 0.10 M HClO_4 .

Detection of an intermediate. In some instances an intermediate 2-hydroxy-1,3-diketone (Scheme 1) was detected by its NMR spectrum prior to the production of organic acids, the final products. The concentration-time profiles for reactant, intermediate, and product are shown in Figure 3 for 2-methyl-1,3-cyclohexanedione. Such intermediates were observed only for 2-methyl-substituted cyclic β -diketones.

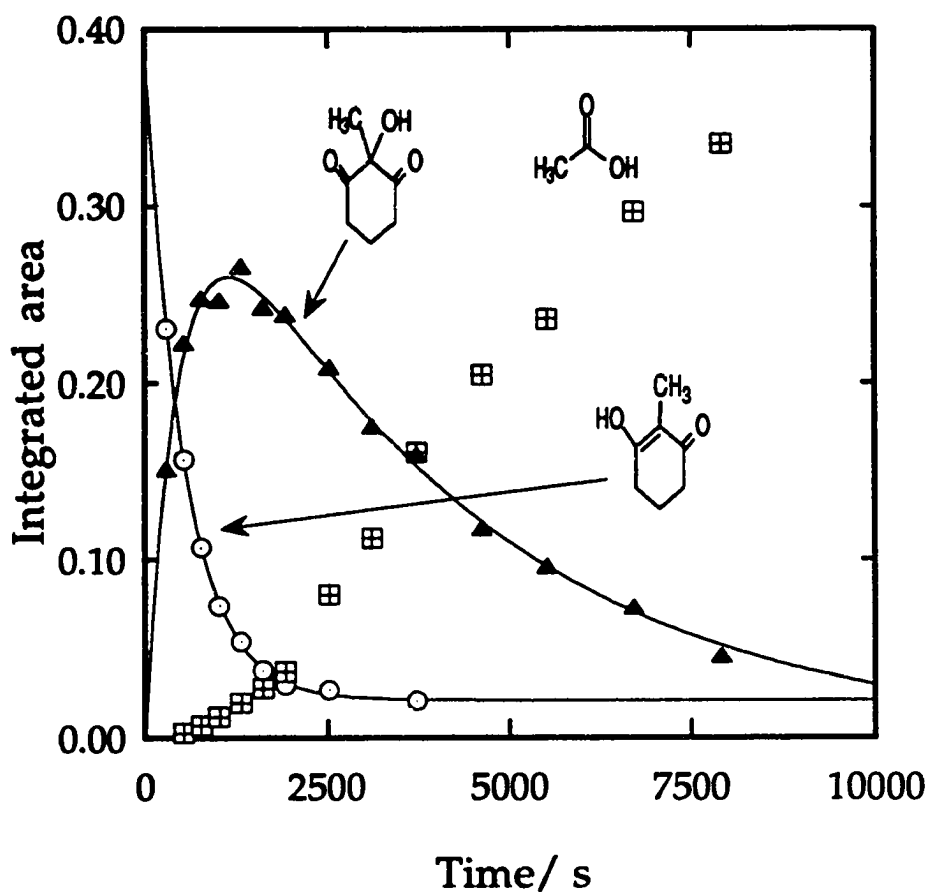


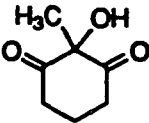
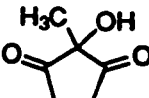
Figure 3. Concentration–time profiles from ^1H NMR data for reactant, intermediate, and product for the oxidation of 2-methyl-1,3-cyclohexanedione. Conditions: 0.080 M 2-Me-1,3-cyclohexanedione, 0.010 M MTO and 0.50 M H_2O_2 in $\text{CD}_3\text{CN}-\text{D}_2\text{O}$ containing 0.10 M DClO_4 at 25 $^\circ\text{C}$. The decay of the starting β -diketone is fitted to a single-exponential decay equation and the intermediate to a biexponential model as in $\text{R} \rightarrow \text{I} \rightarrow \text{P}$.

On the other hand, the buildup and decline of an intermediate were not observed for cyclic β -diketones that had H or Cl in place of methyl on C-2. Since MCD (Cl on C-2) reacts ten times more slowly than the methyl substituted β -diketone (Table 2), one cannot conclude that the 2-hydroxy intermediate for MCD was not observed owing to its greater reactivity in comparison to the 2-methyl substituted β -diketone. Nevertheless, 1,3-cyclohexanedione and 2-methyl-1,3-cyclohexanedione have comparable k_4 values (Table 2), and 2-methyl substituted cyclic ketones exhibit reactivities similar to the unsubstituted ones in Baeyer-Villiger oxidations.¹⁸ Therefore, it is reasonable to assume that the Baeyer-Villiger oxidation (oxygen insertion) of this intermediate proceeds more rapidly for the substrates with H or Cl substituents.

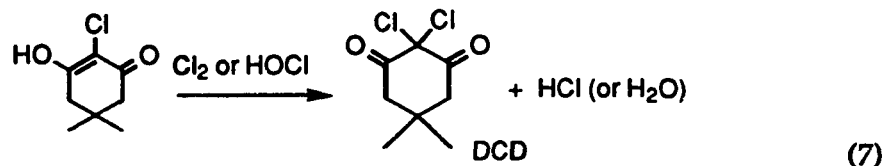
Perhaps the mechanism changes at this stage of the reaction. The 2-hydroxy-1,3-dicarbonyl intermediate behaves like an electrophile in the oxygen insertion step and not like a nucleophile. It is worth noting that the kinetics of formation and disappearance of the 2-hydroxy-1,3-dicarbonyl intermediate are dependent on the rhenium concentration. Therefore, oxygen insertion into C-C bond is accelerated by MTO. Since the intermediate was observed only for cyclic β -diketones having a methyl substituent on C-2, the kinetics of this oxygen insertion step could be determined only for these compounds. Table 3 presents the second order rate constants for the reaction of the 2-hydroxy-1,3-dicarbonyl intermediate with the diperoxorhenium complex B.

Monochlorodimedone. In the case of MCD two products were observed, 3,3-dimethylglutaric acid (70%) and 2,2-dichloro-5,5-dimethyl-1,3-cyclohexanedione (dichlorodimedone or DCD) (25%). The dichlorodimedone product was verified by utilizing the MTO-catalyzed reaction between chloride ions and hydrogen peroxide; this process yielded HOCl and Cl₂ that convert MCD to DCD.¹⁴

Table 3. Rate constants for the Baeyer Villiger oxidation of the 2-hydroxy-1,3-dicarbonyl intermediate by B.^a

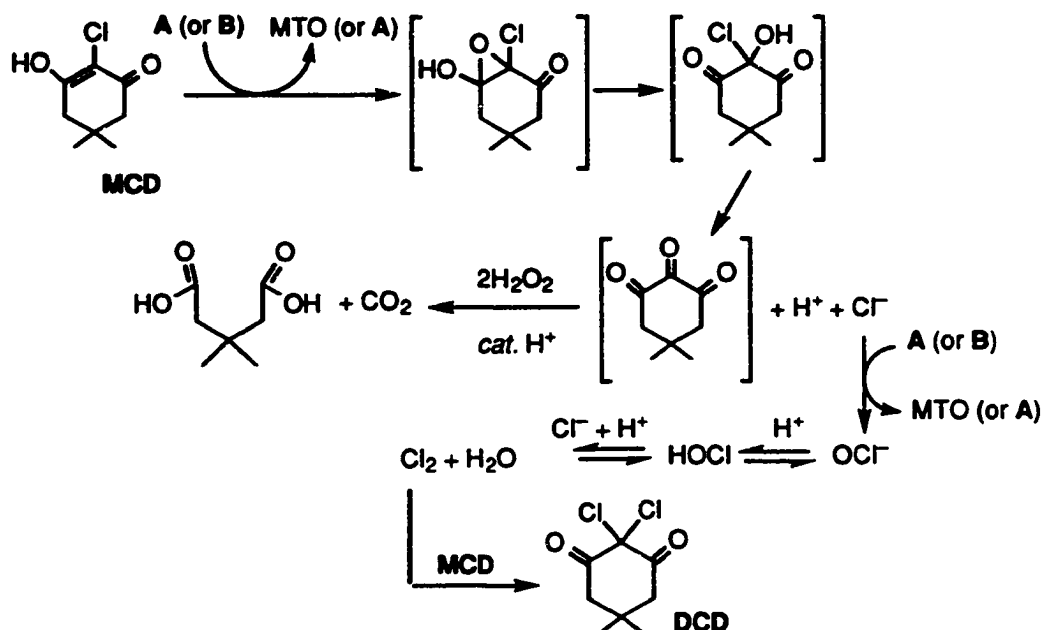
Intermediate	$k_5/\text{L mol}^{-1} \text{s}^{-1}$
	0.02
	0.02

^a At 25 °C in CD₃CN/D₂O (1:1 v/v) containing 1.0 M DClO₄; measured by ¹H-NMR.

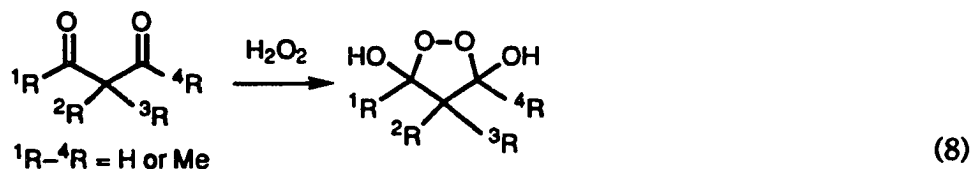


In one experiment with 0.05 M MCD, 1.0 M Cl⁻, 0.010 M MTO, 0.10 M H₂O₂, and 1.0 M DClO₄ in D₂O/CD₃CN, DCD was the only product observed [(90% yield; ¹H-NMR: δ 1.00 ppm (s, 6H) and 3.03 ppm (s, 4H)]. These signals for DCD matched those of the second product observed for the MCD oxidation by MTO-H₂O₂ in the absence of Cl⁻. The chlorine lost from one MCD must be incorporated into a second, by way of the Cl₂/HOCl reaction. The sequence of events we envisage for monochlorodimedone oxidation is shown in Scheme 3.

Scheme 3

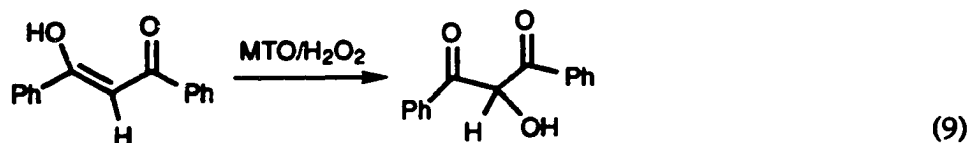


Aliphatic β -diketones. Since non-hindered simple aliphatic dicarbonyl compounds such as pentane-2,4-dione and its derivatives form cyclic peroxo compounds with hydrogen peroxide,³⁰ eq 8, the MTO-catalyzed oxidations could not be studied independently.



However, when bulky substituents were present, hydrogen peroxide and the hindered diketone do not react without a catalyst. MTO catalyzes this oxidation, giving dibenzoylmethanol, eq 9. Since MTO catalyzes the Baeyer-Villiger oxidation of cyclic but not aliphatic ketones,²³ dibenzoylmethanol is not appreciably oxidized to carboxylic acids by MTO- H_2O_2 . In contrast, cyclic β -diketones are cleaved by

MTO-H₂O₂ via a Baeyer-Villiger oxidation step that yields organic acids as the final products.



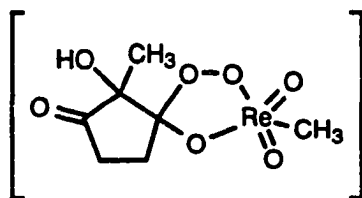
Discussion

The rhenium peroxides **A** and **B** show similar reactivities towards a given β -diketone, as much as they do toward most substrates.^{8,10-14,24} This initial oxidation step is characterized by kinetic trends that suggest nucleophilic attack of the substrate on oxygen atom of a peroxide coordinated to the rhenium atom of **A** and **B**. This trend is most pronounced by MCD and dimedone. For dimedone, k_4 is 0.11 L mol⁻¹ s⁻¹ and for MCD, 0.018 L mol⁻¹ s⁻¹. The rate retardation by substitution of Cl for H in the 2-position of the diketone supports rate-controlling nucleophilic attack by the enol, as does the further enhancement for the 2-methyl derivative, with $k_4 = 0.17$ L mol⁻¹ s⁻¹.

A and **B** are equilibrated more rapidly in eq 3-4 than the oxidation of β -diketones. The concentrations of **A** and **B** therefore remained constant throughout the reaction, given the substantial excess of hydrogen peroxide. In the limit of moderate peroxide concentrations (0.006-0.04 M), [**A**] and [**B**] are of a similar magnitude and each contributes to the overall reaction in proportion with its relative abundance and intrinsic reactivity. Under these conditions the rate is given by eq 6. At higher [H₂O₂], **B** becomes the dominant rhenium species in solution and the rate law simplifies further to $v = k_4[\beta\text{-Diketone}][\text{B}]$. The above statement is true only if **A** is not much more reactive than **B** (i.e., k_3 is comparable to k_4); since k_3 and k_4 are indeed comparable (see Table 2), the simpler form holds at high [H₂O₂]. In such cases, k_4 follows simply from the initial rates: $k_4 = v_i \times [\beta\text{-Diketone}]^{-1} \times [\text{B}]^{-1}$.

The kinetic trends exhibited by the variation of the substituent at the 2-position of cyclic β -diketones were helpful in recognizing the operative mechanism. From them, we infer that the double bond of the enol acts as a nucleophile, attacking the rhenium-bound peroxides **A** and **B**. The difference in reactivities between **A** and **B** is minor, Table 2: k_3 and k_4 differ by less than an order of magnitude. This trend is not at all uncommon, being found for other nucleophilic substrates.^{8,10-14}

Oxygen insertion into a C-C bond, the Baeyer-Villiger oxidation step, implicates a cyclic Re-peroxo intermediate, illustrated below for **A**. Analogous intermediates have been proposed for the rhenium-catalyzed Baeyer-Villiger oxidations of cyclic ketones,²³ as well as for the enzyme catechol dioxygenase,^{31,32} that catalyzes the oxygenation of catechol to 2,4-hexadienedioic acid.

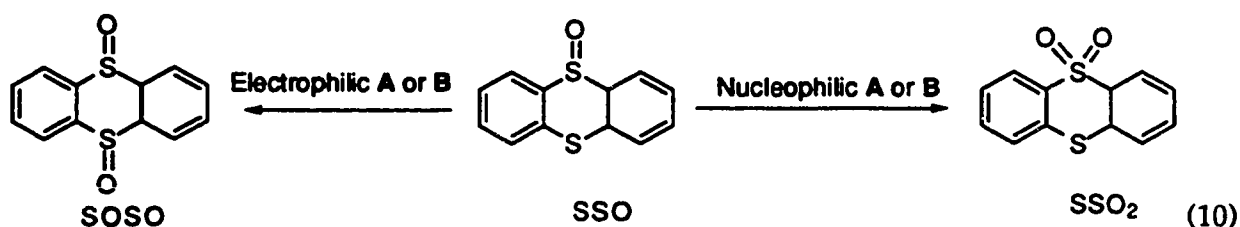


The Baeyer-Villiger oxidation of the 2-hydroxy intermediate follows a trend different from the usual, signaling a change in mechanism. For example, the 2-hydroxy-1,3-dicarbonyl intermediate was sustained at a detectable level only for the cyclic β -diketones with a C-2 methyl group but not for those with H or Cl in place of the methyl. This finding establishes that the 2-hydroxy intermediate disappeared more rapidly for the more electrophilic compounds. Perhaps the rhenium peroxides **A** and **B** behave as nucleophiles in this oxygen insertion step, as observed previously in the MTO-catalyzed oxidations of cyclic ketones to lactones²³ as well as in the Dakin reaction of benzaldehydes with H_2O_2 catalyzed by MTO to give phenols.³³ The changeover between electrophilic and nucleophilic character of the rhenium-bound peroxides in **A** and **B** can be illustrated in reactions of thianthrene-5-oxide

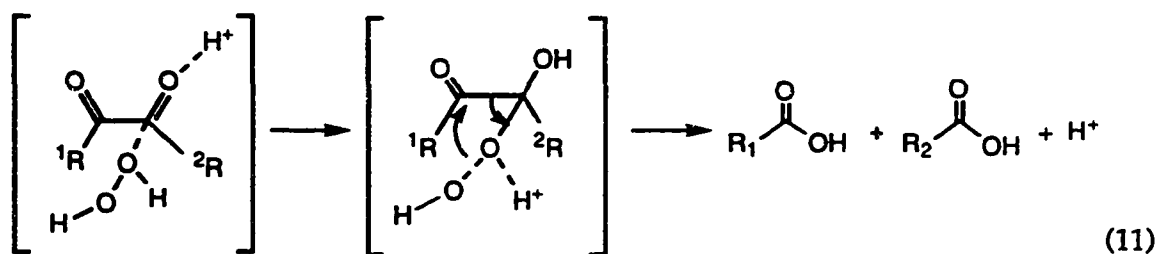
(SSO). This substance is an established mechanistic probe for oxygen transfer reagents, eq 10.^{34,35}

$$X_{\text{SO}} = \frac{n_{\text{SSO}_2}}{[n_{\text{SSO}_2} + n_{\text{SOSO}}]}$$

The oxygen transfer parameter was found²³ to have an intermediate value. However, it has been suggested that SSO is not an ideal probe for the character of peroxo metal complexes.³⁶ Nevertheless, it appears reasonable in light of the results here and those reported previously^{23,33} to suggest that **B** exhibits both nucleophilic and electrophilic reactivity. Therefore, **B** (and **A**) is able to adapt its reactivity as necessitated by the substrate involved. This feature allows **A** and **B** to be versatile oxidation catalysts since they are able to react with a wider range of substrates.



In our case the lactone formed from the oxygen insertion step rearranges to the α -diketone owing to the presence of a hydroxyl group on C-2. The resulting α -diketone is then oxidized by H_2O_2 , this step being catalyzed by the acid present in solution, eq 11.



MTO does not catalyze the Baeyer-Villiger oxidations of aliphatic ketones.²³ Similarly, oxidative cleavage of aliphatic β -diketones is not catalyzed by

methylrhenium trioxide; for example, acacH_2 and its derivatives form organic peroxy compounds, eq 8, and dibenzoylmethane yields dibenzoylmethanol, eq 9. MTO does, however, catalyze oxygen insertion into C–C bond of cyclic β -diketones, resulting in complete cleavage products, organic acids.

Why should the postulated reversal in the mechanism be found for these special cases? In these and other such cases, the substrate has a lead-in oxygen atom capable of coordination to rhenium.³⁷ A situation would then arise where the substrate and peroxide were both bound to rhenium, but the substrate, less nucleophilic than O_2^{2-} , would be polarized to a greater extent. The peroxide in such cases would be a better nucleophile than coordinated substrate. This situation appears to dominate the reactivity of thiophene-based sulfoxides.³⁸ Indeed, some otherwise puzzling data for thianthrene-5-oxide derivatives may be reconciled in this manner.

Acknowledgments. JHE is grateful to Prof. Charles E. Castro for helpful discussions and suggestions. This research was supported by the U. S. Department of Energy, Office of Basic Energy Sciences, Division of Chemical Sciences under contract W-7405-Eng-82 and by a U.S. Department of Education Fellowship awarded to M.M.A.-O.

References

- (1) Strukul, G. *Catalytic Oxidations with Hydrogen Peroxide as Oxidant*; Kluwer Academic Publishers: Dordrecht, 1992.
- (2) Sheldon, R. A. *Topics in Chemistry* 1993, 164, 23-28.
- (3) Heaney, H. *Topics in Chemistry* 1993, 164, 15-16.
- (4) Beattie, I. R.; Jones, P. J. *Inorg. Chem.* 1979, 18, 2318.
- (5) Herrmann, W. A.; Wagner, W.; Flessner, U. N.; Volkhardt, U.; Komber, H. *Angew. Chem. Int. Ed. Engl.* 1991, 30, 1636.

- (6) Herrmann, W. A.; Fischer, R. W.; Rauch, M. U.; Scherer, W. *J. Mol. Catal.* **1994**, *86*, 243.
- (7) Herrmann, W. A. In *Organic Peroxygen Chemistry*; Herrmann, W. A., Ed.; Springer-Verlag: Berlin, 1993; Vol. 164, pp 130.
- (8) Abu-Omar, M. M.; Espenson, J. H. *J. Am. Chem. Soc.* **1995**, *117*, 272.
- (9) Yamazaki, S.; Espenson, J. H.; Huston, P. *Inorg. Chem.* **1993**, *32*, 4683.
- (10) Al-Ajlouni, A.; Espenson, J. H. *J. Am. Chem. Soc.* **1995**, *117*, 9243.
- (11) Vassell, K. A.; Espenson, J. H. *Inorg. Chem.* **1994**, *33*, 5491.
- (12) Zhu, Z.; Espenson, J. H. *J. Org. Chem.* **1995**, *60*, 1326.
- (13) Espenson, J. H.; Pestovsky, O.; Huston, P.; Staudt, S. *J. Am. Chem. Soc.* **1994**, *116*, 2869.
- (14) Hansen, P. J.; Espenson, J. H. *Inorg. Chem.* **1995**, *34*, 5389.
- (15) Payne, G. B. *J. Org. Chem.* **1961**, *26*, 4793.
- (16) Payne, G. B. *J. Org. Chem.* **1959**, *24*, 1830.
- (17) Gusso, A.; Baccin, C.; Strukul, G. *Organometallics* **1994**, *13*, 3442.
- (18) Jacobson, S. E.; Tang, R.; Mares, F. J. *J. Chem. Soc., Chem. Comm.* **1978**, 888.
- (19) Toullec, J. In *The Chemistry of Enols*; Z. Rappoport, Ed.; John Wiley & Sons: New York, 1990; pp Ch. 6.
- (20) Salzmann, T. N.; Ratcliffe, R. W.; Christensen, B. G. *Tet. Lett.* **1980**, *21*, 1193.
- (21) Wasserman, H. H.; Han, W. T. *Tet. Lett.* **1984**, *25*, 3743.
- (22) Herrmann, W. A.; Fischer, R. W.; Marz, D. W. *Angew. Chem., Int. Ed. Engl.* **1991**, *30*, 1638.
- (23) Herrmann, W. A.; Fischer, R. W.; Correia, J. D. G. *J. Mol. Catal.* **1994**, *94*, 213.
- (24) Huston, P.; Espenson, J. H.; Bakac, A. *Inorg. Chem.* **1993**, *32*, 4517.
- (25) Abu-Omar, M. M.; Hansen, P. J.; Espenson, J. H. *J. Am. Chem. Soc.* **1996**, *118*, in press.

- (26) Wasserman, H. H.; Pickett, J. E. *Tetrahedron* **1985**, *41*, 2155.
- (27) Durst, H. D.; Gokel, G. W. *Experimental Organic Chemistry, 2nd ed*; McGraw-Hill: New York, 1987.
- (28) Wolfrom, M. L.; Bobbitt, J. M. *J. Am. Chem. Soc.* **1956**, *78*, 2489.
- (29) Ogata, Y.; Sawaki, Y.; Shiroyama, M. *J. Org. chem.* **1977**, *42*, 4061.
- (30) Cocker, W.; Grayson, D. H. *J. Chem. Soc., Perkin Trans. I* **1975**, 1347.
- (31) Que, L. *J. Chem. Educ.* **1985**, *62*, 938.
- (32) Lippard, S. J.; Berg, J. M. *Principles of Bioinorganic Chemistry*; University Science Books: Mill Valley, CA, 1994, pp 111-112.
- (33) Yamazaki, S. *Chem. Lett.* **1995**, 127-128.
- (34) Adam, W.; Haas, W.; Lohray, B. B. *J. Am. Chem. Soc.* **1991**, *113*, 6202.
- (35) Adam, W.; Lohray, B. B. *Angew. Chem., Int. Ed. Engl.* **1986**, *25*, 188.
- (36) Ballistreri, F. P.; Tomaselli, G. A.; Toscano, R. M.; Conte, V.; Furia, F. D. *J. Am. Chem. Soc.* **1991**, *113*, 6209.
- (37) Brown, K. N., Private Communication.
- (38) Brown, K. N.; Espenson, J. H., submitted for publication.

CHAPTER III

DEACTIVATION OF METHYLRHENIUM TRIOXIDE-PEROXIDE
CATALYST BY DIVERSE AND COMPETING PATHWAYS

A paper published in the *Journal of the American Chemical Society* *

Mahdi M. Abu-Omar, Peter J. Hansen, and James H. Espenson

Abstract

The peroxides from methylrhenium trioxide and hydrogen peroxide, $\text{CH}_3\text{ReO}_2(\eta^2\text{-O}_2)$, **A**, and $\text{CH}_3\text{Re}(\text{O})(\eta^2\text{-O}_2)_2(\text{H}_2\text{O})$, **B**, have been fully characterized in both organic and aqueous media by spectroscopic means (NMR and UV-vis). In aqueous solution, the equilibrium constants for their formation are $K_1 = 16.1 \pm 0.2 \text{ L mol}^{-1}$ and $K_2 = 132 \pm 2 \text{ L mol}^{-1}$ at pH 0, $\mu = 2.0 \text{ M}$, and 25°C . In the presence of hydrogen peroxide the catalyst decomposes to methanol and perrhenate ions with a rate that is dependent on $[\text{H}_2\text{O}_2]$ and $[\text{H}_3\text{O}^+]$. The complex peroxide and pH dependences could be explained by one of two possible pathways: either attack of hydroxide on **A** or HO_2^- on MTO. The respective second-order rate constants for these reactions which were deduced from comprehensive kinetic treatments are $k_A = (6.2 \pm 0.3) \times 10^9$ and $k_{\text{MTO}} = (4.1 \pm 0.2) \times 10^8 \text{ L mol}^{-1} \text{ s}^{-1}$. The plot of $\log k_{\psi}$ versus pH for the decomposition reaction is linear with a unit slope in the pH range 1.77–6.50. The diperoxide, **B**, decomposes much more slowly to yield O_2 and CH_3ReO_3 . This is a minor pathway, however, amounting to <1% of the methanol and perrhenate ions produced from the irreversible deactivation at any given pH. Within the limited precision for this

* Abu-Omar, M. M.; Hansen, P. J.; Espenson, J. H. *J. Am. Chem. Soc.* 1996, 118, 4966.

rate constant, it appears to vary linearly with $[\text{OH}^-]$ with $k = 3 \times 10^{-4} \text{ s}^{-1}$ at pH 3.21, $\mu = 0.10 \text{ M}$, and $25 \text{ }^\circ\text{C}$. Without peroxide, CH_3ReO_3 is stable below pH 7, but decomposes in alkaline aqueous solution to yield CH_4 and ReO_4^- . As a consequence, the decomposition rate rises sharply with $[\text{H}_2\text{O}_2]$, peaking at the concentration at which $[\text{A}]$ is a maximum, and then falling to a much smaller value. Variable-temperature $^1\text{H-NMR}$ experiments revealed the presence of a labile coordinated water in **B**, but supported the anhydride form for **A**.

Introduction

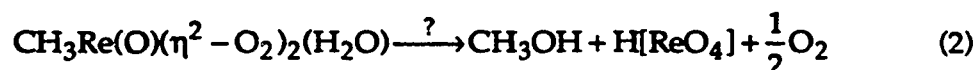
Methylrhenium trioxide (CH_3ReO_3 , MTO) catalyzes a broad spectrum of oxygen atom transfer reactions. It commonly assists in the transfer of an O atom from hydrogen peroxide to a suitable substrate, **S**, as represented by this generalized chemical equation,



A wide range of substrates can participate in this reaction: alkenes,^{1,2} phosphines,³ sulfides,⁴ metal thiolate complexes,⁵ bromide ions,⁶ amines,⁷ and so on. We and others are studying how MTO functions as a catalyst. We must also define any limitations to its use. Two catalytically-active peroxorhenium complexes, with 1:1 and 2:1 peroxide:rhenium ratios, are involved. They are $\text{CH}_3\text{Re}(\text{O})_2(\eta^2\text{-O}_2)$ (**A**) and $\text{CH}_3\text{Re}(\text{O})(\eta^2\text{-O}_2)_2(\text{H}_2\text{O})$ (**B**). We address here not the catalytic reactions per se, but solvolytic and other reactions that the peroxorhenium complexes undergo on their own, which lead to deactivation of MTO.

Alone in water and in mixed aqueous-organic solvents, dilute solutions of CH_3ReO_3 persist for days with minimal (<5%) decomposition. When CH_3ReO_3 and H_2O_2 are present together, however, decomposition ensues, usually over the course of a few hours, depending on the peroxide concentration and the pH.

Generally speaking, the system is more stable against decomposition at high $[\text{H}_3\text{O}^+]$. In organic solvents, however, **B** is stable at ambient temperature provided hydrogen peroxide is in excess. We thus undertook a study of how this catalytic system decomposes in an aqueous medium. Over time, both methanol and oxygen can be detected, and both methylrhenium trioxide and hydrogen peroxide decrease in concentration. Others have claimed⁸ that the products form together, and have described the major decomposition pathway by this equation:



We shall see, however, that eq 2 is not a correct representation of the deactivation processes; oxygen is a minor byproduct compared to methanol and perrhenate ions.

In the early stages of this investigation it became evident that an array of methods would be needed to characterize the chemical events taking place. We have employed several experimental techniques: ^1H NMR, stopped-flow, oxygen-sensing electrodes, UV-visible spectroscopy, kinetics, and gas chromatography.

As it turns out, the decomposition reactions in the MTO- H_2O_2 system are of interest in their own right, independent from their implications for catalyst stability. These reactions speak to the different modes by which peroxo-metal complexes can react, a subject that has commanded considerable independent interest.^{9,10}

In addition, **A** was further characterized spectroscopically. We sought to resolve the issue of whether **A**, like **B**, has a water molecule coordinated to rhenium. Also, the equilibrium constants for peroxide binding and the spectrum of **A** were determined more precisely.

Experimental Section

Materials. HPLC grade tetrahydrofuran (Fisher) was used, and high-purity water was obtained by passing laboratory distilled water through a Millipore-Q water purification system. Hydrogen peroxide solutions, prepared by diluting 30% H_2O_2 (Fisher), were standardized by iodometric titration. The purity of starting reagents was checked by ^1H NMR.

Methylrhenium trioxide was prepared by a literature method¹¹ or purchased from Aldrich. Stock solutions of CH_3ReO_3 were prepared in water, protected from light and stored at -5°C . The solutions were used within 3 days. Their concentrations were determined spectrophotometrically prior to each use.¹² Labeled hydrogen peroxide- O^{18} was purchased from ICON Services, Inc. as 1.4% solution in H_2^{16}O , and 94% H_2^{18}O from ISOTEC, Inc.

Instrumentation. ^1H NMR spectra were obtained with either a Nicolet 300 MHz or a Varian VXR-300 spectrometer. NMR spectra recorded in THF-d^8 were referenced to Me_4Si . Tert-butanol (δ 1.27) was used as internal reference for spectra obtained in D_2O .¹³ For spectrophotometric measurements, conventional (Shimadzu UV-2101PC and UV-3101PC) and stopped-flow (Sequential DX-17MV, Applied Photophysics Ltd.) instruments were used with quartz cells (1 or 2 cm optical path length). The pH was measured using a Corning pH meter model 320. Molecular oxygen production was measured using a YSI Model 5300 Biological Oxygen Monitor with a Model 5331 Oxygen Probe. All measurements were made at $25.0 \pm 0.2^\circ\text{C}$ and the instrument was calibrated using air-saturated water assuming $[\text{O}_2] = 0.27 \text{ mM}$.¹⁴ Methane production was measured with an HP 5790A Series Gas Chromatograph using an Alltech VZ-10 packed column and an HP 3390A Integrator. Electrospray mass spectra of perrhenate were obtained using a Finnigan TSQ 700 operated in the single quad mode for negative ions.

Results

Identification of A by NMR. The chemical shift of A in THF-d⁸ was recently reported to be 3.2 ppm.¹⁵ When we mixed equimolar amounts of MTO and H₂O₂ (50 mM each) in THF-d⁸ and recorded the ¹H NMR spectrum, three CH₃ signals were apparent: $\delta(\text{CH}_3) = 2.1$ (MTO), 2.4 (A), and 3.3 ppm (CH₃OH, from partial decomposition). The peak of A at 2.4 ppm increased with time, as did the methanol signal at 3.3 ppm, although at different rates. When more hydrogen peroxide was added to this solution (10 × the initial MTO concentration), the peaks of MTO and A diminished and a new peak emerged at 2.7 ppm, corresponding to the bis(η^2 -peroxo) complex (B). The signal for methanol did not continue to increase once A and MTO were converted to B by the addition of a sufficiently high concentration of hydrogen peroxide. We infer that the first-reported¹⁵ chemical shift of A was in fact that of the methanol formed by partial decomposition.

The rates of formation of A and B in THF depend on the water concentration; the source of water in this experiment was the 30% H₂O₂. Drying H₂O₂ solutions in THF proved difficult, since the formation of A and B yields water, free or coordinated. Hence, complete exclusion of water was not attempted; the amount of water present, however, was limited to that introduced by the 30% H₂O₂. Figure 1 shows the time profile for the formation of A (2.4 ppm) from MTO (2.1 ppm) in THF-d⁸ from an equimolar mixture of MTO and H₂O₂ (50 mM). The curve for A constitutes a rise-and-fall pattern according to which A first forms from MTO and H₂O₂, and then the [A] drops as MeOH (3.3 ppm) is produced from catalyst degradation. In THF, the pseudo first-order rate constant for the formation of A is $(3.7 \pm 0.2) \times 10^{-3} \text{ s}^{-1}$, and that for its decomposition is $(3.1 \pm 0.3) \times 10^{-4} \text{ s}^{-1}$.

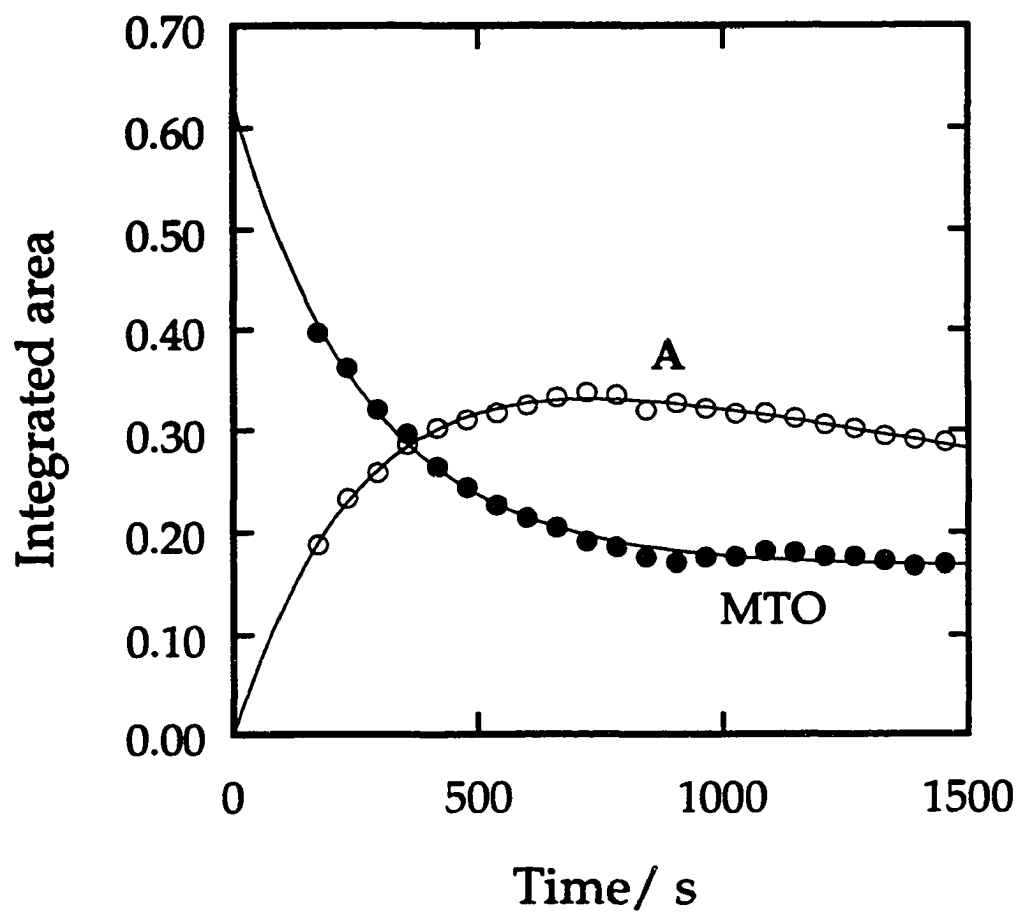


Figure 1. Kinetic traces obtained by NMR spectroscopy for the formation of **A** in THF- d^8 . Conditions: $[MTO] = [H_2O_2] = 50$ mM at 25.0 °C. The fit for **A** is based on the model $MTO + H_2O_2 \rightarrow A \rightarrow MeOH + H^+ + ReO_4^-$.

At high $[\text{H}_2\text{O}_2]$, where **A** forms very rapidly, the reaction of **A** with one additional mole of peroxide to form **B** could also be followed by ^1H -NMR. The first-order rate constant for the formation of **B** from **A** in THF-d^8 with 40 mM MTO and 0.30 M H_2O_2 is $(2.05 \pm 0.04) \times 10^{-3} \text{ s}^{-1}$.

Is water coordinated to A and B? This issue was examined by variable temperature ^1H NMR. Solutions of H_2O_2 in THF-d^8 were dried over MgSO_4 . Although fully-dried peroxide was not obtained, the water concentration was quite significantly reduced. In one set of conditions, high $[\text{H}_2\text{O}_2] = 1.0 \text{ M}$ and $[\text{MTO}] = 0.08 \text{ M}$ were used, so that only **B** would be present. The temperature was varied from $+20 \text{ }^\circ\text{C}$ to $-50 \text{ }^\circ\text{C}$. At $-40 \text{ }^\circ\text{C}$ two water peaks were evident, one for free water at 5.3 ppm and the other at 6.2 ppm for coordinated water. As shown in **Figure 2**, the two are well separated. The low temperature was needed to separate the coordinated water peak from that of free water, since this water is reasonably labile. This finding contradicts another report¹⁵, wherein water is said to be tightly bound to **B** and not exchanging, with a chemical shift of 9.4 ppm. We found no chemical shift that high in the variable-temperature NMR experiments. In general, we find that the peaks broadened and coalesced as the temperature was raised. The rate of water exchange proved to be dependent on the concentration of water, consistent with the following exchange process.



A second set of experiments employed a low $[\text{H}_2\text{O}_2] = 80 \text{ mM}$ and $[\text{MTO}] = 80 \text{ mM}$ to give a solution containing predominantly **A** and MTO and little **B**. The temperature was again varied from $+20 \text{ }^\circ\text{C}$ to $-55 \text{ }^\circ\text{C}$. The separation of a coordinated water peak for **A** was not observed. We conclude, therefore, either that **A** lacks a coordinated water or that its coordinated water is much more labile

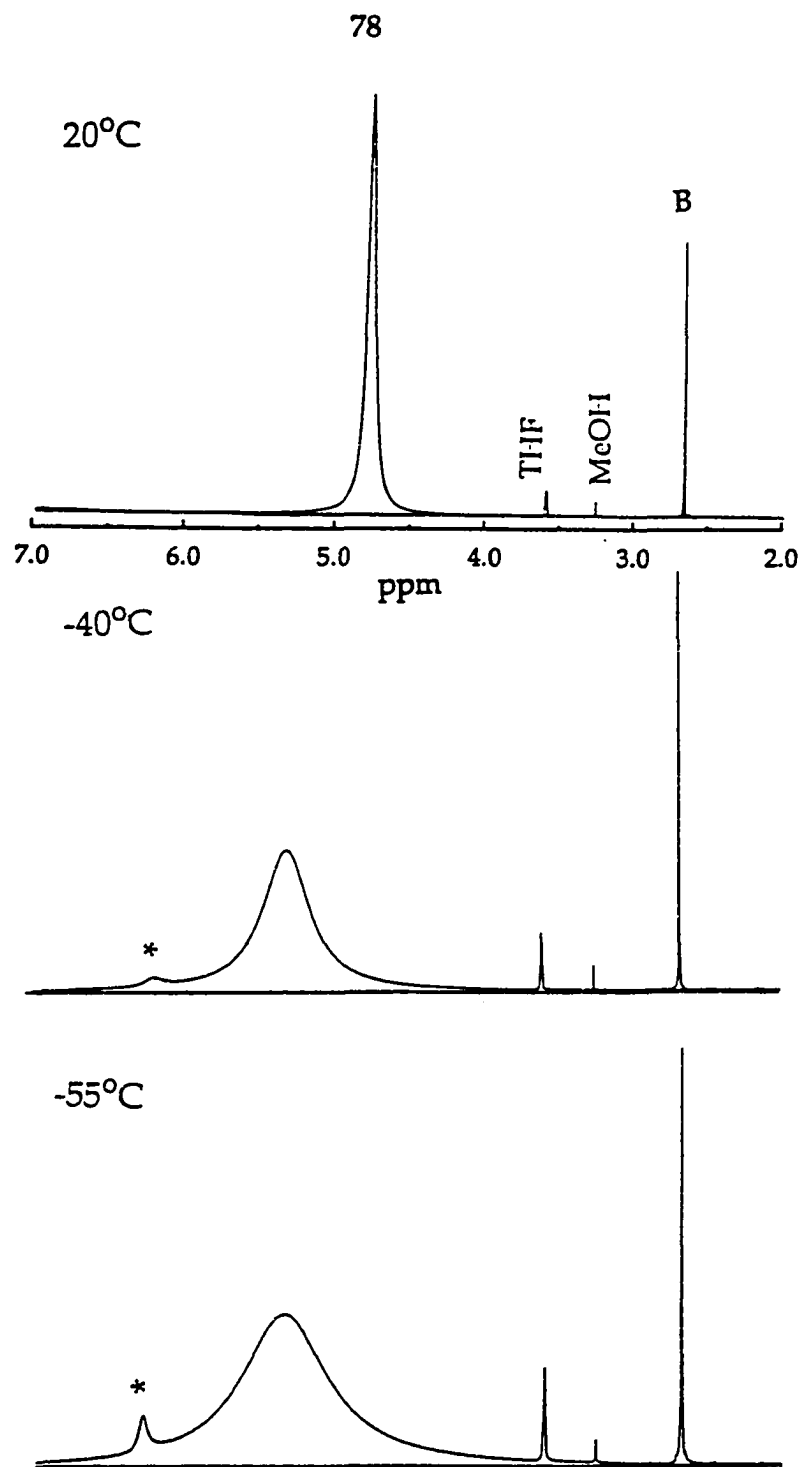


Figure 2. Variable-temperature ^1H -NMR spectra of B (generated in situ) in THF-d^8 . Conditions: 80 mM MTO and 1.0 M H_2O_2 . (*)- Coordinated H_2O .

than that of **B**. Because of other results from the pH-dependent kinetics, as presented in a later section, we are inclined to the first interpretation.

Catalyst deactivation—general observations. Compound **B** is stable in organic solvents including tetrahydrofuran, acetonitrile and acetone, especially with excess peroxide. In aqueous solutions, however, the peroxides are prone to decompose, although the addition of acid greatly improves their stability. NMR experiments in THF-d⁸, similar to the ones described previously, revealed that at low peroxide (generally $\leq Re_{tot}$, such that $[A] \gg [B]$), methanol is the decomposition product. Perrhenate ions were detected from the distinctive UV band at 225 nm after decomposing the interfering hydrogen peroxide by adding NaOH and heating to 100 °C or by adding MnO₂. Perrhenate ions were also detected by their distinctive UV absorption without the need to decompose hydrogen peroxide when [H₂O₂] was low enough, that is ≤ 5 mM. Hence, methanol and perrhenate ions are formed concurrently by either one of the following net reactions:

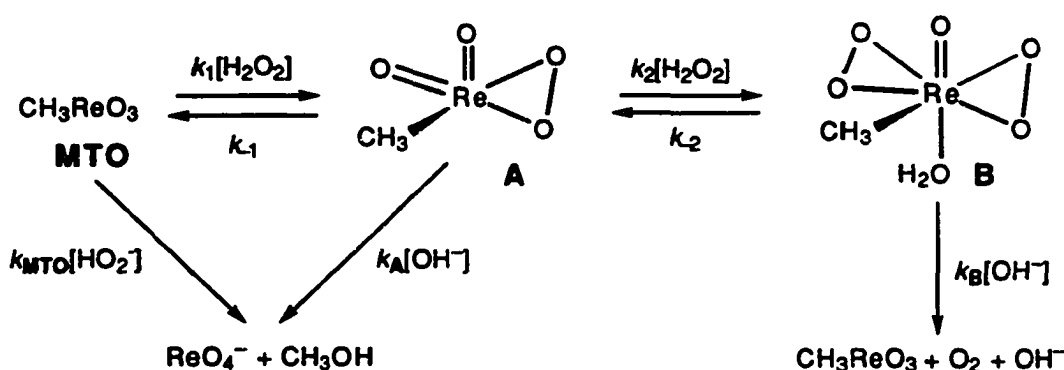


Even under acidic aqueous conditions the same reaction occurred, albeit more slowly. Based on the equilibrium constants for peroxide binding (K_1 and K_2 were determined here as subsequently described), we settled on conditions where there are comparable concentrations of all three rhenium species, for example: 60 mM MTO, 70 mM H₂O₂, 1.0 M DClO₄ in D₂O. The ¹H NMR spectrum was run as soon as practicable (ca. 4 min. after mixing). Along with a substantial amount of CH₃OD (δ 3.4 ppm), the spectrum showed MTO (δ 2.5), A (δ 2.6), and B (δ 3.0) in ratios that agree with those predicted from the equilibrium constants.

When this experiment was repeated with a large excess of H_2O_2 , B was the only methylrhenium compound detected and little methanol was seen.

Catalyst decomposition-kinetics. This system is sufficiently intricate in its pattern of kinetic behavior that it seems worthwhile to display all the plausible reactions before presenting the data from which they were constructed. The reactions are given in Scheme 1.

Scheme 1



The two reactions in Scheme 1 that account for the production of methanol and perrhenate ions are kinetically indistinguishable, since they both give rise to an identical transition state, namely, $[\text{CH}_3\text{ReO}_5\text{H}^-]^\ddagger$. The rate equations for this scheme will be written so as to presume the two peroxide binding steps are sufficiently rapid that they can be treated as prior equilibria, a point that we verified independently. It should be noted from this scheme that the irreversible decomposition of the catalyst proceeds either via the reaction of A with hydroxide or MTO with HO_2^- , whereas B regenerates MTO upon expulsion of dioxygen. The kinetic equations for Scheme 1 will be derived here, since we are not aware of a prior derivation. Let C_t represent at any time t all the forms of rhenium other than perrhenate ions:

$$[\text{Re}]_T = C_t + [\text{ReO}_4^-]_t \quad (6)$$

By differentiating this equation, and assuming perrhenate ions originate from A only, we have

$$+\frac{d[\text{ReO}_4^-]}{dt} = -\frac{dC}{dt} = k_A[\text{A}][\text{OH}^-] = k_A f_A [\text{OH}^-] C_t \quad (7)$$

where $f_A = [\text{A}]_t / C_t$ is given by

$$f_A = \frac{K_1[\text{H}_2\text{O}_2]}{1 + K_1[\text{H}_2\text{O}_2] + K_1K_2[\text{H}_2\text{O}_2]^2} \quad (8)$$

Integration of this equation, noting that $C_0 = [\text{Re}]_T$, affords

$$C_t = [\text{Re}]_T \exp(-k_A f_A [\text{OH}^-] t) \quad (9)$$

On the other hand, assuming perrhenate ions originate from the reaction of MTO and HO_2^- , we obtain

$$+\frac{d[\text{ReO}_4^-]}{dt} = -\frac{dC}{dt} = k_{\text{MTO}} [\text{MTO}] [\text{HO}_2^-] = k_{\text{MTO}} f_{\text{MTO}} [\text{HO}_2^-] C_t \quad (10)$$

where $f_{\text{MTO}} = [\text{MTO}]_t / C_t$ is given by

$$f_{\text{MTO}} = \frac{1}{1 + K_1[\text{H}_2\text{O}_2] + K_1K_2[\text{H}_2\text{O}_2]^2} \quad (11)$$

and $[\text{HO}_2^-]$ expressed relative to $[\text{H}_2\text{O}_2]$ is

$$[\text{HO}_2^-] = \frac{K_a^{\text{H}_2\text{O}_2} [\text{OH}^-] [\text{H}_2\text{O}_2]}{K_w} \quad (12)$$

Therefore, eq 7 and 10 differ only in the identities of the equilibrium and rate constants while maintaining the same dependences on hydrogen peroxide, hydroxide, and rhenium concentrations. In summary, both methanol producing reactions in Scheme 1 give rise to indistinguishable rate laws as shown by eq 7 and 10. This treatment accounts for the main pathway following first-order kinetics at constant pH and at constant f_A or f_{MTO} , which also implies at constant $[\text{H}_2\text{O}_2]$, by virtue of it being taken in excess.

The quantitative kinetic study of the decomposition pathways was carried out spectrophotometrically by monitoring the absorbance at 360 nm, where A

and especially B ($\epsilon_{\max} 1.1 \times 10^3 \text{ L mol}^{-1} \text{ cm}^{-1}$) absorb. In an extensive series of experiments $[\text{Re}]_{\text{T}}$ was maintained at 1.00 mM and the pH at 2.0 with perchloric acid. The concentration of hydrogen peroxide was varied in the range 0.007–0.50 M. The data from each experiment followed first-order kinetics, and the value of k_{ψ} was evaluated from nonlinear least-squares fitting of the absorbance-time curves to a single exponential function.

A plot of k_{ψ} versus $[\text{H}_2\text{O}_2]$ was made, as shown in Figure 3. The rate constant rises very near zero without peroxide, and after peaking it falls, following the proportion of A. According to eqs 7-8 and 10-12. The fit to eq 9 yielded $k_{\text{A}}[\text{OH}^-] = (6.2 \pm 0.3) \times 10^{-3} \text{ s}^{-1}$ or $k_{\text{MTO}}[\text{OH}^-] = (4.1 \pm 0.2) \times 10^{-4} \text{ s}^{-1}$ at pH 2.00 and $\mu = 0.01 \text{ M}$.

As shown in Scheme 1, B decomposes to yield O_2 . Again from this scheme the rate of buildup of oxygen, for the moment using k'_{B} to symbolize the rate constant at a particular pH, is given by:

$$\frac{d[\text{O}_2]}{dt} = k'_{\text{B}}[\text{B}] = f_{\text{B}}k'_{\text{B}}C_{\text{t}} = f_{\text{B}}k'_{\text{B}}[\text{Re}]_{\text{T}}e^{-f_{\text{A}}k_{\text{A}}[\text{OH}^-]t} \quad (13)$$

where

$$f_{\text{B}} = \frac{K_1K_2[\text{H}_2\text{O}_2]^2}{1 + K_1[\text{H}_2\text{O}_2] + K_1K_2[\text{H}_2\text{O}_2]^2} \quad (14)$$

Since $k_{\text{A}}[\text{OH}^-] = k_{\psi}/f_{\text{A}}$, regardless of whether k_{ψ} is measured spectrophotometrically or from O_2 buildup, the value of k'_{B} can be obtained from the yield of oxygen at the end of the reaction. Integration of eq 13 and rearrangement affords the expression

$$k'_{\text{B}} = \frac{f_{\text{A}}k_{\text{A}}[\text{OH}^-]}{f_{\text{B}}} \times \frac{[\text{O}_2]_{\infty}}{[\text{Re}]_{\text{T}}} \quad (15)$$

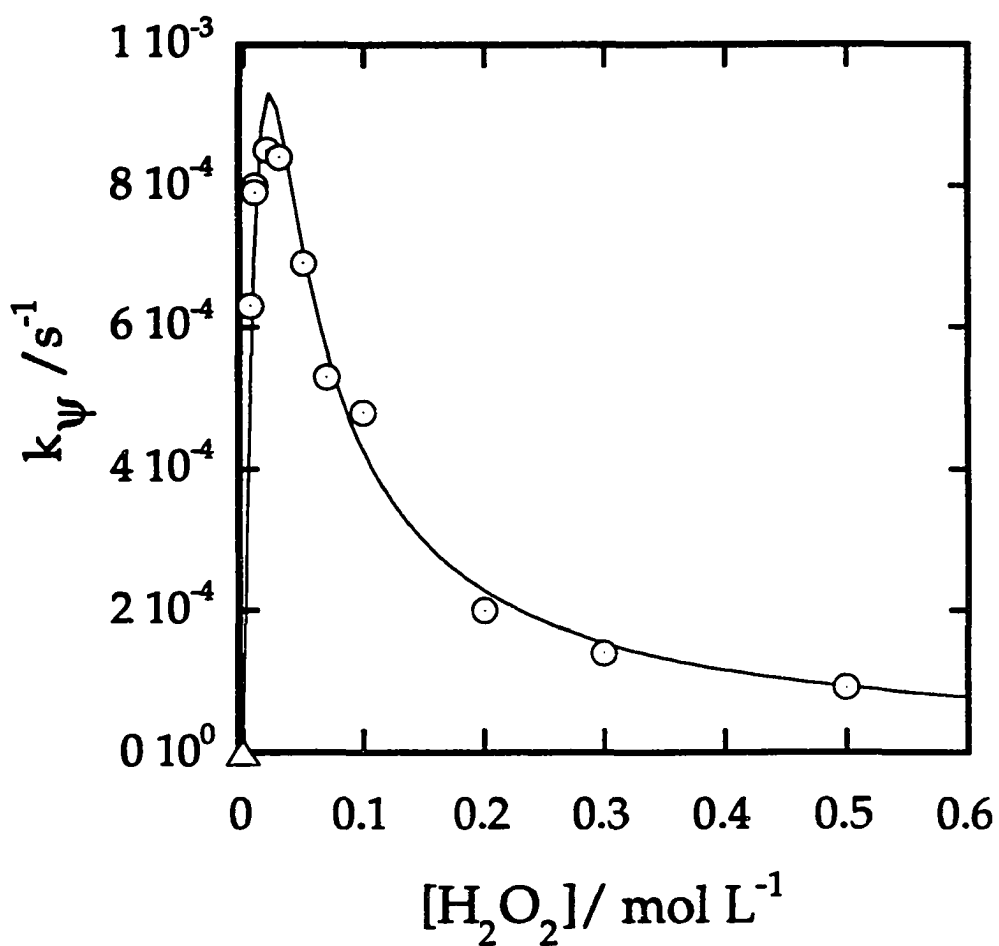


Figure 3. Plot of the pseudo-first-order rate constant for the decomposition of the catalyst as a function of $[\text{H}_2\text{O}_2]$. The fit to eq 9 (or the integral of eq 10) yields $k_A[\text{OH}^-]$ (or $k_{\text{MTO}}K_a^{\text{H}_2\text{O}_2}/K_1K_w$)[OH^-] = $0.0062 \pm 0.0003 \text{ s}^{-1}$. Conditions: 1.0 mM MTO, 0.010-0.50 M H_2O_2 , and $\mu = [\text{HClO}_4] = 0.010 \text{ M}$ at 25.0 °C.

Similar expressions, of course, could be written using the MTO and HO_2^- reaction as the decomposition pathway by relating k_A to k_{MTO} as shown in the following relation

$$k_A = \frac{k_{\text{MTO}}K_a^{\text{H}_2\text{O}_2}}{K_1K_w} \quad (16)$$

The overall relationship between k_B and $[\text{O}_2]$ remains unchanged. The only difference lies in expressions of rate and equilibrium constants for the formation of methanol and perrhenate.

Oxygen buildup, detected with an oxygen electrode, was used to monitor the decomposition processes at high $[\text{H}_2\text{O}_2]$, 0.2–0.8 M. These experiments had $[\text{Re}]_T = 1.00$ mM at pH 3.21 ($\text{H}_3\text{PO}_4/\text{KH}_2\text{PO}_4$ buffer) and 25 °C. The final O_2 concentration varied linearly with $[\text{H}_2\text{O}_2]$ and the plot of k_ψ shows a hyperbolic dependence on $[\text{H}_2\text{O}_2]$. These relationships are depicted in Figure 4. Since the expression for f_A at high $[\text{H}_2\text{O}_2]$ reduces to $f_A = f_A/f_B = 1/K_2[\text{H}_2\text{O}_2]$, these forms are expected from, and are consistent with, Scheme 1. The average value of k_B at pH 3.21 and $\mu = 0.10$ M is $(2.9 \pm 0.6) \times 10^{-4} \text{ s}^{-1}$. Increasing $[\text{H}_2\text{O}_2]$ results in an increased ratio of B to A and MTO, thus enhancing the relative importance of the O_2 -producing reaction of B. At the same time, however, the destruction of the catalyst is slowed since A decomposes irreversibly. Nonetheless, decomposition of B is minor (<1%) compared to the irreversible decomposition leading to methanol and perrhenate ions. This means that the kinetic data for this very minor pathway are of considerably lower quality; this point must be kept in mind in considering the data obtained.

The results of these experiments are given in Table 1, which includes values of the rate constants that were calculated from values of K_1 and K_2

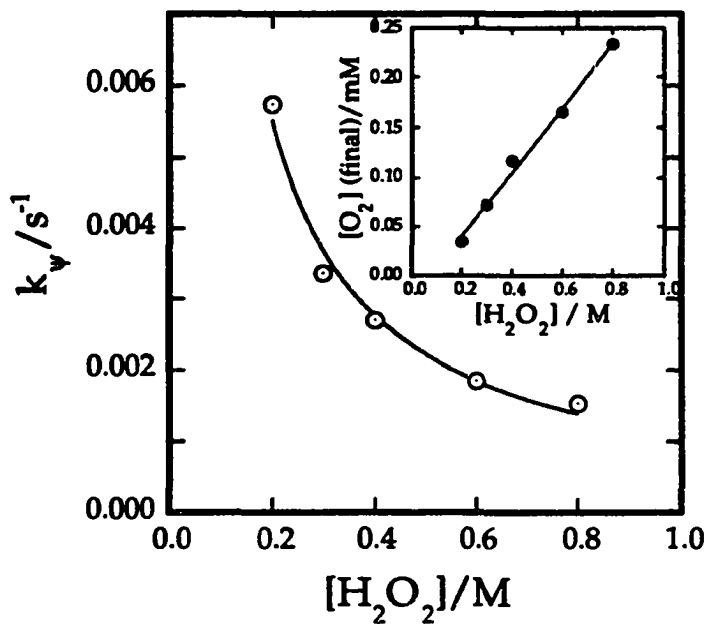


Figure 4. The plot of the pseudo-first-order rate constant from O_2 measurements as a function of $[\text{H}_2\text{O}_2]$. Conditions: 1.0 mM MTO, 0.2–0.8 M H_2O_2 , pH 3.21, $\mu = 0.10$ M at 25.0 °C. Inset: The linear relationship between the amount of O_2 produced and the $[\text{H}_2\text{O}_2]$ as required by eq 17.

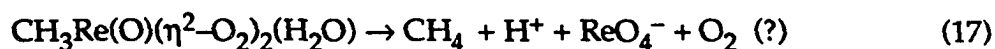
Table 1. Kinetic results and yields from the measurement of O₂ production. ^a

[H ₂ O ₂]/M	k _ψ /10 ⁻³ s ⁻¹	[O ₂] _∞ /mM	k' _A /s ⁻¹	k' _B /10 ⁻⁴ s ⁻¹	f _A	f _B
0.20	5.7	0.035	0.16	2.1	0.036	0.95
0.30	3.4	0.073	0.14	2.5	0.025	0.97
0.40	2.7	0.12	0.14	3.2	0.019	0.98
0.60	1.8	0.17	0.15	3.1	0.013	0.99
0.80	1.5	0.23	0.16	3.6	0.0094	0.99
			av.: 0.15	2.9 × 10 ⁻⁴		

^a Experimental conditions: 1.0 mM MTO, pH 3.21 (H₃PO₄/KH₂PO₄ buffer), μ = 0.10 M at 25 °C. The f_A and f_B values were calculated with K₁ = 16.1 L mol⁻¹ and K₂ = 132 L mol⁻¹.

determined at pH 0 (see later). The peroxide-binding equilibria are not noticeably pH-dependent and this treatment should be fully reliable.

The possibility was considered that methane formation might accompany the decomposition of B:



Although this would yield stable products, we reject this alternative based on the results of GC analyses for methane. Only a trace of CH₄ could be detected from a reaction between MTO (1.0 mM) and H₂O₂ (0.8 M) at pH 3.21. It amounted to only 2.2(±0.3)% of the amount of O₂ formed under these conditions, after calibration

of the GC with pure methane from the decomposition of MTO in NaOH solutions (see later).

Catalyst decomposition–pH profile. The kinetic dependence of the rate of decomposition on $[\text{H}_3\text{O}^+]$ was investigated with $[\text{Re}]_{\text{T}} = 0.10$ mM and at $[\text{H}_2\text{O}_2] = 2.00$ mM to maximize the accuracy. At this concentration f_{A} reduces to $f_{\text{A}} = K_1[\text{H}_2\text{O}_2]$, and k_{ψ} to $k_{\text{A}}[\text{OH}^-]K_1[\text{H}_2\text{O}_2]$ or to $(k_{\text{MTO}}K_{\text{a}}^{\text{H}_2\text{O}_2}/K_{\text{w}})[\text{OH}^-][\text{H}_2\text{O}_2]$ (refer to eq 7, 8, and 16). For each of 15 experiments a constant pH was maintained using HClO_4 (pH < 3), or one of a series of buffers, $\text{H}_3\text{PO}_4/\text{KH}_2\text{PO}_4$ (pH 2.9-3.8), HOAc/NaOAc (pH 3.8-5.8), or $\text{KH}_2\text{PO}_4/\text{K}_2\text{HPO}_4$ (pH 5.8-6.8). A constant ionic strength of 0.050M was maintained with lithium perchlorate.

The pH profile ($\log k_{\psi}$ versus pH), shown in Figure 5, is linear with a slope of 0.95 ± 0.01 . The inset shows the fitting of k_{ψ} directly to the expression $k_{\psi} = k'/[\text{H}_3\text{O}^+]$. The value of k' is $(9.76 \pm 0.06) \times 10^{-7}$ mol L⁻¹ s⁻¹, and therefore $k_{\text{A}} = 3.05 \times 10^9$ L mol⁻¹ s⁻¹ and $k_{\text{MTO}} = 2.03 \times 10^8$ L mol⁻¹ s⁻¹ at $\mu = 0.050$ M. For now, we simply take this to be the basis on which the decomposition of the catalyst in Scheme 1 is written with a direct dependence upon $[\text{OH}^-]$. The molecular basis for this chemistry will be presented in the Discussion.

The pH profile for the decomposition of B is harder to define with certainty, since so little decomposition leads to oxygen. The conclusion we have reached is that B probably reacts with a first-order dependence on $[\text{OH}^-]$, just like A and MTO do. Rearrangement of eq 15, after substitution of the expressions for f_{A} and f_{B} , affords this relation between $[\text{O}_2]_{\infty}$ and $[\text{H}_2\text{O}_2]$:

$$[\text{O}_2]_{\infty} = \frac{k_{\text{B}}'}{[\text{OH}^-]} \times \frac{K_2[\text{Re}]_{\text{T}}[\text{H}_2\text{O}_2]}{k_{\text{A}}} \quad (18)$$

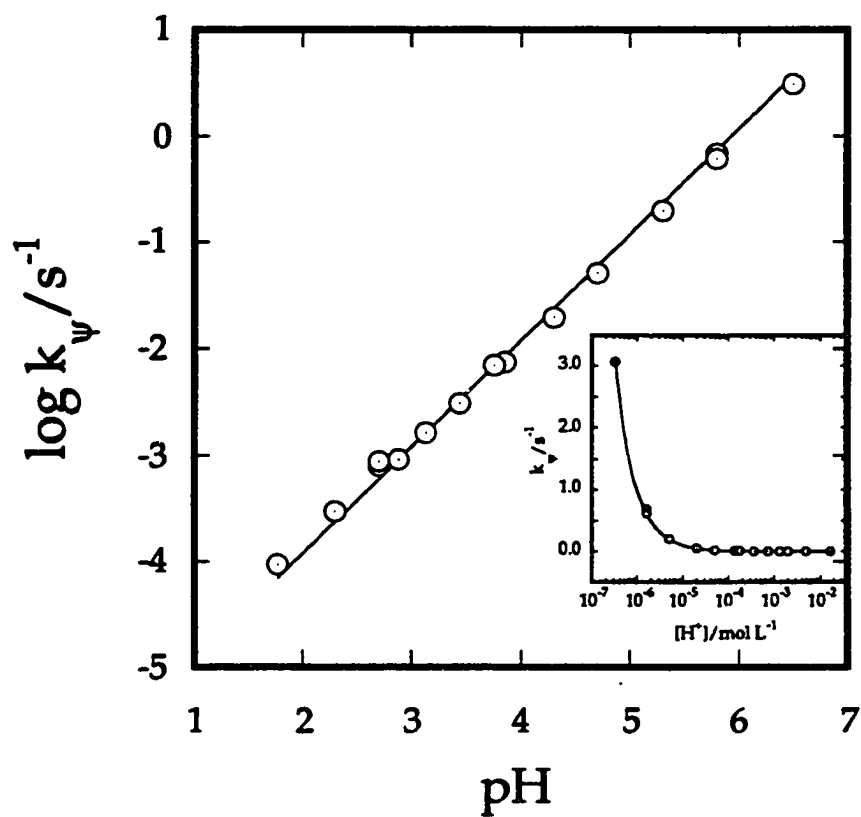
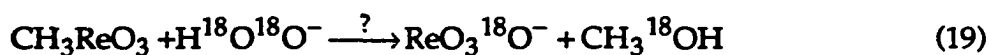


Figure 5. The plot of k_ψ for the irreversible decomposition reaction as a function of pH. Conditions: 0.10 mM MTO, 2.0 mM H_2O_2 at $\mu = 0.05$ M at 25.0 °C. Inset: Plot of k_ψ versus $[\text{H}^+]$ (log scale). The fit shown is that to $k_\psi = k'/[\text{H}^+]$.

The plot suggested by this equation, $[O_2]_{\infty}$ versus $K_2[Re]_T[H_2O_2]/k_A$, where each individual k_A value and not the average was taken, is shown in Figure 6 for data taken at two ionic strengths, 0.1 and 0.2 M. Each of the plots approximates a straight line, but the precision is evidently fairly low. Again, this reflects the fact that oxygen evolution is a quite minor pathway. At any rate, within the precision of the data, the values determined over the accessible pH interval (2.6–3.5) fall on a straight line, indicating that the slope is roughly pH-independent. For that to be the case, the denominator term in $[OH^-]$ must be canceled by a corresponding term in the numerator, or $k_B = k_B[OH^-]$. The values of k_B are $(3.0 \pm 0.2) \times 10^7$ and $(2.0 \pm 0.1) \times 10^7$ L mol⁻¹ s⁻¹, at $\mu = 0.10$ M and 0.20 M, respectively.

Labeling Studies. Since all the kinetic data presented thus far for the irreversible decomposition reaction could be rationalized by either the reaction of HO_2^- upon MTO or that of hydroxide upon A, we resorted to labeling experiments utilizing O-18 enriched hydrogen peroxide and water in an effort to distinguish between the two pathways. The reaction of A with hydroxide ions would result in the incorporation of two peroxide oxygens into the final perrhenate ions (eq 20); on the other hand, if MTO reacts with HO_2^- and a peroxide oxygen is used to form MeOH, then only one peroxide oxygen would remain on the final perrhenate (eq 19). It is worth noting here that the peroxide oxygens of A and B in this catalytic system neither exchange with the oxo ligands on the rhenium nor with water molecules.



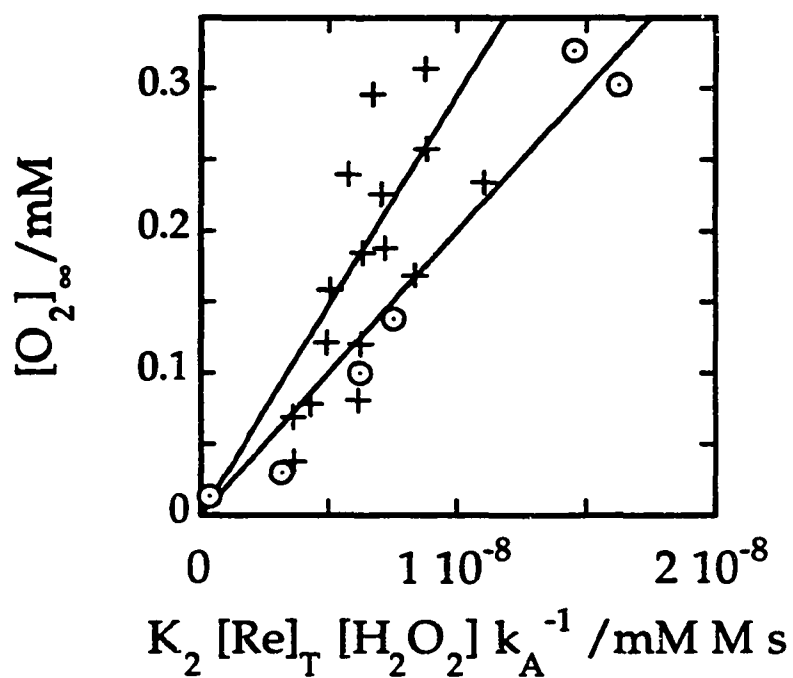


Figure 6. The plot of $[O_2]_\infty$ as a function of $(K_2[Re]_T[H_2O_2]) / k_A$ (see eq 18).
 Conditions: 1.0 mM MTO, 0.15-1.00 M H_2O_2 , pH = 2.6-3.5 (H_3PO_4/KH_2PO_4 buffer), 25.0 ± 0.2 °C, $\mu = 0.10$ M (+), 0.20 M (o).

The perrhenate ions from catalyst decomposition were isolated as the potassium salt. 15 mg (60 μmol) of MTO was dissolved in 0.60 mL of H_2O^{16} containing 6 mg (60 μmol) KHCO_3 . 120 μL of 1.5% $\text{H}_2^{18}\text{O}_2$ (90% ^{18}O enrichment) was added and allowed to stir for few minutes to ensure complete decomposition. The presence of bicarbonate is necessary to neutralize the produced perrhenic acid, since perrhenate oxygen exchange reaction is very rapid at acidic pHs.¹⁶

The solvent was removed under vacuum and the resulting KReO_4 collected. The KReO_4 was dissolved in methanol and the mass of the anion determined. A similar experiment was performed by labeling the MTO oxygens with H_2^{18}O and using unlabelled $\text{H}_2^{16}\text{O}_2$.

The major perrhenate species detected by electrospray mass spectrometry corresponded to the fully exchanged anion, that is $\text{Re}^{18}\text{O}_4^-$ in the case of using $\text{H}_2^{18}\text{O}/\text{H}_2^{16}\text{O}_2$ and $\text{Re}^{16}\text{O}_4^-$ when $\text{H}_2^{16}\text{O}/\text{H}_2^{18}\text{O}_2$ are used. Evidently, the oxygen-exchange between the produced ReO_4^- and water¹⁶ made these labeling experiments inconclusive with regards to resolving the true pathway of decomposition.

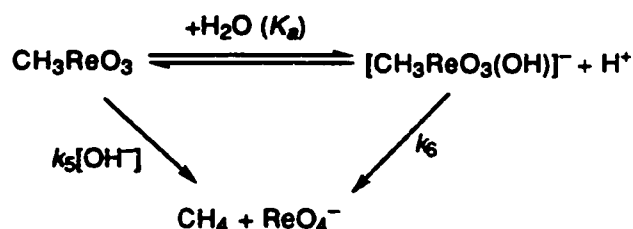
The decomposition of MTO itself. MTO is known to decompose to CH_4 and ReO_4^- in alkaline solutions, and was assumed to proceed via a hydroxide ion adduct.^{17,18} We monitored the rate of eq 21 by both ^1H NMR and UV-visible methods.



Addition of NaOH to 50 mM MTO in D_2O resulted in an immediate color change from clear to yellow, followed by gas evolution over a period of time. The NMR peak of MTO (δ 2.5 ppm) shifted to 1.9 ppm, and then disappeared after some hours. The UV-vis spectrum of 0.1 mM MTO changed immediately with

30 mM NaOH. The new yellow compound displays an absorption maximum at 340 nm (ϵ 1500 L mol⁻¹ cm⁻¹). This lends support to the existence of an intermediate, as presented in Scheme 2.

Scheme 2



The dependence of the experimental reaction rate upon $[\text{OH}^-]$ is shown in Figure 7. The experimental conditions were as follows: 0.20 mM MTO, 0.0050–0.70 M NaOH, and $\mu = 1.0$ M (LiClO_4) at 25.0 °C. The kinetic scheme gives the rate law

$$v = \frac{(k_5 K_w + k_6 K_a)[\text{OH}^-]}{K_w + K_a[\text{OH}^-]} \cdot [\text{Re}]_T \quad (22)$$

A nonlinear least squares fit gives $K_a = (1.2 \pm 0.2) \times 10^{-12}$ mol L⁻¹ and $(k_5 K_w + k_6 K_a) = 2.7 \times 10^{-16}$ mol L⁻¹ s⁻¹. The matter cannot be resolved further on the basis of kinetic data unless one assumes that only the k_5 path is important (giving $k_5 = (2.7 \pm 0.3) \times 10^{-2}$ L mol⁻¹ s⁻¹); or assuming the obverse, in which case $k_6 = (2.23 \pm 0.06) \times 10^{-4}$ s⁻¹. The value of K_a for MTO at 25 °C and $\mu = 1.0$ M was confirmed by a spectrophotometric titration of MTO and NaOH; measured absorbances at 360 and 390 nm yield an average K_a of 2.2×10^{-12} mol L⁻¹.

Equilibrium constants for peroxide coordination. The equilibrium constants for the formation of A and B in aqueous solution were determined at 25.0 °C. These are the values of K_1 and K_2 from Scheme 1. The solutions contained 1.0 M HClO_4 , 1.0 M LiClO_4 , 0.74 mM MTO and variable $[\text{H}_2\text{O}_2]$, 0.0071–0.22 M. The spectra of 15 such solutions were recorded in the range 280–420 nm

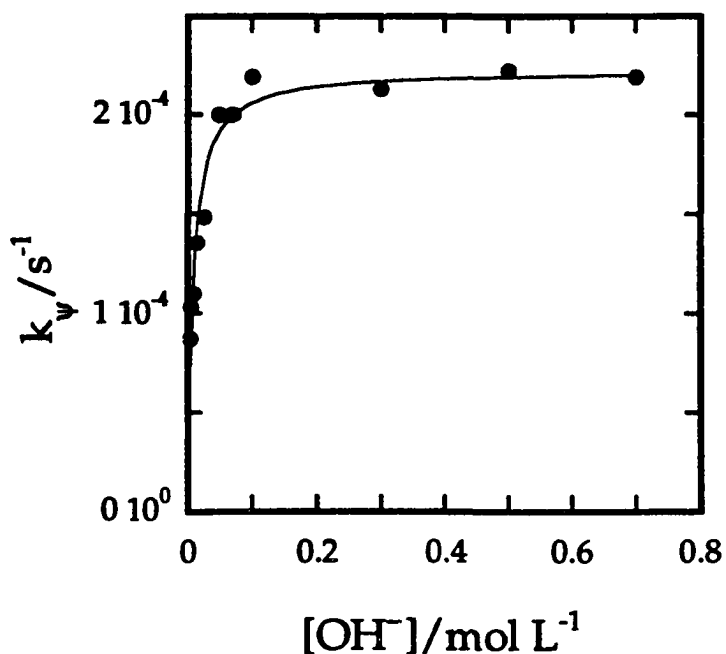


Figure 7. The plot of the pseudo-first-order rate constants in alkaline solution for the decomposition of MTO to CH_4 and ReO_4^- . Conditions: 0.20 mM MTO, 0.0050–0.70 M OH^- , $\mu = 1.0$ M (LiClO_4) at 25.0 °C.

at intervals of 0.2 nm. The absorbance readings were fit globally using the program SPECFIT.¹⁹ The known spectra of MTO and H_2O_2 were entered and held constant. This fitting gives $K_1 = 16.1 \pm 0.2$ L mol⁻¹ and $K_2 = 132 \pm 2$ L mol⁻¹. The calculated spectra of A and B are shown in Figure 8.

Timed repetitive scan spectra were also taken at a fixed $[\text{H}_2\text{O}_2] = 10$ mM and $[\text{MTO}] = 1.0$ mM in THF. The overlaid spectra, Figure 9, feature an isosbestic point at 290 nm, indicating that no intermediates attain an appreciable concentration. In THF, A has a maximum at 305 nm (ϵ 730 L mol⁻¹ cm⁻¹

compared to a literature value¹⁵ of ϵ 600 L mol⁻¹ cm⁻¹). Addition of 0.47 M H₂O increased the rate at which A formed. The decomposition of the catalyst is also accelerated by water.

Repetitive scan spectra for the formation of B from MTO via A show the expected two stages, Figure 10. The concentrations were [MTO] = 1.0 mM and [H₂O₂] = 0.20 M. Following formation of A, the repetitive spectra show an isosbestic point for A and B at 340 nm (ϵ 900 L mol⁻¹ cm⁻¹). B itself has a maximum at 360 nm (ϵ 1.10 × 10³ L mol⁻¹ cm⁻¹). This is close to values we have found in earlier work,²⁰ but considerably larger than one literature value¹⁵ of 700 L mol⁻¹ cm⁻¹.

Discussion

The results on catalyst deactivation can be interpreted by means of a relatively small number of chemical reactions. They are summarized in Scheme 1, which presents all of the reactions that are of importance in the MTO–H₂O₂ system. The essence of the reaction scheme is this: MTO and H₂O₂ form two species that contain rhenium and peroxide in 1:1 and 1:2 ratios, A and B. Under the conditions used, the two peroxide-binding reactions can be treated as rapid prior equilibria, even though in catalytic systems they are kinetic steps.

The irreversible destruction of the catalyst to give methanol and perrhenate proceeds via compound A or an analogous rhenium hydroperoxide complex, [CH₃Re(η^1 -OOH)(O₃)]⁻. Compound B, on the other hand, releases molecular oxygen, thereby restoring MTO, the parent form of the catalyst. That is to say, decomposition of B does not really destroy the catalyst, although it does decompose a corresponding amount of peroxide.

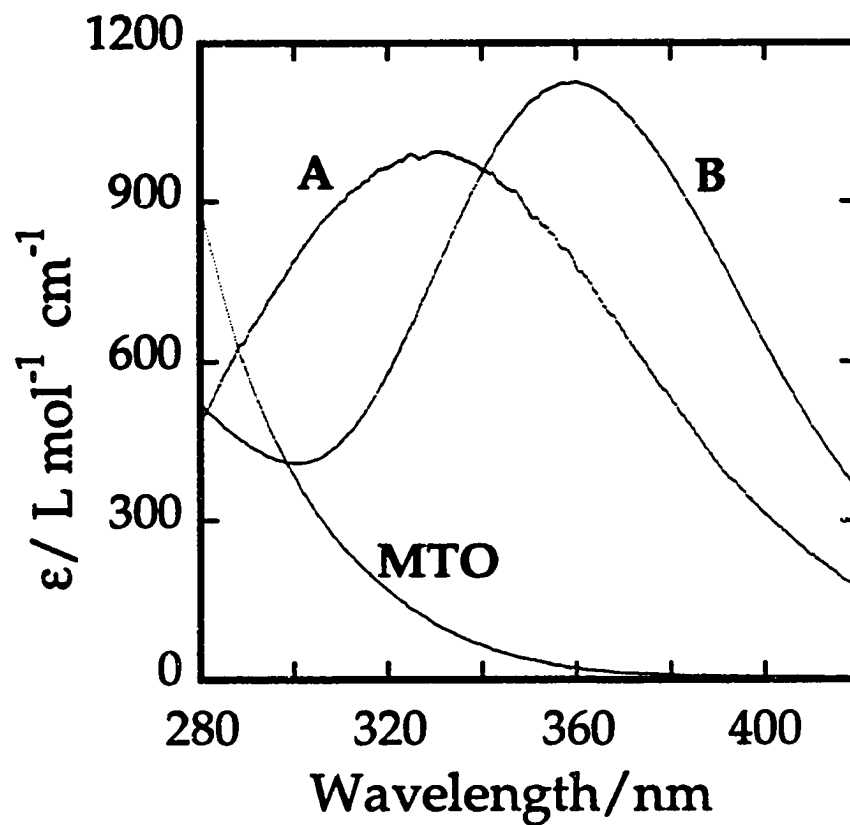


Figure 8. The spectra of A and B obtained from SPECFIT fitting are shown alongside that of MTO in the range 280–420 nm.

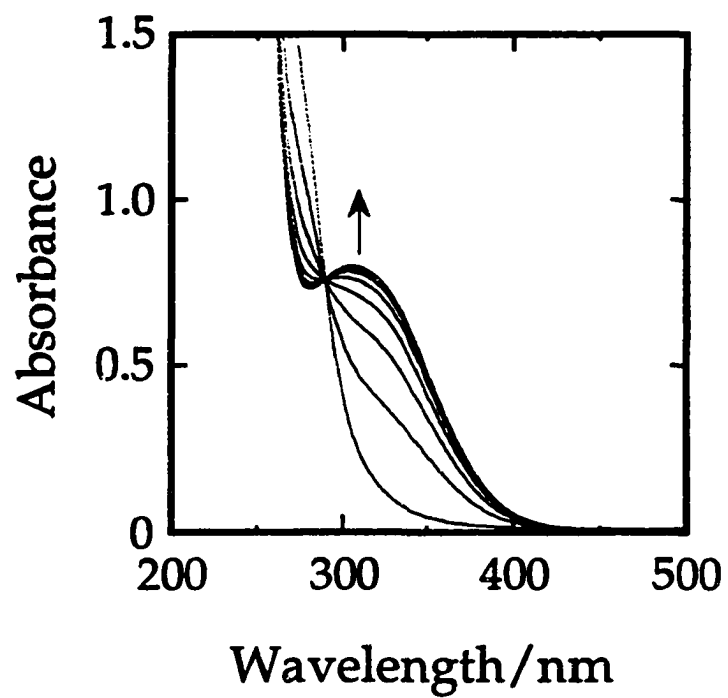


Figure 9. Repetitive spectral changes at 60 min. intervals for the formation of **A** from 1.0 mM MTO and 0.010 M H_2O_2 in THF at 25.0 ± 0.2 °C.

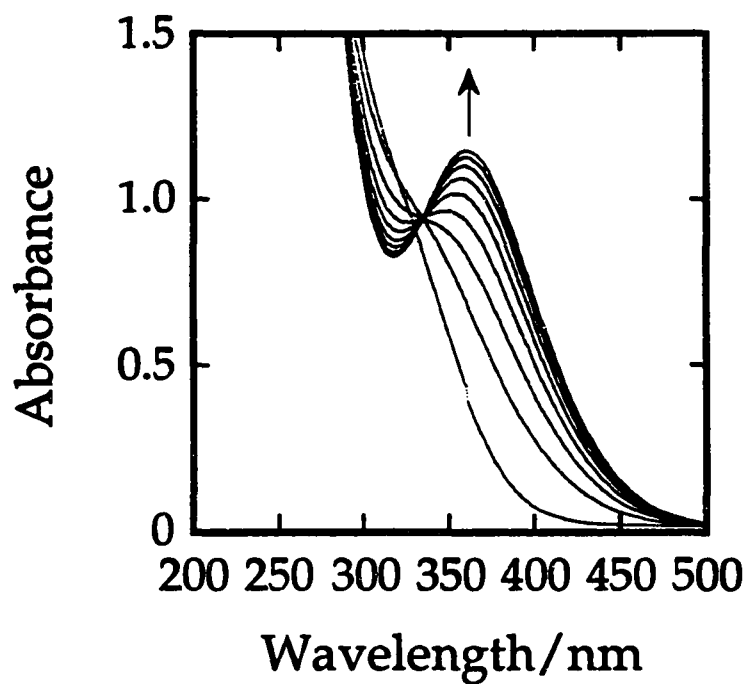
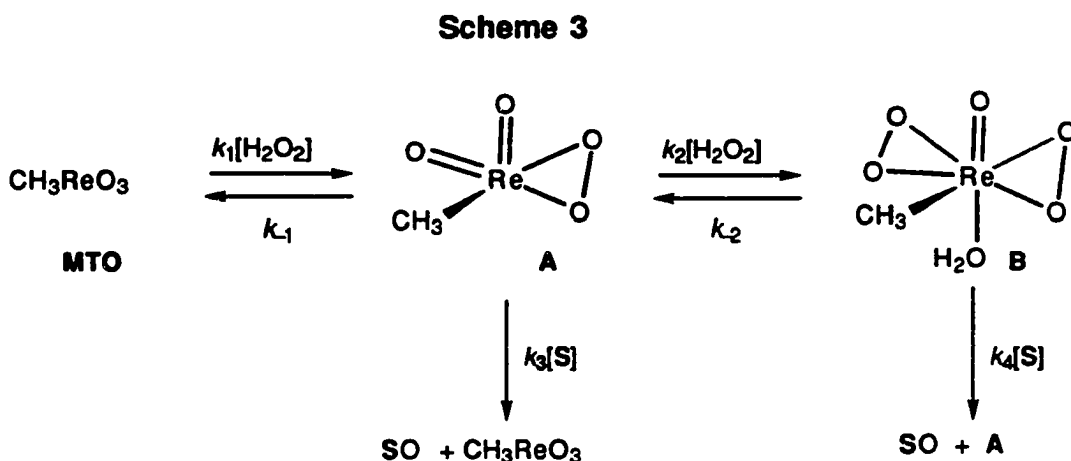


Figure 10. Repetitive spectral changes at 5 min. intervals for the formation of **B** in THF from MTO *via* **A**. The first spectrum does not coincide with the isosbestic point, since the MTO to **A** conversion is still in progress. Conditions: [MTO] = 1.0 mM, [H₂O₂] = 0.20 M, and 25.0 ± 0.2 °C.

Neglected reactions. The reactions shown in Scheme 1 suffice to account for all the observations. Other chemical equations can be written; at face value, they might appear to be as plausible as the ones given, yet they do not participate. For example, the answer is "no" to the question of whether B, like A, will release methanol, and "no" again to the question of whether A, like B, will release oxygen. Put more precisely, the two alternatives can be demonstrated to be of negligible importance compared to the ones found. The finding that A and B undergo distinctive reactions is intriguing, because, when it comes to their role in catalysis, A and B act as virtual stand-ins for one another. We have shown that, with few exceptions,^{5,21} each peroxorhenium compound transfers a peroxidic oxygen to a given substrate with comparable kinetic efficiency. To illustrate this point, refer to Scheme 3, which gives the essence of the catalytic cycle.



Indeed, one of the messages we have presented previously is that the rate constants for the oxygen-transfer reactions of the two intermediates A and B are nearly the same. Here, for example, are values of k_3 and k_4 for a few typical oxygen-accepting substrates that suffice to make the point:^{2-4,6}

Substrate	$k_3/\text{L mol}^{-1} \text{s}^{-1}$	$k_4/\text{L mol}^{-1} \text{s}^{-1}$
$\text{C}_6\text{H}_5\text{SCH}_3$	2.65×10^3	0.97×10^3
Br^-	3.5×10^2	1.9×10^2
PPh_3	7.3×10^5	21.6×10^5
$\text{PhCH}=\text{CMe}_2$	1.00	0.70

Clearly, **A** and **B** exhibit comparable catalytic reactivities for a given substrate. That is not to say, of course, that a comparable concentration of product is produced from **A** and from **B** in any of these transformations. The contribution of each catalytic transfer step is defined not only by k_3 versus k_4 , but also by the concentration of hydrogen peroxide and by the rate constants that characterize the formation of the active intermediates (k_1 , k_{-1} , k_2 , and k_{-2}). A combination of these quantities determines the proportion of each peroxorhenium species present in the system and its conversion to product. The extent of the two O-atom transfer processes is determined by the peroxide concentration and all six rate constants, not simply k_3 and k_4 . Moreover, the thermodynamic binding constants K_1 and K_2 are of less relevance than the constituent rate constants, since the peroxide binding steps are not instantaneous under catalytic conditions, but are kinetically competitive.

One means of gaining insight into the decompositions, where **A** and **B** behave so differently, is to examine what would happen were the role of each to be interchanged in the respective processes. For example, were **B** to release methanol upon attack by hydroxide ion, the chemical equation would be



This reaction offers an unappealing prospect, however, in contrast with the corresponding one for **A** in Scheme 1, since the trioxo(peroxo)rhenate(VII) ion is not a known or stable species. Indeed, we have found that mixtures of ReO_4^- and H_2O_2 show no indication of peroxo-complex formation, whereas the corresponding combination of CH_3ReO_3 and H_2O_2 readily results in the formation of **A**. So our contention is that reaction 23 is not important because it would give rise to a thermodynamically unfavorable product.

For a similar reason, we rationalize the lack of oxygen evolution from **A**:



This event, were it to occur, would produce a rhenium(V) product. While this substance is known, oxygen atom abstraction from MTO takes a species with a very avid affinity for oxygen (e. g. PPh_3 and H_3PO_2);^{22,23} in such cases CH_3ReO_2 can be formed slowly.²³⁻²⁵ It seems unlikely, however, that conversion of peroxide to dioxygen can bring about this transformation. As to the parallel event that **B** undergoes (refer to the k_B step in Scheme 1), the bis(peroxo) species upon oxygen release generates a stable rhenium(VII) product, MTO itself. That is to say, one peroxide anion of **B** is released as elemental oxygen and the other is converted into a pair of O^{2-} ions that are automatically incorporated into the newly-formed MTO. This is how the more energetic Re(V) is avoided when **B** evolves oxygen. If **A**, however, were to disproportionate H_2O_2 like **B** does, it would necessarily require a bimolecular pathway, which would be unlikely considering the low concentrations of **A** at equilibrium.

The process for oxygen release has just been described in somewhat simplistic terms, with the goal in mind of rationalizing the absence of two decomposition pathways. In fact, there are some very fundamental matters that need to be addressed about the reactions that do take place. The timing of the

events for oxygen release from **B** and the chemical mechanism by which MTO is released is one of these. The balance of the discussion focuses on these events and on plausible mechanisms by which methanol and perrhenate are released.

Oxygen evolution from B. The evolution of oxygen upon decomposition of **B** to MTO is one of the reactions shown in Scheme 1. In practice the yield of O₂ is rather low compared to [B]₀, the reason being the relative values of k'_A (k'_{MTO}) and k'_B. The decomposition of **B** occurs relatively slowly. The electrochemical determination of O₂ buildup showed that [O₂]_∞ increased linearly with [H₂O₂]₀. This substantiates that **B** is the source of oxygen, as given by the kinetic scheme and eq 15 once the peroxide dependence of f_A (or f_{MTO}) is taken into account. The experimental rate constants obtained for O₂ release at various concentrations of [H₂O₂] decreased hyperbolically as [H₂O₂] increased; see Figure 4. This agrees with eq 15 and with the spectrophotometric kinetic measurements, Figure 3.

Precedents for oxygen release from η²-peroxides are not very common. A bis(η²-peroxo)Mo^{VI}(porphyrin) is photochemically converted to oxygen and the cis-(dioxo)Mo^{VI}(porphyrin).⁹ Although the mechanism has not been established, an intermediate Mo^{IV}-peroxo complex has been proposed.²⁶ This is analogous to the mode of decomposition by which we propose **B** reverts to the parent MTO.

On the other hand, the rhenium(V) peroxo complex (HBpz₃)Re(O)(O₂) decomposes to (HBpz₃)ReO₃ bimolecularly, rather than losing O₂ directly.¹⁰ The authors attribute the failure of dioxygen release from a single site, despite a substantial driving force, to a symmetry restriction against the interconversion of a d²-metal peroxide to a d⁰-metal dioxo species. If this symmetry-derived restriction is general to all d² complexes, the decomposition of **B** to MTO and O₂

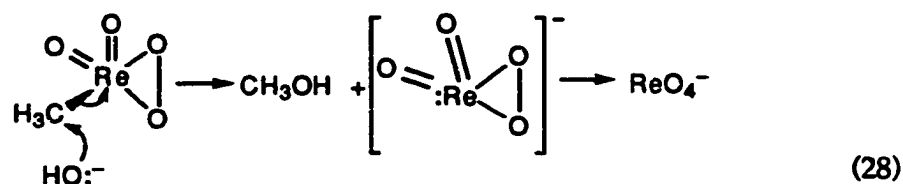
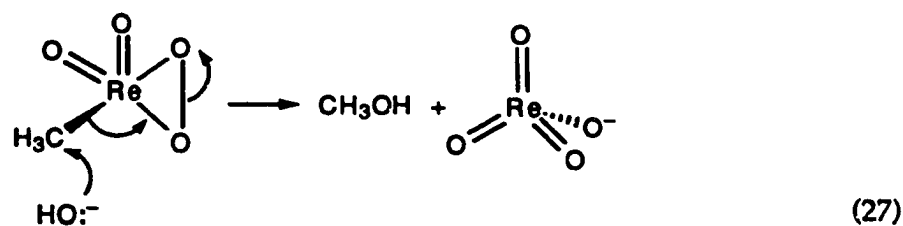
would proceed via a concerted mechanism rather than a step-wise transformation that involves a Re(V) peroxo intermediate.

Methanol formation. Since the two possible pathways for the production of methanol (Scheme 1) cannot be resolved further on the basis of kinetics and the labeling studies were inconclusive due to the oxygen-exchange of perrhenate, we will discuss the molecular mechanisms by which each pathway may proceed. The decomposition of **A** may occur by the direct attack of OH⁻ on the methyl group of **A**, in effect, an S_N2 displacement, eq 27 or 28. Alternatively, a species with OH⁻ coordinated to rhenium may be responsible, which is represented by this sequence of steps:

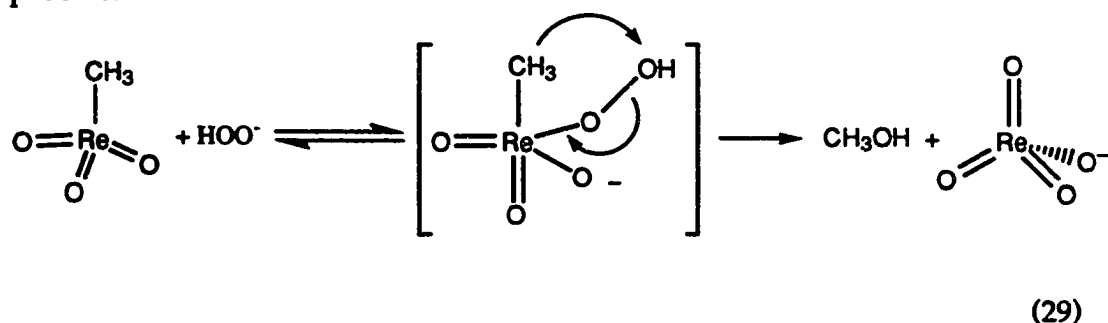


with $k_A = k_{25}K_a^A / K_w$, which affords $k_{25}K_a^A = 6.2 \times 10^{-5} \text{ mol L}^{-1} \text{ s}^{-1}$. If we approximate K_a^A as equal to the K_a^{MTO} ($1.2 \times 10^{-12} \text{ mol L}^{-1}$, see eq 21), then $k_{25} = 5 \times 10^7 \text{ s}^{-1}$. This is not an implausible formulation, save for the fact that eq 26 does not seem to represent particularly well the molecular changes that might lead to methanol.

Returning to the first formulation, in which OH⁻ attacks nucleophilically at the methyl group, we envisage that this step either leads directly to the products, in which case the requisite electronic rearrangement of the η²-peroxide group is presumed to be relatively rapid, eq 27, or we invoke a sequential process in which a first-formed peroxorhenium(V) intermediate yields the final products after internal electron shifts, eq 28.



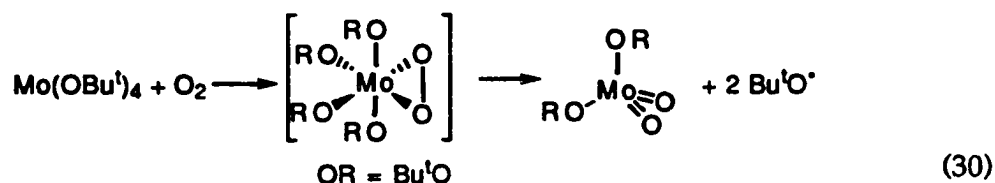
The alternative route for production of methanol and perrhenate ions involves the attack of HO_2^- on MTO. This proceeds most likely via a rhenium hydroperoxo complex that is analogous to compound A, eq 29. Following its coordination to the rhenium(VII) center, the hydroperoxide ligand becomes electrophilically activated and more susceptible to attack by the methyl group bound to rhenium. The outcome of this rearrangement (as illustrated by eq 29) is the elimination of methanol leaving behind perrhenate as the final rhenium product.



Although neither kinetics nor labeling experiments were successful in discriminating between mechanisms 27-28 on the one hand and 29 on the other, a comment on which pathway would be more chemically sound based on our present knowledge is in order at this stage. Since k_A and k_{MTO} are close to the diffusion limit and the hydroperoxide anion is notably more nucleophilic than

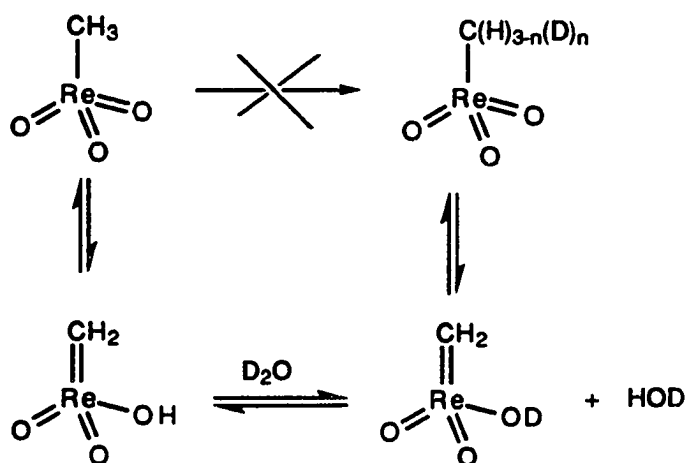
hydroxide,²⁷ one expects to see diffusion-controlled peroxide-induced rather than hydroxide-induced decomposition. Therefore, in light of these considerations and the fact that dilute MTO solutions without H₂O₂ persist for days in aqueous solution, we are inclined to favor the mechanism shown in eq 29 as the route by which the catalyst is irreversibly deactivated.

A precedent relating to the decomposition of MTO is the formation of (Bu^tO)₂Mo(O)₂ from the reaction of Mo(OBu^t)₄ with molecular oxygen in dilute solutions.²⁸ In concentrated solution, however, the product is (Bu^tO)₄MoO, from bimolecular oxygen activation. The dilute reaction appears to be unimolecular, as in eq 30.

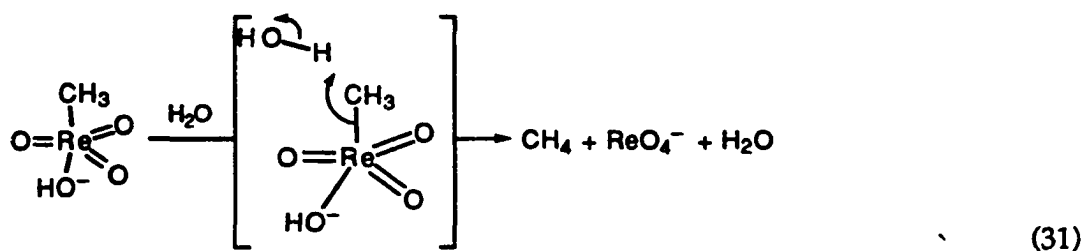


Any mechanism that would involve deprotonation of the methyl group is disregarded because deuterium incorporation into MTO does not occur in D₂O, Scheme 4. The lack of hydrogen exchange for deuterium in D₂O deems the carbene tautomer of MTO insignificant.

Scheme 4



Methane formation. The decomposition of (peroxide-free) CH_3ReO_3 in alkaline solutions produces methane quantitatively. The kinetic and spectroscopic data show that an intermediate is "instantly" formed between MTO and hydroxide ions. This is reasonably a coordination compound, analogous to the adducts formed between MTO and chloride ions and nitrogen bases.²⁹ The short sequence of subsequent events that leads to methane formation can easily be depicted, as in eq 31.



Formation of A and B. The equilibrium constants K_1 and K_2 were previously determined from absorbance readings at selected wavelengths.^{6,20} The re-determinations given here were based on a global fitting routine¹⁹ that in effect uses the continuous spectra. This treatment resulted not only in improved values and statistics for the equilibrium constants, but it was also able to resolve the spectrum of A. Except at the lowest peroxide concentrations, the equilibrium situation is such that A in water is present at relatively low levels compared to MTO and B. The spectrum of A could be obtained independently in THF, where the formation reactions for A and B are much slower than in water. Although the spectrum of A in water from SPECFIT fitting does not match exactly with that measured in THF, they are in reasonable agreement considering the procedures and fitting errors.

We contend that the monoperoxorhenium compound, **A**, was incorrectly identified in the NMR spectrum previously.¹⁵ It seems likely to us that the reported chemical shift can be attributed to methanol, a decomposition product.

The rates at which methanol is produced and **B** decomposed are very sensitive to the solvent and pH. In both aqueous and semi-aqueous environments, these compounds are stabilized by acid. In neat organic solvents the peroxides form more slowly than in water, and their temporal stabilities are greatly enhanced. For example, at pH 2 in water, the experimental rate constant is $6.2 \times 10^{-3} \text{ s}^{-1}$ whereas in THF it is $3.1 \times 10^{-4} \text{ s}^{-1}$. As a result **B** is stable in the presence of excess peroxide for days in organic solvents, whereas 1 M acid is required to stabilize **B** comparably in water.

Summary. The important reactions are shown together in Scheme 5, and the rate and equilibrium constants are given in Table 2.

Scheme 5

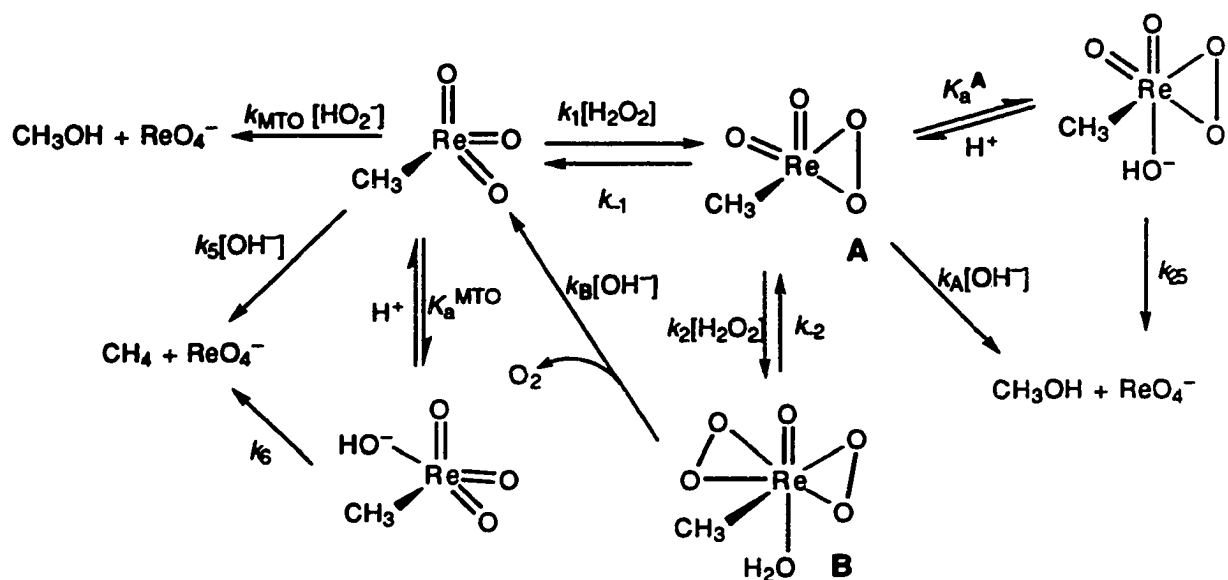


Table 2. Summary of equilibrium and rate constants at 25 °C

Reaction	Symbol	Value
$\text{CH}_3\text{ReO}_3 + \text{H}_2\text{O}_2 = \text{CH}_3\text{Re}(\text{O})_2(\text{O}_2)(\text{A}) + \text{H}_2\text{O}$	K_1	$16.1 \pm 0.2 \text{ L mol}^{-1}$
$\text{A} + \text{H}_2\text{O}_2 = \text{CH}_3\text{Re}(\text{O})(\text{O}_2)_2(\text{OH}_2)(\text{B})$	K_2	$132 \pm 2 \text{ L mol}^{-1}$
$\text{CH}_3\text{ReO}_3 + \text{H}_2\text{O} = \text{CH}_3\text{ReO}_3(\text{OH})^- + \text{H}^+$	K_a^{MTO}	$1.2 \pm 0.2 \times 10^{-12} \text{ mol L}^{-1}$
$\text{CH}_3\text{ReO}_3 + \text{OH}^- \rightarrow \text{ReO}_4^- + \text{CH}_4^{\text{a}}$	k_5	$2.7 \pm 0.3 \times 10^{-2} \text{ L mol}^{-1} \text{ s}^{-1}$
$\text{CH}_3\text{ReO}_3(\text{OH})^- \rightarrow \text{ReO}_4^- + \text{CH}_4^{\text{a}}$	k_6	$2.2 \pm 0.1 \times 10^{-4} \text{ s}^{-1}$
$\text{A} + \text{OH}^- \rightarrow \text{CH}_3\text{OH} + \text{ReO}_4^{-\text{b}}$	k_A	$6.2 \pm 0.2 \times 10^9 \text{ L mol}^{-1} \text{ s}^{-1}$
$\text{CH}_3\text{ReO}_3 + \text{HO}_2^- \rightarrow \text{ReO}_4^- + \text{CH}_3\text{OH}^{\text{b}}$	k_{MTO}	$4.1 \pm 0.1 \times 10^8 \text{ L mol}^{-1} \text{ s}^{-1}$
$\text{B} + \text{OH}^- \rightarrow \text{CH}_3\text{ReO}_3 + \text{O}_2^{\text{c}} + \text{OH}^-$	k_B	$2 \times 10^7 \text{ L mol}^{-1} \text{ s}^{-1}$

^a The reaction represented by k_5 is written in an alternative form represented by k_6 . ^b $\mu = 0.010 \text{ M}$ and $25 \text{ }^\circ\text{C}$. ^c $\text{pH } 3.21$, $\mu = 0.10 \text{ M}$ and $25 \text{ }^\circ\text{C}$.

Acknowledgment. This research was supported by the U. S. Department of Energy, Office of Basic Energy Sciences, Division of Chemical Sciences under contract W-7405-Eng-82. PJH is indebted to the administration and Board of Trustees of Northwestern College (Iowa) for their award of sabbatical leave. We are grateful to Kamel Harrata for the mass spectra determinations. JHE is grateful to S. N. Brown and J. E. Bercaw for helpful comments.

References

- (1) Herrmann, W. A.; Fischer, R. W.; Marz, D. W. *Angew. Chem., Int. Ed. Engl.* **1991**, *30*, 1638.
- (2) Al-Ajlouni, A.; Espenson, J. H. *J. Am. Chem. Soc.* **1995**, *117*, 9243.
- (3) Abu-Omar, M. M.; Espenson, J. H. *J. Am. Chem. Soc.* **1995**, *117*, 272.
- (4) Vassell, K. A.; Espenson, J. H. *Inorg. Chem.* **1994**, *33*, 5491.
- (5) Huston, P.; Espenson, J. H.; Bakac, A. *Inorg. Chem.* **1993**, *32*, 4517.
- (6) Espenson, J. H.; Pestovsky, O.; Huston, P.; Staudt, S. *J. Am. Chem. Soc.* **1994**, *116*, 2869.
- (7) Zhu, Z.; Espenson, J. H. *J. Org. Chem.* **1995**, *60*, 1326.
- (8) Herrmann, W. A.; Fischer, R. W.; Rauch, M. U.; Scherer, W. *J. Mol. Catal.* **1994**, *86*, 243.
- (9) Ledon, H.; Bonnet, M.; Lallemand, J.-Y. *J. Chem. Soc., Chem. Comm.* **1979**, 702.
- (10) Brown, S. N.; Mayer, J. M. *Inorg. Chem.* **1992**, *31*, 4091.
- (11) Herrmann, W. A.; Kühn, F. E.; Fischer, R. W.; Thiel, W. R.; Ramao, C. C. *Inorg. Chem.* **1992**, *31*, 4431.
- (12) Kunkely, H.; Turk, T.; Teixeira, C.; Bellefon, C. d. M. d.; Herrmann, W. A.; Volger., A. *Organometallics* **1991**, *10*, 2090.
- (13) Gordon, A. J.; Ford, R. A. *The Chemist's Companion*; Wiley: 1972.
- (14) Fogg, P. C. T.; Gerrard, W. *Solubility of Gases in Liquids*; Wiley: New York, 1991, pp 293.
- (15) Herrmann, W. A.; Fischer, R. W.; Scherer, W.; Rauch, M. H. *Angew. Chem., Int. Ed. Engl.* **1993**, *32*, 1157.
- (16) Murmann, R. K. *J. Phys. Chem.* **1967**, *71*, 974.
- (17) Herrmann, W. A. *Angew. Chem., Int. Ed. Engl.* **1988**, *27*, 1297.

- (18) Herrmann, W. A.; Kuchler, J. G.; Weichselbaumer, G.; Herdtweck, E.; Kiprof, P. *J Organomet. Chem.* **1989**, *372*, 351.
- (19) Binstead, R. A.; Zuberbühler, A. D. *Specfit*; Spectrum Software Associates, P.O. Box 4494, Chapel Hill, NC 27515: .
- (20) Yamazaki, S.; Espenson, J. H.; Huston, P. *Inorg. Chem.* **1993**, *32*, 4683.
- (21) One exception appears to be the cobalt thiolate complex $(en)_2Co(SCH_2CH_2NH_2)^{2+}$, for which $k_3 \gg k_4$.
- (22) Holm, R. H.; Donahue, J. P. *Polyhedron* **1993**, *12*, 571-589.
- (23) Abu-Omar, M. M.; Espenson, J. H. *Inorg. Chem.* **1995**, *34*, 6239.
- (24) Herrmann, W. A.; Roesky, P. W.; Wang, M.; Scherer, W. *Organometallics* **1994**, *13*, 4531.
- (25) Zhu, Z.; Espenson, J. H. *J. Mol. Catal.* **1995**, *103*, 87.
- (26) Ledon, H. J.; Bonnet, M.; Gillard, D. *J. Am. Chem. Soc.* **1981**, *103*, 6209.
- (27) Carey, F. A.; Sundberg, R. J. *Advanced Organic Chemistry*; Plenum Press: Part A, 3rd Ed.: New York, 1990, pp 268.
- (28) Chisholm, M. H.; Folting, K.; Huffman, J. C.; Kirkpatrick, C. C. *Inorg. Chem.* **1984**, *23*, 1021.
- (29) Herrmann, W. A.; Kuchler, J. G.; Kiprof, P.; Riede, J. *J. Organomet. Chem.* **1990**, *395*, 55.

CHAPTER IV

OXIDATIONS OF ER₃ (E = P, As, or Sb) BY HYDROGEN PEROXIDE:
METHYLRHENIUM TRIOXIDE AS CATALYST

A paper published in the *Journal of the American Chemical Society* *

Mahdi M. Abu-Omar and James H. Espenson

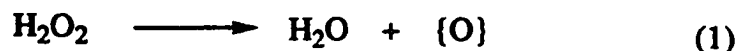
Abstract

Catalytic and noncatalytic conversions of tertiary phosphines to their oxides by hydrogen peroxide have been investigated. The catalyst is methylrhenium trioxide, CH₃ReO₃. The kinetics were investigated in acetonitrile–water (1:1 by volume) at 25 °C. Stepwise interactions between CH₃ReO₃ and H₂O₂ form CH₃Re(η²-O₂)(O)₂(OH₂), **A**, and CH₃Re(η²-O₂)₂(O)(OH₂), **B**. In CH₃CN–H₂O (1:1 v/v) the equilibrium constants are $K_1 = 13 \pm 2 \text{ L mol}^{-1}$ and $K_2 = 136 \pm 28 \text{ L mol}^{-1}$ at pH 1.0 and 25 °C. The forward and reverse rate constants for the formation of **A** in this medium are $k_1 = 32.5 \pm 0.3 \text{ L mol}^{-1} \text{ s}^{-1}$ and $k_{-1} = 3.0 \pm 0.2 \text{ s}^{-1}$. Systematic changes in the substituents on phosphorus were made to vary the nucleophilicity of the phosphine and its cone angles; the kinetic effects are discernible, although they lie in a narrow range. Triphenylarsine and triphenylstibine were also studied, and their rates are within a factor of two of that for PPh₃. The rhenium peroxides **A** and **B** show a small difference in reactivity. The bimolecular reactions between **A** and most of the phosphines have rate constants of the order $10^5 \text{ L mol}^{-1} \text{ s}^{-1}$. The kinetic data support a mechanism that allows nucleophilic attack of the substrate at the rhenium peroxides.

* Abu-Omar, M. M.; Espenson, J. H. *J. Am. Chem. Soc.* 1995, 117, 272.

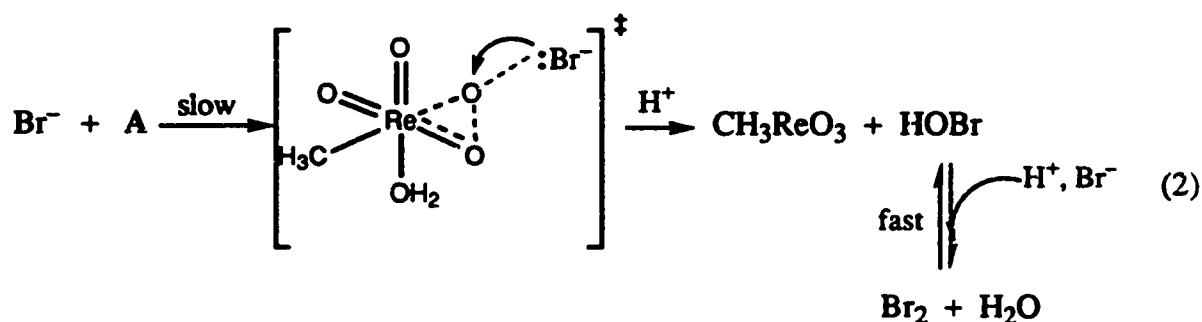
Introduction

More severe environmental constraints and regulations necessitate the reduction of waste by-products in chemical processes. Most widely used oxidants, such as permanganate and dichromate salts, suffer from high costs for waste and by-product clean up.¹ Hydrogen peroxide is an appealing substitute since its only reduction product is water, eq 1.



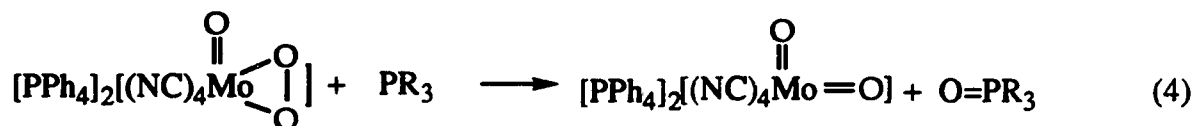
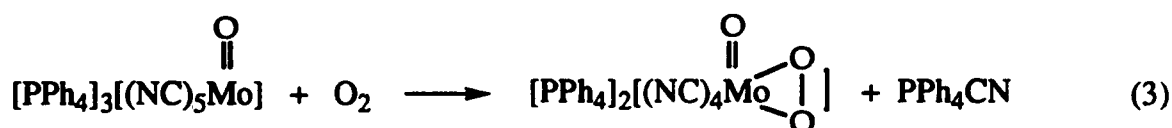
Since hydrogen peroxide reactions are often very slow, a catalyst is needed in most instances to activate H_2O_2 . Such a catalyst must be able to transfer a single oxygen atom to a substrate, and to accelerate the reaction to by-pass the free-radical side-reactions of peroxide. An organometallic oxide, CH_3ReO_3 , was reported to be an excellent catalyst for olefin epoxidation by hydrogen peroxide.² The $\text{CH}_3\text{ReO}_3\text{-H}_2\text{O}_2$ system generates a potent oxidant far more kinetically competent than H_2O_2 itself. This catalyst offers these advantages: it is soluble and stable in many solvents including water, stable towards high concentrations of acid (pH 0–3), air-stable, easily purified by sublimation and recrystallization, and employable either homogeneously or (after immobilization) heterogeneously.

We have recently reported³ the catalytic conversion of the thiolatocobalt complex $(\text{en})_2\text{CoSCH}_2\text{CH}_2\text{NH}_2^{2+}$ (here CoSR^{2+}) by $\text{CH}_3\text{ReO}_3\text{-H}_2\text{O}_2$ to the sulfenato complex (CoS(O)R^{2+}) , then much more slowly to the sulfinato complex $(\text{CoS(O)}_2\text{R}^{2+})$ by a mechanism in which the coordinated sulfur nucleophilically attacks the 1:1 η^2 -peroxo-rhenium compound. The catalytic oxidation of bromide ions was studied by following the formation of bromine and the concurrent catalytic disproportionation of hydrogen peroxide.⁴ The mechanism proposed for bromine formation involved a nucleophilic attack of Br^- on a peroxide oxygen, the result of which is oxygen transfer to substrate:



The investigation of the rhenium catalyst has now been extended to organic phosphines: Ar_3P mostly, and to triphenylarsine and triphenylstibine. We have determined the different reactivities of these substrates toward the catalytically active 1:1 adduct in the $\text{CH}_3\text{ReO}_3\text{-H}_2\text{O}_2$ system, and in two instances toward the 2:1 adduct as well. Systematic changes of the nucleophilicity and the cone angles of phosphorus were made.

The peroxide oxidation of PR_3 is catalyzed by Mo(VI) , an electrophilic, high-oxidation state complex, eq 3-4.^{5,6} It remains to be seen whether the mechanisms are similar.



Experimental Section

Materials. The solvent was a mixture of acetonitrile and water (1:1 v/v). HPLC grade acetonitrile (Fisher) was used, and high-purity water was obtained by passing laboratory distilled water through a Millipore-Q water purification system. Hydrogen peroxide solutions prepared by diluting 30% H_2O_2 were standardized daily by iodometric titration. Triphenylphosphine was recrystallized from diethyl

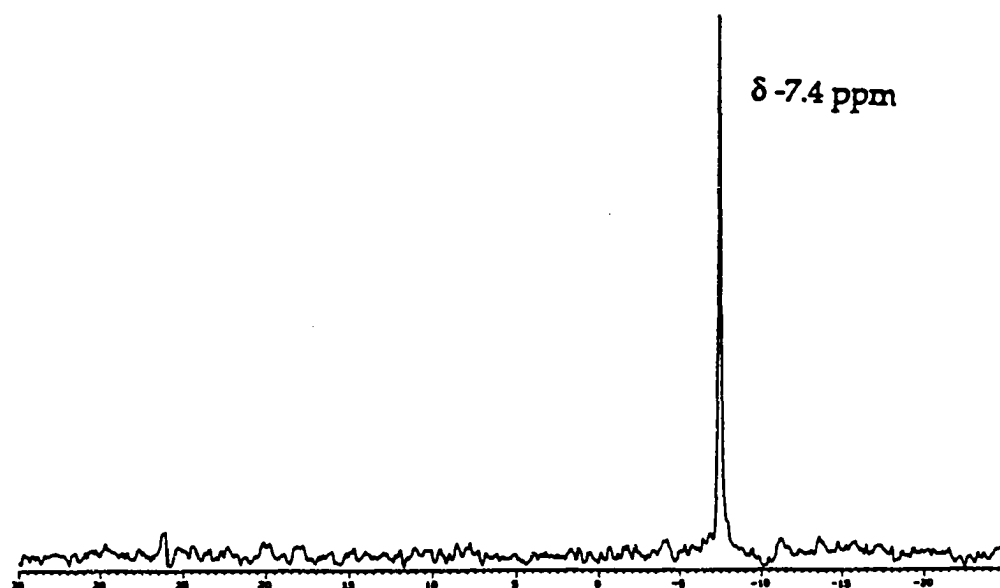
ether. The other phosphines were purchased commercially. 1,3,5-Triaza-7-phosphaadamantane (PTA), a gift from D. J. Darensbourg, was recrystallized from ethanol.⁷ The purity of the starting reagents was checked by ¹H and ³¹P NMR.

Methylrhenium trioxide⁸ was purified first by vacuum sublimation, followed by recrystallization from CH₂Cl₂-hexane, and a final sublimation. The purity of the final product was checked in CH₂Cl₂ solution spectroscopically. IR: 1000 (w), 967 cm⁻¹ (vs);⁹ ¹H NMR: δ 2.63 ppm in CDCl₃,¹⁰ and UV-vis in H₂O: 239 nm (ε 1900 L mol⁻¹ cm⁻¹), 270 nm (ε 1300 L mol⁻¹ cm⁻¹).¹¹ Stock solutions of CH₃ReO₃ were prepared in water, protected from light, stored at -5 °C, and used within ten days. The concentration was determined spectrophotometrically each day.

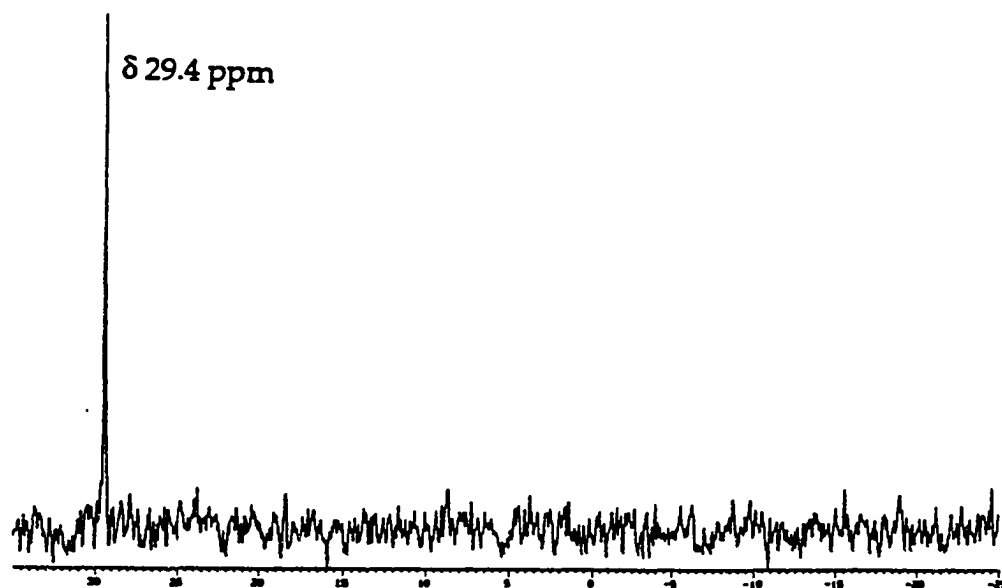
¹H NMR spectra were obtained with a Nicolet 300 MHz spectrometer, referenced to Me₄Si. ³¹P (¹H) NMR spectra were recorded on a Varian VXR-300 spectrometer, with neat H₃PO₄ as the external reference.

Product Analysis. The phosphine oxides were characterized by ¹H and ³¹P NMR. Figure 1 shows representative ³¹P{¹H} spectra of tris(*p*-chlorophenyl)phosphine and the oxide it produced. The near-UV spectra of the products showed the vibronic structure characteristic of phosphine oxides.¹² In addition to the ³¹P NMR identification, 1,3,5-triaza-7-phosphaadamantane oxide was characterized by mass spectrometry: EI m/z: 173 (M); CI m/z: 174 (M + 1), 191 (M + 1 + NH₃).

Kinetic Studies. The kinetic studies were performed at 25.0 ± 0.2 °C in 1:1 (v/v) CH₃CN-H₂O, containing 0.10 M perchloric acid unless specified otherwise. The acid was present since it greatly stabilizes the CH₃ReO₃-H₂O₂ mixture against decomposition in aqueous and semi-aqueous solutions. The air-sensitive substrates, methyldiphenylphosphine, tri-*p*-tolylphosphine, and tri-*o*-tolylphosphine, were studied under argon. Substrates that are not air-sensitive behaved the same whether



(a).



(b).

Figure 1. $^{31}\text{P}\{^1\text{H}\}$ NMR spectra of $(p\text{-ClC}_6\text{H}_4)_3\text{P}$ (a) with a catalytic amount of CH_3ReO_3 , and (b) after addition of H_2O_2 to give $(p\text{-ClC}_6\text{H}_4)\text{P}=\text{O}$.

protected by argon or not. Quartz cuvettes with different optical path lengths (0.1–10 cm) were used. The temperature was maintained by a thermostated water-filled cuvette holder. The reaction mixtures were incubated in the holder for at least 10 minutes to allow for temperature equilibration.

For kinetic studies by spectrophotometry, conventional (Shimadzu UV-2101PC) and stopped-flow (Sequential DX-17MV, Applied Photophysics Ltd.) instruments were used. The absorbance loss of the phosphine in the near-UV region (250–285 nm) was recorded. The product also absorbs in this region, but <0.2 times as strongly.¹² For example, the molar absorptivity of triphenylphosphine at 265 nm is $1.10 \times 10^4 \text{ L mol}^{-1} \text{ cm}^{-1}$ and that of triphenylphosphine oxide at 265 nm is $2.0 \times 10^3 \text{ L mol}^{-1} \text{ cm}^{-1}$.¹² Typical repetitive spectral scans for the reaction of tris(*p*-trifluoromethylphenyl)phosphine are displayed in Figure 2.

In many circumstances the most useful kinetic data were from the initial stage of the reaction, although the reactions were usually followed over the full time course. The initial reaction rates were calculated from the initial 5–7% of reaction. Under other conditions, however, the reactions followed first-order kinetics. The pseudo-first-order rate constant was evaluated by nonlinear fitting of the absorbance-time curves to a single-exponential decay equation, with $k_y = k_1[\text{Re}]_T$:

$$\text{Abs}_t = \text{Abs}_\infty + (\text{Abs}_0 - \text{Abs}_\infty)e^{-k_y t} \quad (5)$$

Equilibrium Studies. The adoption of 1:1 CH₃CN–H₂O as solvent required the remeasurement of the equilibrium constants for the formation of A and B, eq 6 and 7. They were determined from the absorbances in the range 360–420 nm over a wide range of hydrogen peroxide concentrations. The data were fit to eq 8:¹³

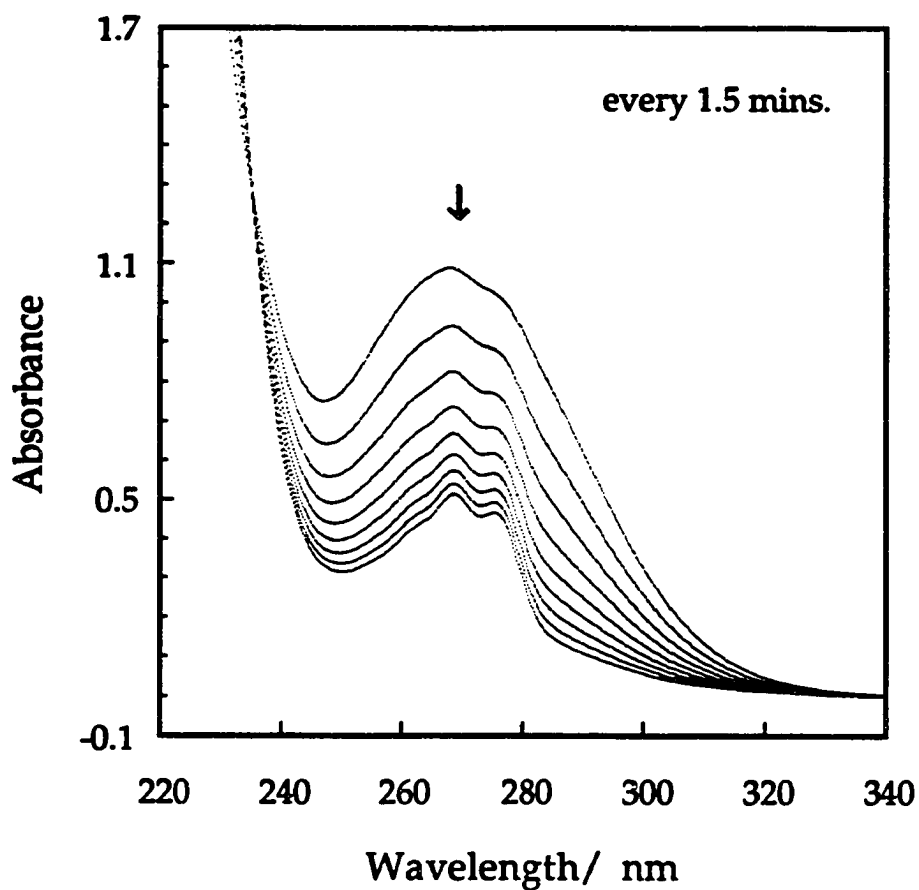
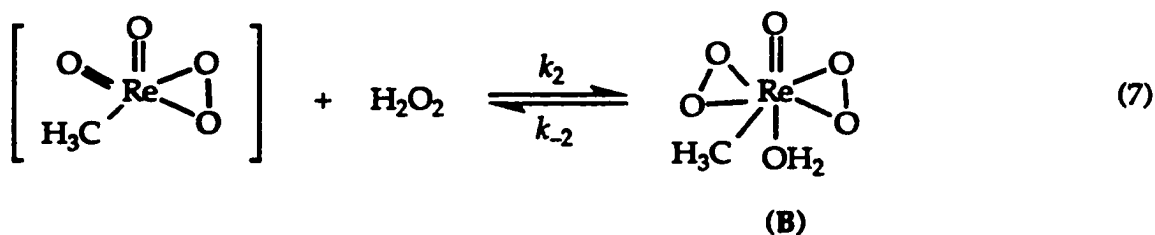
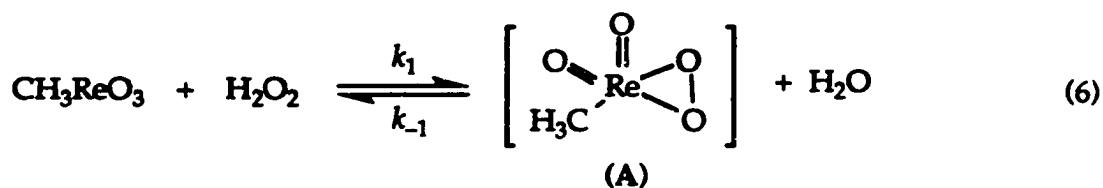


Figure 2. Repetitive spectral changes at 1.5 min intervals for the oxidation of 1.0×10^{-4} M (*p*-CF₃C₆H₄)₃P with 3.0×10^{-3} M H₂O₂ in the presence of 2.0×10^{-6} M MTO at pH 1.0 in 1:1 CH₃CN-H₂O.



$$\frac{(\text{Absorbance})_\lambda}{[\text{Re}]_T} = \frac{\varepsilon_A K_1 [\text{H}_2\text{O}_2] + \varepsilon_B K_1 K_2 [\text{H}_2\text{O}_2]^2}{1 + K_1 [\text{H}_2\text{O}_2] + K_1 K_2 [\text{H}_2\text{O}_2]^2} \quad (8)$$

Results

Equilibrium Constants. Compounds A and B are the mono-peroxo and di-peroxo derivatives of hydrogen peroxide and CH_3ReO_3 .¹³ The binding of water to the rhenium atom of B was shown in solution at -20°C by ^{17}O -NMR and in its diglyme adduct in the solid-state by X-ray diffraction.¹⁴ Proton transfer from the entering hydrogen peroxide to an oxo ligand has been suggested as the mechanism for the formation of A.¹⁵

The new spectrophotometric determinations of K_1 and K_2 were carried out in 1:1 v/v $\text{CH}_3\text{CN}-\text{H}_2\text{O}$ at 25°C ; the solutions contained 0.10 M perchloric acid, 1.00 mM MTO and 0.0010–0.70 M H_2O_2 . The spectra were recorded at wavelengths of 360, 380, 400, and 420 nm. A typical fit to eq 8 of the data at one of the wavelengths is shown in Figure 3. Absorbance data collected at the four different wavelengths were then fit globally to eq 8 with the program GraFit. The equilibrium constants are $K_1 = 13 \pm 2 \text{ L mol}^{-1}$ and $K_2 = 136 \pm 28 \text{ L mol}^{-1}$. The values obtained here are not much

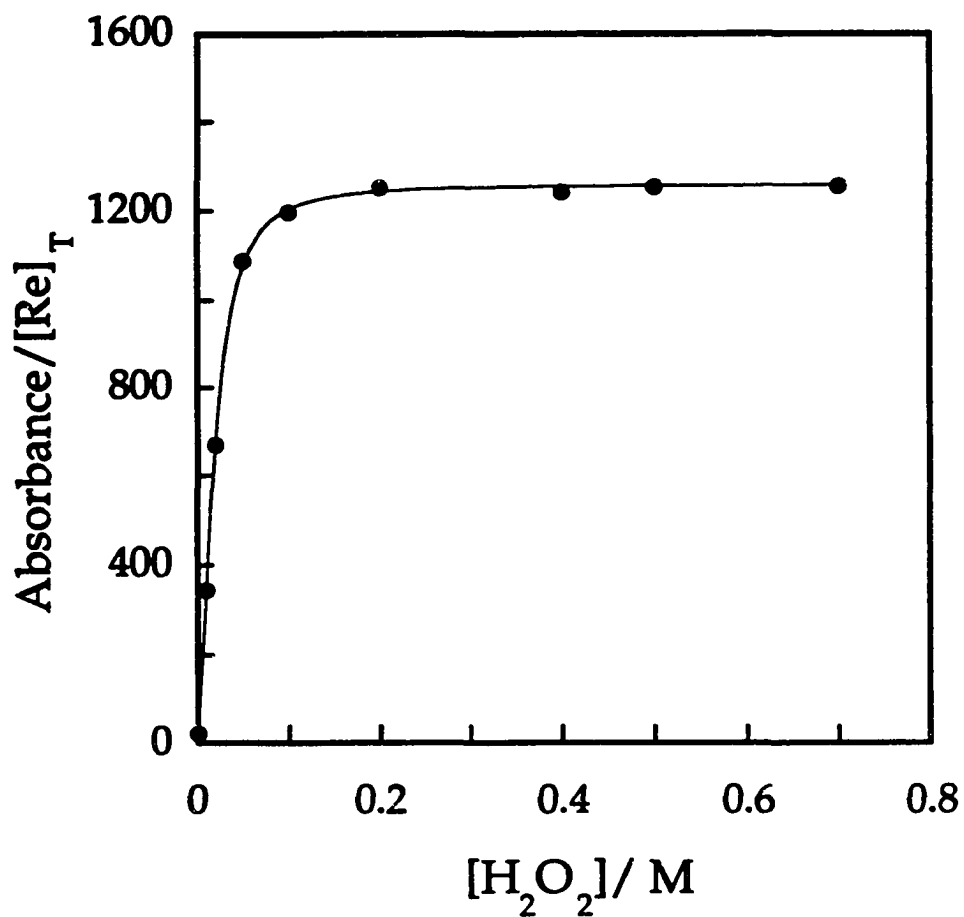


Figure 3. Plot of the absorbance at 360 nm of MTO- H_2O_2 solutions as a function of $[H_2O_2]$ at $[Re]_T = 1.0$ mM. The fit to eq 8 yields $K_1 = 14 \pm 2$ M^{-1} and $K_2 = 128 \pm 22$ M^{-1} . Conditions: pH 1.0 in 1:1 CH_3CN-H_2O at 25.0 ± 0.2 $^{\circ}C$.

different from those reported at $\mu = 0.10$ M in aqueous solution, $K_1 = 7.7$ L mol⁻¹ and $K_2 = 145$ L mol⁻¹.¹³

Oxygen transfer from CH₃ReO₃. We investigated the possibility of transfer of an oxygen atom from CH₃ReO₃ to PPh₃ under the conditions used in this study. This reaction had been reported elsewhere¹⁶ albeit under different conditions. With [PPh₃] and [MTO] on the order of 10⁻⁴ M, the peroxide-free reaction took approximately four days, Figure 4. In comparison, the catalytic reactions of PPh₃ with the H₂O₂-MTO system under these conditions take five minutes or less to reach completion. Since the oxo-transfer reaction from CH₃ReO₃ to PPh₃ is much slower than the reaction of PPh₃ with H₂O₂-CH₃ReO₃ catalytic system, reaction 9 could be neglected.



The uncatalyzed oxidations. Reactions in the absence of CH₃ReO₃ were examined with [H₂O₂] ≥ 10 × [ER₃], the same conditions used for the catalyzed reactions. The disappearance of the substrate was followed in the near UV region, 260-285 nm. The uncatalyzed oxidations followed first-order kinetics in both phosphine and hydrogen peroxide, eq 10. The second-order rate constants for the uncatalyzed reactions, k_u , are reported in Table 1.

$$\left(\frac{d[\text{ER}_3]}{dt} \right)_u = k_u [\text{H}_2\text{O}_2][\text{ER}_3] \quad (10)$$

Catalysis with CH₃ReO₃: An Overview. Typical repetitive-scan spectra for the catalytic oxidation of tris(*p*-trifluoromethylphenyl)phosphine are shown in Figure 2. The overlaid spectra feature an isosbestic point at 235 nm, indicating that no intermediates attain an appreciable concentration. Addition of small amounts (≤ 10⁻⁵ M) of CH₃ReO₃ dramatically changed the shape of the kinetic traces. The

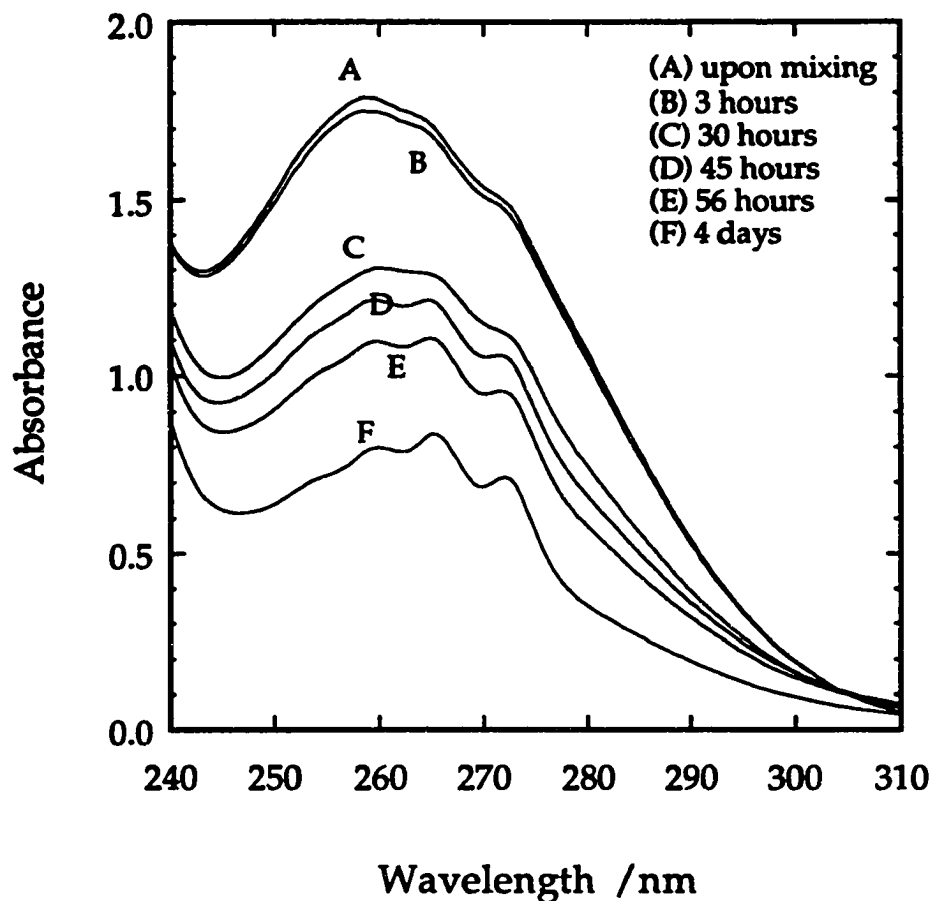


Figure 4. Changes in the UV spectrum of 1.8×10^{-4} M PPh_3 and 1.0×10^{-4} M MTO over a period of four days in 1:1 $\text{CH}_3\text{CN-H}_2\text{O}$ at 0.10 M HClO_4 .

reactions with rhenium were much faster and appeared to follow zeroth-order kinetics during the initial part of the reaction, but an approximate single exponential toward the end. This is illustrated in Figure 5 for a tris(pentafluorophenyl)phosphine. At high substrate concentrations, a zeroth-order limit in substrate was reached (see eq 12 below); this is demonstrated in the inset of

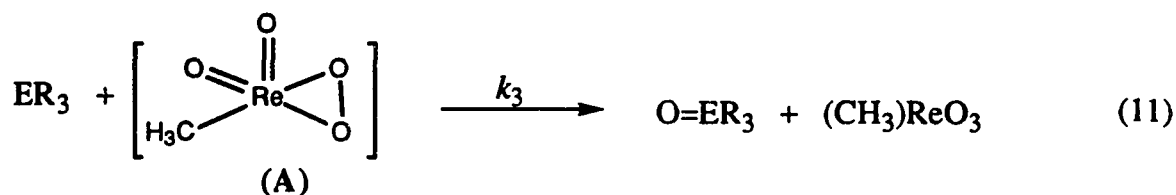
Table 1. Summary of rate constants for reactions of **A** and **B**^a

Substrate	k_u (L mol ⁻¹ s ⁻¹)	k_3 (L mol ⁻¹ s ⁻¹)	k_4 (L mol ⁻¹ s ⁻¹)	activation =
	uncatalyzed	catalyst A	catalyst B	k_3/k_u
P(<i>p</i> -CH ₃ C ₆ H ₄) ₃	4.1 ± 0.4	(9.4 ± 0.6) × 10 ⁵		2.3 × 10 ⁵
P(C ₆ H ₅) ₃	3.0 ± 0.1	(7.4 ± 0.5) × 10 ⁵	(21.6 ± 0.5) × 10 ⁵	2.4 × 10 ⁵
P(<i>p</i> -ClC ₆ H ₄) ₃	1.86 ± 0.06	(4.8 ± 0.2) × 10 ⁵		2.6 × 10 ⁵
P(<i>p</i> -CF ₃ C ₆ H ₄) ₃	0.71 ± 0.04	(3.2 ± 0.2) × 10 ⁵		4.8 × 10 ⁵
P(<i>o</i> -CH ₃ C ₆ H ₄) ₃	0.119 ± 0.002	(1.9 ± 0.1) × 10 ⁵		1.6 × 10 ⁶
p(C ₆ H ₅) ₂ *CH ₃ ^b	7.5 ± 0.6	(40 ± 4) × 10 ⁵		5.2 × 10 ⁵
PTA		(3.2 ± 0.3) × 10 ³		
P(C ₆ F ₅) ₃	0.0016 ± 0.0001	130 ± 4	347 ± 25	8 × 10 ⁴
As(C ₆ H ₅) ₃	0.084 ± 0.001	(3.7 ± 0.3) × 10 ⁵		4.4 × 10 ⁶
Sb(C ₆ H ₅) ₃	1.33 ± 0.04	(5.3 ± 0.4) × 10 ⁵		4 × 10 ⁵

^a In 1:1 CH₃CN-H₂O at 0.10 M HClO₄ and 25 °C. ^b 1.0 × 10⁻⁴M HClO₄.

Figure 5 for PPh₃. The rate of the catalyzed reaction showed first-order dependences on [H₂O₂] and [Re]_T.

When [B] was negligible (*i.e.* eq 7 was unimportant), which was realized at low [H₂O₂],¹³ the reactive form of the catalyst was A (the 1:1 adduct); hence, the simplified catalytic scheme is described by eq 6 and 11.



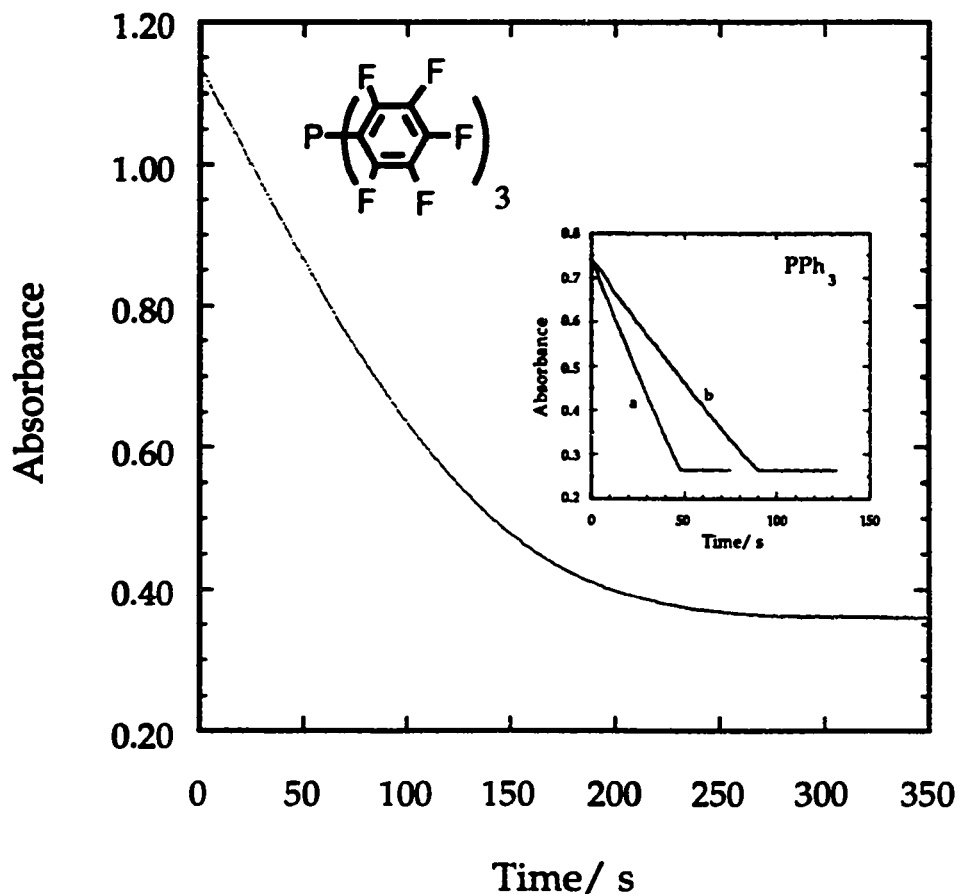


Figure 5. A typical kinetic trace for a catalytic phosphine oxidation monitored spectrophotometrically at 260 nm. Conditions: 25.0 °C, 0.10 M HClO_4 , 5.0×10^{-5} M CH_3ReO_3 , 0.03 M H_2O_2 , and 8.0×10^{-5} M $\text{P}(\text{C}_6\text{F}_5)_3$. Inset: Kinetic data in the form of Absorbance ($\lambda = 270 \text{ nm}$)-time curves for two experiments with $[\text{PPh}_3]_0 = [\text{Re}]_{\text{T}} = 8.0 \times 10^{-5}$ M at $[\text{H}_2\text{O}_2] = 2.5 \times 10^{-4}$ M (a) and 5.0×10^{-4} M (b).

The rate equation derived from these two reactions by means of the steady-state approximation for [A] is given by eq 12, in which $[\text{Re}]_{\text{T}} = [\text{CH}_3\text{ReO}_3] + [\text{A}]$. The rate equation here applies to conditions where [B] was negligible, and therefore, oxidation of the ER_3 by B is unimportant (unless, of course, the trace of B was exceptionally reactive compared to a larger amount of A, a possibility that will be ruled out subsequently).

$$V_c = \left(\frac{d[\text{ER}_3]}{dt} \right)_c = \frac{k_1 k_3 [\text{Re}]_{\text{T}} [\text{H}_2\text{O}_2] [\text{ER}_3]}{k_{-1} + k_3 [\text{ER}_3] + k_1 [\text{H}_2\text{O}_2]} \quad (12)$$

Kinetics at high $[\text{PPh}_3]$. Inspection of eq 12 reveals that at high concentrations of PPh_3 , such that $k_3[\text{PPh}_3] \gg k_{-1}$, the limiting form of the rate law is:

$$V_c = \left(\frac{d[\text{PPh}_3]}{dt} \right)_c = k_1 [\text{Re}]_{\text{T}} [\text{H}_2\text{O}_2] \quad (13)$$

An extensive set of experiments was carried out with limiting $[\text{H}_2\text{O}_2]$ (5.0×10^{-5} M), high $[\text{PPh}_3]$ (0.5×10^{-3} M), over a wide range of $[\text{Re}]_{\text{T}}$ (0.22 – 4.0×10^{-4} M). The kinetic traces under these conditions were fit by a single-exponential, eq 5, indicating that eq 13 was then valid.

In a series of such experiments, changes in the initial concentrations of H_2O_2 and PPh_3 had no effect on the apparent first-order rate constants. As eq 13 suggests, the values of k_y were directly proportional to $[\text{Re}]_{\text{T}}$. A plot of the values of the experimental rate constants corrected for the uncatalyzed contribution versus $[\text{Re}]_{\text{T}}$ is given in Figure 6. The slope of this line gives the value of $k_1 = 32.5 \pm 0.3 \text{ L mol}^{-1} \text{ s}^{-1}$ at 25°C in 1:1 $\text{CH}_3\text{CN-H}_2\text{O}$ at 0.10 M HClO_4 .

Kinetics at variable $[\text{ER}_3]$: Initial-rate method. As can be seen from eq 12, the conditions needed to evaluate k_3 and k_{-1} are low $[\text{H}_2\text{O}_2]$, with $[\text{ER}_3]$ varied in the region where k_{-1} and $k_3[\text{ER}_3]$ are comparable. These conditions were achieved in a series of experiments using the substrates Ph_3P and Ph_3As . The concentrations for

the first series were: 3.0×10^{-4} M H_2O_2 , 4.0×10^{-5} M CH_3ReO_3 , and $(1-15) \times 10^{-5}$ M PPh_3 . The second series was performed with 4.9×10^{-4} M H_2O_2 , 3.5×10^{-6} M CH_3ReO_3 and $(0.50-10) \times 10^{-5}$ M Ph_3As . Representative traces are shown for $[\text{Ph}_3\text{As}]$ variation in Figure 7. The shapes of the absorbance-time recordings, as mentioned previously, are typical of Michaelis-Menten kinetics, being zeroth-order during the initial part of the reaction and approaching first-order towards the end.

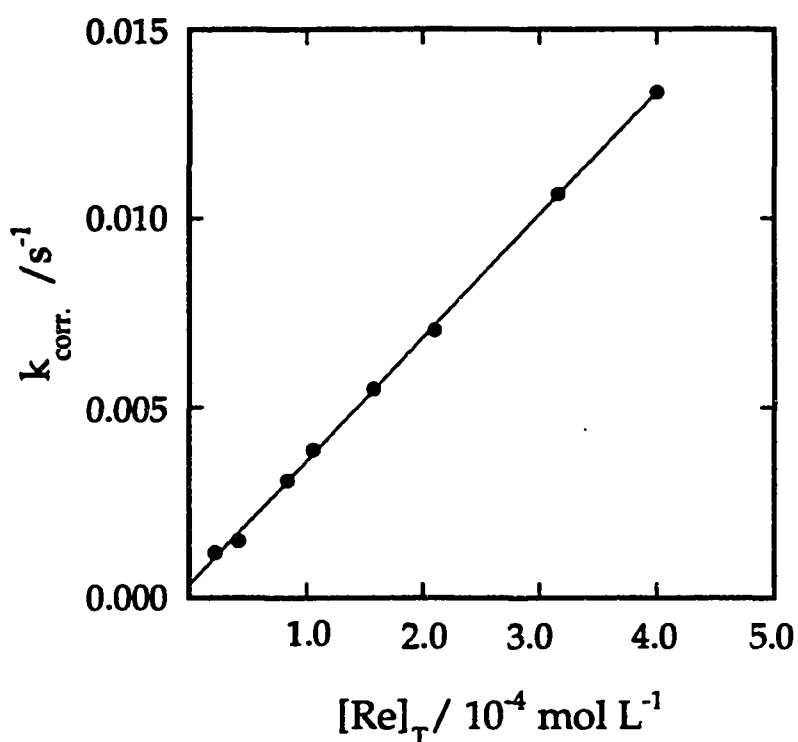


Figure 6. The plot of the pseudo-first-order rate constants, corrected for the contribution of the uncatalyzed reaction, for the oxidation of PPh_3 (0.5×10^{-3} M) by H_2O_2 (5.0×10^{-5} M) at 25.0°C and pH 1.0 in 1:1 $\text{CH}_3\text{CN}-\text{H}_2\text{O}$. The linear variation of $k_{\text{corr.}}$ with the catalyst concentration affords $k_1 = 32.5 \pm 0.3 \text{ L mol}^{-1} \text{ s}^{-1}$.

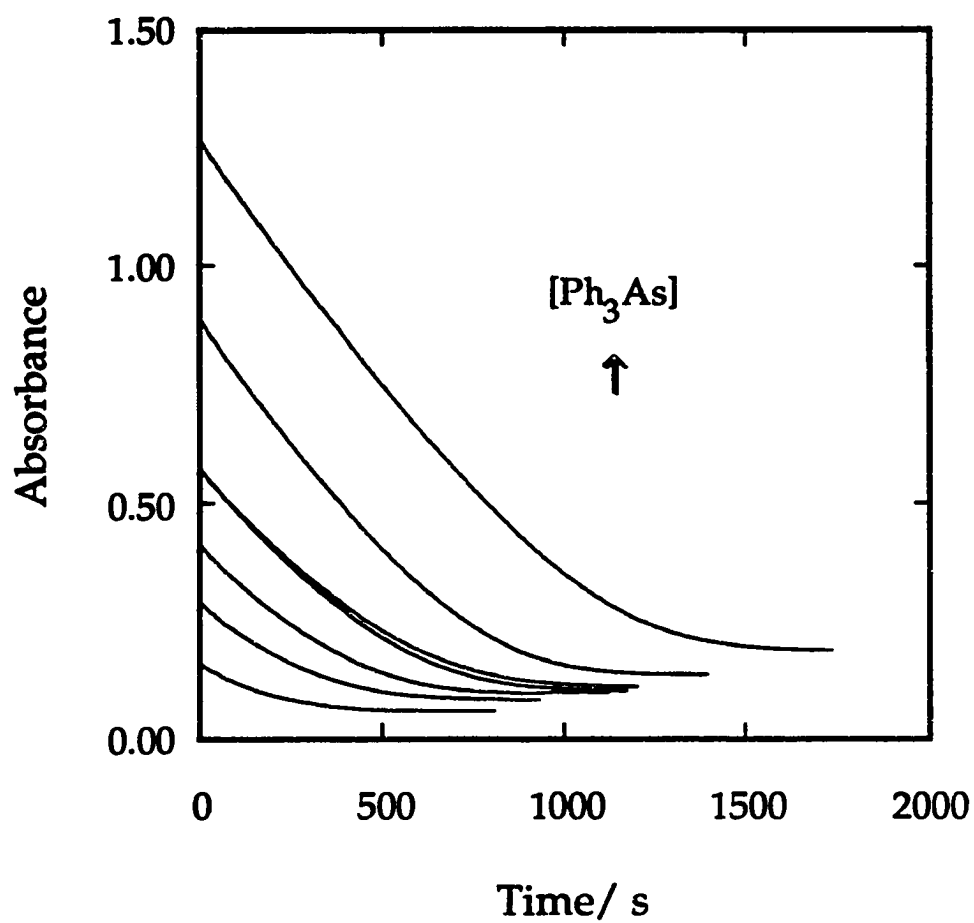


Figure 7. A family of kinetic traces for the oxidation of triphenylarsine, monitored spectrophotometrically at 250 nm. Conditions: 25 °C, pH 1.0, 3.5×10^{-6} M CH_3ReO_3 , 4.9×10^{-4} M H_2O_2 , with $[\text{Ph}_3\text{As}]/10^{-5}$ M = 0.5, 1.0, 1.5, 2.1, 2.5, 3.5, and 5.0.

The initial rate method was applied in each case and gave a value of V_i that was then corrected for the contribution of the uncatalyzed reaction. In every case the correction amounted to no more than 10% of the total rate ($V_{\text{Tot}} = V_u + V_c$). The plots of initial rate, so corrected, vs. $[\text{PPh}_3]$ and $[\text{AsPh}_3]$ are shown in Figure 8. In the limit of high $[\text{PPh}_3]$ or $[\text{Ph}_3\text{As}]$, the initial-rate reached a plateau that gives the already-determined value of k_1 ; in this limit, recall that the rate-law is reduced to the form shown in eq 13. Visual inspection of the plots in Figure 8 confirms this.

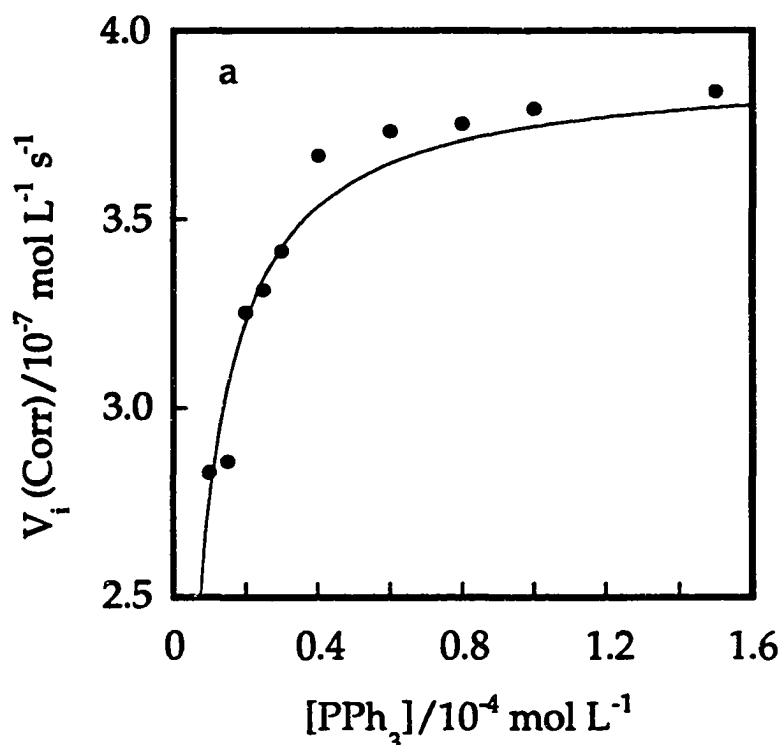


Figure 8. Variations of the initial rate of reaction, corrected for the contribution, of the uncatalyzed reaction, with (a) $[\text{PPh}_3]$ and (b) $[\text{Ph}_3\text{As}]$. The curves show the fit of these data to the rate law (eq 12) applicable when $[\text{B}]$ is negligible. Conditions: 25 °C, pH 1.0, (a) $4.0 \times 10^{-5} \text{ M}$ MTO, $3.0 \times 10^{-4} \text{ M}$ H_2O_2 ; (b) $3.5 \times 10^{-6} \text{ M}$ CH_3ReO_3 , $4.9 \times 10^{-4} \text{ M}$ H_2O_2 .

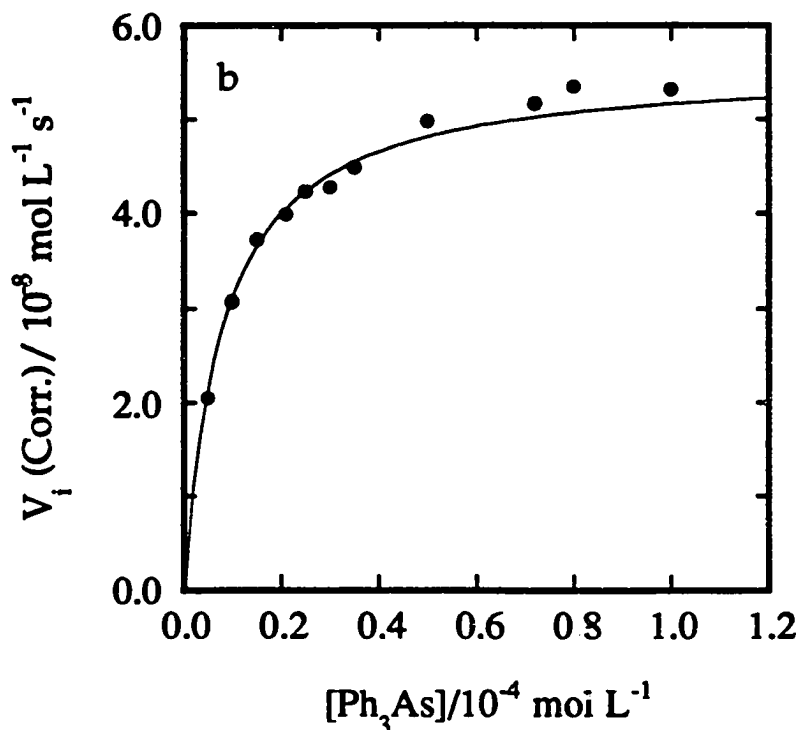


Figure 8b. (Continued)

The value for k_{-1} was obtained from the fit to eq 12. In this calculation, k_1 was fixed at $32.5 \text{ L mol}^{-1} \text{ s}^{-1}$, as given above, and (from the next section) $k_3(\text{PPh}_3) = 7.3 \times 10^5 \text{ L mol}^{-1} \text{ s}^{-1}$ and $k_3(\text{Ph}_3\text{As}) = 3.7 \times 10^5 \text{ L mol}^{-1} \text{ s}^{-1}$. This led¹⁷ to $k_{-1} = 3.0 \pm 0.2 \text{ s}^{-1}$ at 25°C in $\text{CH}_3\text{CN-H}_2\text{O}$ at pH 1.0. The value of k_{-1} from these kinetic investigations is consistent with that calculated independently from the equilibrium study, with $k_{-1} = k_1/K_1 = 2.5 \pm 0.3 \text{ s}^{-1}$.

Catalysis with CH_3ReO_3 : Determination of k_3 for all substrates. Two types of initial-rate studies were performed to determine the values for the k_3 's. Both were carried out at low $[\text{H}_2\text{O}_2]$, so the amount of $[\text{B}]$ present would be negligible. The order of mixing was also significant; in order that $[\text{B}]$ be negligible, hydrogen

peroxide was added last. This prior equilibration is needed, since the rate at which **A** reacts with a phosphine is higher than that at which it is converted to **B**, or at least comparable; without this as a part of the protocol, **B** would not carry much of the reaction, and the kinetic situation would be rather more complex. In one series of experiments, $[\text{Re}]_{\text{T}}$ was varied $0\text{--}20 \times 10^{-5} \text{ M}$ in the presence of $0.5\text{--}1.0 \times 10^{-5} \text{ M ER}_3$ and $\sim 1.0 \times 10^{-4} \text{ M H}_2\text{O}_2$. The relationship between the corrected initial rate, $V_i(\text{corr})$ (corrected for the uncatalyzed contribution, which amounts to no more than 10% of the total rate), and $[\text{Re}]_{\text{T}}$ is linear as expected from eq 12. The data were fit to eq 12, fixing k_1 and k_{-1} at $32.5 \text{ L mol}^{-1} \text{ s}^{-1}$ and 3.0 s^{-1} , respectively. This yielded k_3 values for the different substrates used in this study. Figure 9b illustrates the linear relationship between V_i and $[\text{Re}]_{\text{T}}$ for Ph_3Sb .

In the second series of experiments, $[\text{H}_2\text{O}_2]$ was varied in the range $(0.5\text{--}3.5) \times 10^{-4} \text{ M}$. A plot of the corrected V_i versus $[\text{H}_2\text{O}_2]$ was linear at this low $[\text{H}_2\text{O}_2]$, where the denominator term in eq 12 that contains $[\text{H}_2\text{O}_2]$ is negligible. These data were fit to eq 12 to yield values for k_3 's. The values of k_3 obtained from these two studies were consistent with each other; see, for example, the k_3 value for Ph_3Sb given in Figure 9.

A global fit of the initial rates from both studies to eq 12 yielded a single k_3 value for each substrate. These second-order rate constants for the catalyzed reactions are tabulated alongside those for the uncatalyzed reactions in Table 1. The activation power of methylrhenium trioxide, defined as k_3/k_{-1} , is also presented in Table 1. It shows an acceleration of $10^5\text{--}10^6$ when compared with H_2O_2 alone.

Catalysis with CH_3ReO_3 : The role of **B**. Since **B**, like **A**, contains η^2 -peroxide ligands, it is reasonable to anticipate its ability to oxidize phosphines as illustrated in reaction 14.

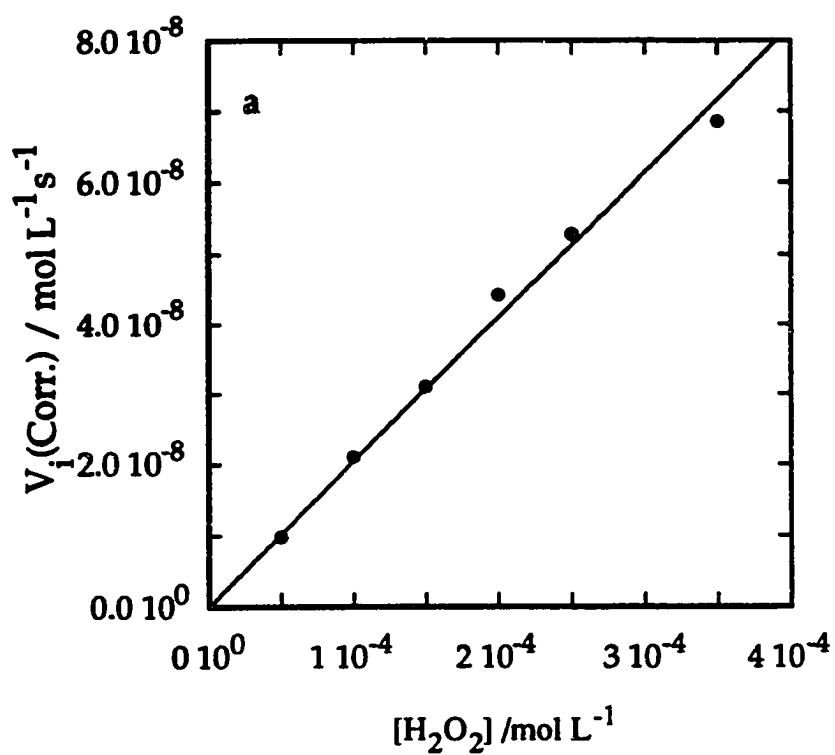


Figure 9. Variation of the initial rate of reaction, corrected for the uncatalyzed reaction, with (a) $[H_2O_2]$, $k_3 = (5.3 \pm 0.4) \times 10^5 \text{ L mol}^{-1} \text{ s}^{-1}$ and (b). $[Re]_T$, $k_3 = (5.2 \pm 0.3) \times 10^5 \text{ L mol}^{-1} \text{ s}^{-1}$ for Ph_3Sb at $25^\circ C$ and pH 1.0. Conditions: (a) $1.5 \times 10^{-5} \text{ M } Ph_3Sb$, $8.0 \times 10^{-6} \text{ M MTO}$; (b). $1.5 \times 10^{-5} \text{ M } Ph_3Sb$, $1.0 \times 10^{-4} \text{ M } H_2O_2$.

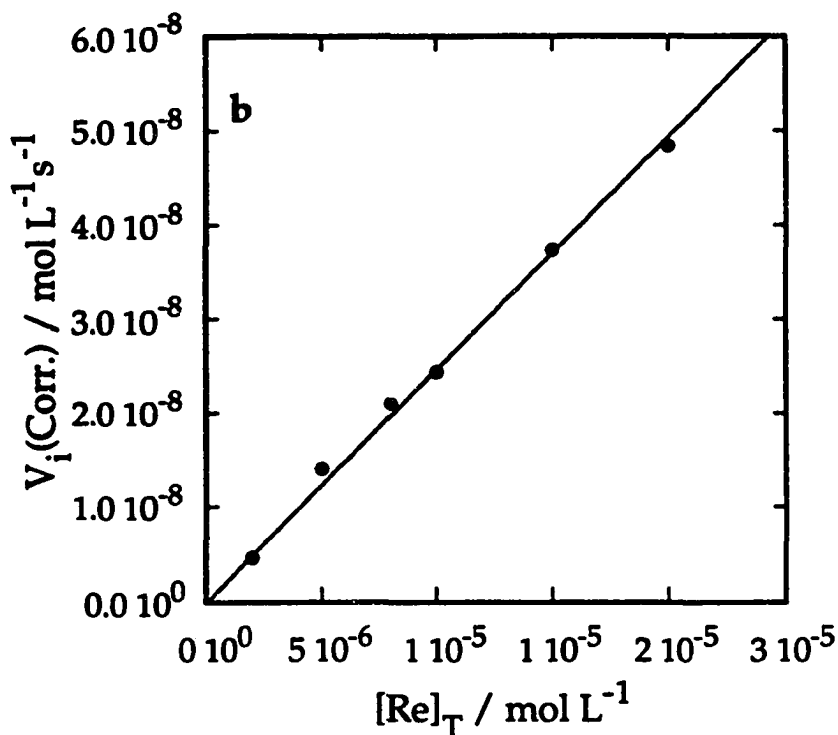
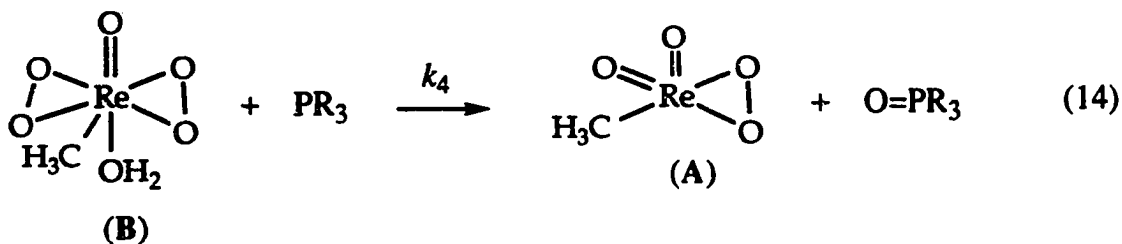


Figure 9b. (Continued)



The catalytic activity and kinetics of **B** were studied for two different phosphines, PPh_3 and $\text{P}(\text{C}_6\text{F}_5)_3$. Pseudo-first-order conditions were satisfied by using $[\text{B}] \geq 10 \times [\text{PR}_3]_0$ and $[\text{H}_2\text{O}_2]_0 \geq 100 \times [\text{Re}]_T$ with CH_3ReO_3 and H_2O_2 equilibrated prior to addition of substrate. These conditions were simulated with the program KINSIM,¹⁸ which uses Runge-Kutta and Gear methods to generate concentration-time profiles for the reaction scheme, given the rate constants and

starting concentrations. The simulations showed that under the conditions stated above, the rate should show be first-order with respect to $[PAr_3]$, as was indeed observed.

The reactions under these conditions occur much more rapidly, and so were studied with the stopped-flow technique. For triphenylphosphine, $[Re]_T$ was varied from $(1.5\text{--}14.5) \times 10^{-5}$ M, with $[H_2O_2] = 0.10$ M, and $[PPh_3] = 4.0 \times 10^{-6}$ M. The solutions of CH_3ReO_3 and H_2O_2 were allowed to equilibrate for a few minutes before PPh_3 was added. Under these conditions k_ψ becomes

$$k_\psi = k_4 [B] + \frac{k_3 [B]}{K_2 [H_2O_2]} \quad (15)$$

The concentrations of **B** were calculated from K_1 and K_2 from the equilibrium study, and k_3 was fixed at 7.3×10^5 L mol⁻¹ s⁻¹, determined independently (see above). The plot of k_ψ vs $[B]$ is linear, with k_4 as the slope, Figure 10. The fit to eq 15 provided $k_4 = (2.16 \pm 0.05) \times 10^6$ L mol⁻¹ s⁻¹ in 1:1 $CH_3CN\text{--}H_2O$ at pH 1.0. It turned out that k_4 is about three times larger than k_3 for PPh_3 . Although **B** is more reactive towards PPh_3 than **A**, the difference in reactivity is not very substantial, with k_4 not even an order of magnitude larger than k_3 .

For tris(pentafluorophenyl)phosphine, k_4 is 347 ± 27 L mol⁻¹ s⁻¹. Again, $P(C_6F_5)_3$ shows the same trend demonstrated by PPh_3 , with $k_4 \sim 3 \times k_3$.

The case of PTA: competition kinetics. We chose to study this compound, 1,3,5-triaza-7-phospha-adamantane, because of the three electronegative nitrogen atoms; we sought to learn whether it is less reactive than PAr_3 , as one might infer from the kinetic effects of varying the substituents on the aryl groups. Since PTA does not absorb in the UV region, the direct spectrophotometric method used with the other substrates could not be applied to its catalytic reaction with $MTO\text{--}H_2O_2$. Therefore, the reaction was investigated indirectly by utilizing competition reactions with a substrate that met two requirements: (1) it reacts with $MTO\text{--}H_2O_2$ at a rate

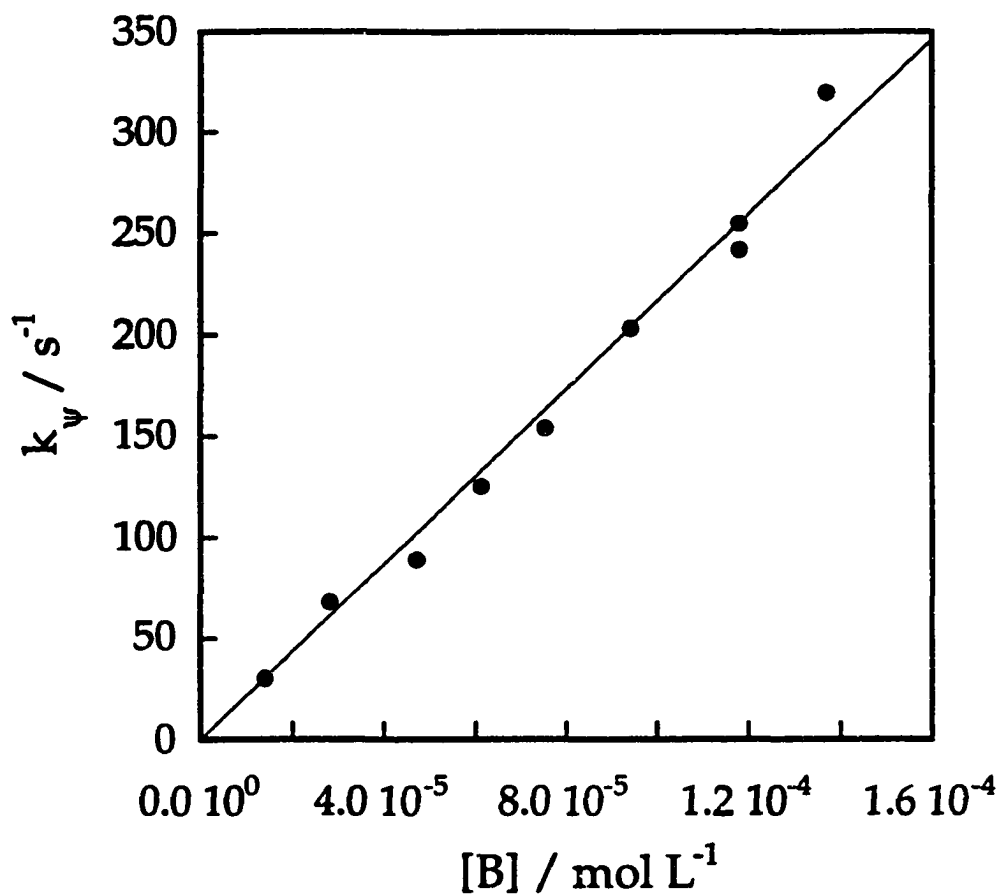
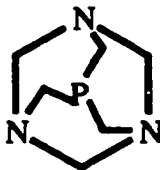


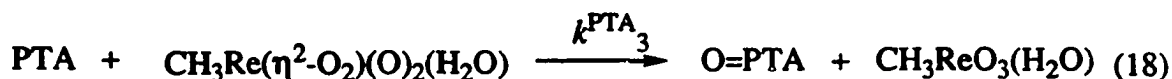
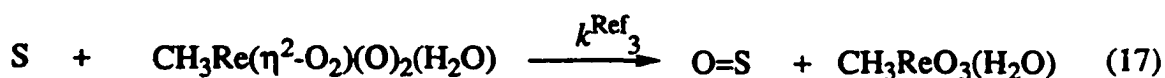
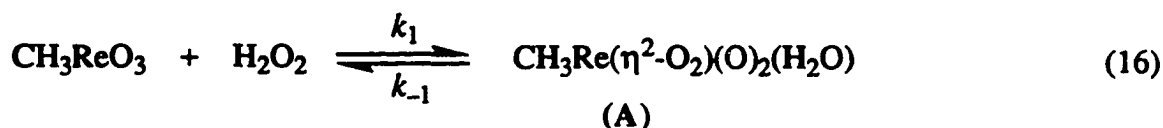
Figure 10. Plot of the pseudo-first-order rate constant for the oxidation of PPh_3 ($4.0 \times 10^{-6} \text{ M}$) by **B** showing linear variation of k_{ψ} with $[\text{B}]$. The curve is a fit to the rate law under these conditions (eq 15). Conditions: $25.0 \text{ }^{\circ}\text{C}$, $\text{pH } 1.0$, $4.0 \times 10^{-6} \text{ M PPh}_3$, $0.10 \text{ M H}_2\text{O}_2$.

comparable to that of PTA, and (2) it could be directly monitored spectrophotometrically. The rate constant for the reference substrate with A must be known independently.



1,3,5-Triaza-7-phosphadamantane (PTA)

The idea in such a competition reaction is to have both substrates, PTA and PAr_3 (where Ar = aromatic), for the catalytic active species A as illustrated by eqs 16-18. The concentrations must be adjusted so that the two rates are not too dissimilar.



The difference in initial-rates for the reaction of S with MTO- H_2O_2 in the presence and absence of PTA gives the solution presented in eq 19, which is used in the competition reactions to evaluate k_3^{PTA} , the only unknown.

$$\frac{v_{\text{Ref}} - v}{v} = \frac{k_3^{\text{PTA}}[\text{PTA}]}{k_{-1} + k_3^{\text{Ref}}[\text{S}] + k_1[\text{H}_2\text{O}_2]} \quad (19)$$

Three different substrates were used independently to determine the rate constant for the reaction of PTA with A. Two of the substrates were aromatic phosphines, $\text{P}(\text{C}_6\text{F}_5)_3$ and $\text{P}(p\text{-CF}_3\text{C}_6\text{H}_4)_3$. In the case of $\text{P}(\text{C}_6\text{F}_5)_3$, 3.0×10^{-4} M MTO,

5×10^{-4} M of $P(C_6F_5)_3$, and 1.0×10^{-4} M H_2O_2 were used; and [PTA] was varied from $0-1.5 \times 10^{-3}$ M. The values of $k_3(P(C_6F_5)_3)$, k_{-1} and k_1 were fixed at $130 \text{ L mol}^{-1} \text{ s}^{-1}$, 3.0 s^{-1} , and $32.5 \text{ L mol}^{-1} \text{ s}^{-1}$, respectively. The plot of $[V_{\text{Ref}}(P(C_6F_5)_3) - V]/V$, where V here and in eq 19 represents the rinital rate of disappearance of the reference substrate, versus [PTA] is shown in Figure 11. The fit to eq 19 provided $k^{\text{PTA}}_3 = (3.24 \pm 0.06) \times 10^3 \text{ L mol}^{-1} \text{ s}^{-1}$.

For the second substrate, $(p\text{-CF}_3\text{C}_6\text{H}_4)_3\text{P}$, the following concentrations were used: $[(p\text{-CF}_3\text{C}_6\text{H}_4)_3\text{P}] = 8.0 \times 10^{-6}$ M, $[H_2O_2] = 0.6 \times 10^{-3}$ M, $[\text{Re}]_{\text{T}} = 2.8 \times 10^{-6}$ M, and $[\text{PTA}] = 0-8.5 \times 10^{-4}$ M. The fit to eq 19 gave $k^{\text{PTA}}_3 = (3.4 \pm 0.2) \times 10^3 \text{ L mol}^{-1} \text{ s}^{-1}$.

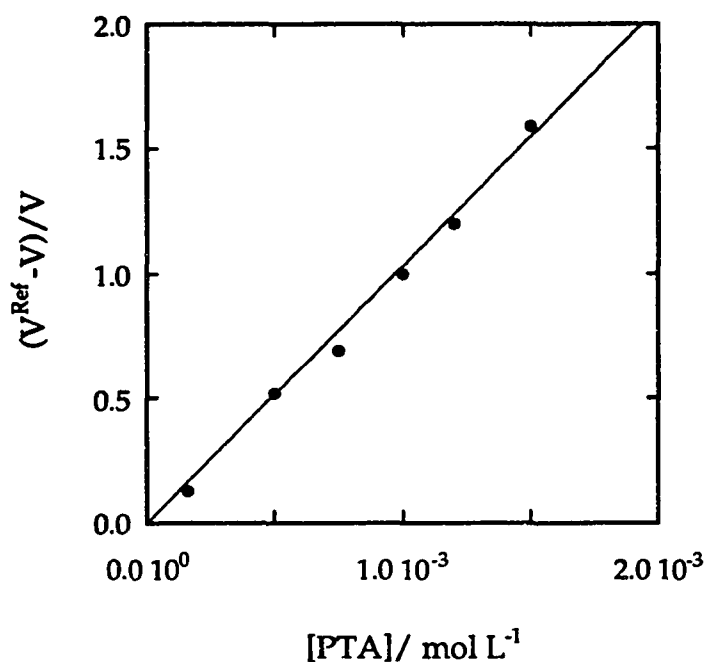


Figure 11. The rate enhancement function, $[V_p(P(C_6F_5)_3) - V_s(\text{PTA})]/V_s(\text{PTA})$, varies linearly with [PTA] according to eq 19 for competition experiments. Conditions: $25 \text{ }^\circ\text{C}$, $\text{pH } 1.0$, 2.5×10^{-4} M $P(C_6F_5)_3$, 3.0×10^{-4} M CH_3ReO_3 , 1.0×10^{-4} M H_2O_2 .

p-Tolyl methyl sulfide, (*p*-CH₃C₆H₄)SCH₃, was also employed in this competition study, since its rate constant is closer to that for PTA. This thioether reacts cleanly with **A** to form the sulfoxide.¹⁹ The rate constant $k^{\text{Ref}_3(p\text{-tolyl)SMe}}$ is $4.3 \times 10^3 \text{ L mol}^{-1} \text{ s}^{-1}$.¹⁸ The concentrations used in this investigation were: [ArSMe] = $1.0 \times 10^{-3} \text{ M}$, [H₂O₂] = 0.010 M, [CH₃ReO₃] = $6.0 \times 10^{-5} \text{ M}$, and [PTA] = $0\text{--}4.3 \times 10^{-3} \text{ M}$. The fit to eq 19 gave $k^{\text{PTA}_3} = (3.5 \pm 0.2) \times 10^3 \text{ L mol}^{-1} \text{ s}^{-1}$. The k^{PTA_3} values from three independent studies agree within acceptable precision. In the competition experiments the concentrations of hydrogen peroxide used were low enough to avoid significant formation of **B**. Also, hydrogen peroxide was added to the reaction mixture last to assure that negligible amounts of **B** were present at the outset.

The integrity of the catalyst. Several tests were run to examine the stability of the catalyst under our reaction conditions. In one experiment that demonstrates the stability of the catalyst after many turnovers, [substrate] = 100 × [CH₃ReO₃] was employed. The concentrations used were as follows: $6.0 \times 10^{-5} \text{ M}$ Ph₃As, $6.0 \times 10^{-7} \text{ M}$ CH₃ReO₃, and $5.0 \times 10^{-3} \text{ M}$ H₂O₂. After the reaction was done, additional $4.0 \times 10^{-5} \text{ M}$ of Ph₃As was added. The rate of catalytic oxidation was similar (93%) to that with the initial batch of Ph₃As, indicating stability and high percent of catalyst recovery. On a preparatory scale, 0.20g (97% yield) of O=P(C₆F₅)₃ were isolated from the reaction of 0.20g ($3.8 \times 10^{-4} \text{ mol}$) P(C₆F₅)₃ with $1.0 \times 10^{-3} \text{ mol}$ H₂O₂, employing 1.0 mg ($4.0 \times 10^{-6} \text{ mol}$, 1% of substrate) of catalyst, CH₃ReO₃. In a ¹H NMR experiment, conducted in CD₃CN as solvent, concentrations of Ph₃As and H₂O₂ that were > 25 times that of CH₃ReO₃ were used. The intensity of the methyl-protons signal (H₃C-ReO₃) at 2.8 ppm indicated that all of the CH₃ReO₃ remained at the end of the reaction, within the limits of detection.

Discussion

It has been shown¹³ that CH_3ReO_3 reversibly forms compounds A and B with H_2O_2 in aqueous solutions. We have also demonstrated that the same holds in 1:1 $\text{CH}_3\text{CN}-\text{H}_2\text{O}$. This points to a mechanism in which eqs 6 and 7 are involved in the catalytic cycle. In other words, the mono-peroxo and di-peroxo species from the interaction of CH_3ReO_3 and H_2O_2 could be anticipated to be the catalytically active ones. Under conditions where [B] is negligible, at low peroxide concentrations, eq 6 is analogous to the formation of the Michaelis–Menten complex. The fact that the CH_3ReO_3 catalytic system follows Michaelis–Menten kinetics is of no surprise, since many catalytic systems tend to do so.

The experimentally-determined rate law in eq 12 has a denominator term containing $[\text{ER}_3]$ as well as one containing $[\text{H}_2\text{O}_2]$. Therefore, this is a two-substrate system in its kinetics as well as in its chemistry. The key step in the catalytic cycle involves the reaction of one of the rhenium-peroxide complexes, A or B, with the substrate ER_3 , as in eqs 11 and 14. This step is the stage at which the peroxide oxygen atom is excised by the substrate.

At low concentrations of peroxide, and in the presence of excess (ER_3) , the reaction is first-order with respect to $[\text{H}_2\text{O}_2]$. This indicates that the active species under these conditions is adduct A, formed from the first equivalent of hydrogen peroxide. Were B the active species under these conditions, meaning that $k_4 \gg k_3$, even with $[\text{B}] \ll [\text{A}]$, second-order kinetics with respect to $[\text{H}_2\text{O}_2]$ should have been observed. This can be seen by inspection of the full rate law. With the steady-state approximations for both peroxides, then the full rate equation is given by

$$-\frac{d[\text{PAr}_3]}{dt} = \frac{k_1 k_3 [\text{Re}]_T [\text{H}_2\text{O}_2] [\text{PAr}_3] + \frac{k_1 k_2 k_4 [\text{Re}]_T [\text{PAr}_3] [\text{H}_2\text{O}_2]^2}{k_4 [\text{PAr}_3] + k_{-2}}}{k_{-1} + k_3 [\text{PAr}_3] + k_1 [\text{H}_2\text{O}_2] + \frac{k_1 k_2 [\text{H}_2\text{O}_2]^2}{k_4 [\text{PAr}_3] + k_{-2}}} \quad (20)$$

In the limit where $[\text{H}_2\text{O}_2]$ is very small, the rate is given by

$$V = \left\{ \frac{K_1 k_2 k_4 [\text{Re}]_T [\text{PAr}_3]}{k_{-2} + k_4 [\text{PAr}_3]} \right\} [\text{H}_2\text{O}_2]^2 \quad (21)$$

From this treatment the value of k_1 is $32.5 \pm 0.3 \text{ L mol}^{-1} \text{ s}^{-1}$, which agrees with that obtained in the same medium using a different substrate, methyl tolyl sulfide.¹⁹ The reverse rate constant for the formation of A, $k_{-1} = 3.0 \pm 0.2 \text{ s}^{-1}$, also agrees with an independent determination.¹⁹

Also from eq 20, one can see that the limit of the rate at high $[\text{H}_2\text{O}_2]$, where B comes into play, will be $V = k_4 [\text{Re}]_T [\text{PAr}_3]$. To attain this, the prior equilibration of peroxide and CH_3ReO_3 as a part of the experimental protocol was necessary to simplify the kinetic treatment to this form. The experimental observation that the reaction followed pseudo-first-order kinetics at high $[\text{H}_2\text{O}_2]$ was also confirmed to be consistent with the entire kinetic model by simulations with the program KINSIM.¹⁸ The second-order rate constants, k_4 , for the reaction of B with PPh_3 and $\text{P}(\text{C}_6\text{F}_5)_3$ differ by a factor of < 3 from those for the reactions of A. This difference being less than an order of magnitude could be easily understood in light of the presence of two peroxo ligands in B rather than only one for A. Since the differences between the respective values of k_3 and k_4 for PPh_3 and $\text{P}(\text{C}_6\text{F}_5)_3$ are not very significant (only a factor of 3), the only conclusion that could be reached here is that both A and B have similar reactivities toward the phosphines.

The structure-reactivity correlations devised by Hammett^{20, 21} account for various reactions of *meta* and *para* substituted aromatic compounds. The values of σ , characteristic of substituent X in either *meta* or *para* position, are available from the pK_a 's of benzoic acids. Tri-aryl phosphines from this study with different substituents on the *para* position were examined. Values for σ_p ²² are listed in Table 2 along with the k_3 values for the different phosphines. Figure 12 shows a plot of $\log(k_{3X}/k_{3H})$ versus σ_p . The slope affords the reaction constant, $\rho = -0.63$. The linear Hammett correlation suggested that all the phosphines react by the same mechanism

in the MTO–H₂O₂ catalytic system. The negative sign of the reaction constant is in agreement with nucleophilic attack of the phosphine on the electrophilic oxygen of the rhenium-bound peroxide. The fact that the reaction constant is near –1.0 suggests an early transition-state with little P—O bond formation. One might also conclude, as suggested by a referee that this value of the reaction constants shows that there is little change in charge density at phosphorus in the transition state.

Table 2. Substituent effects on the rate constants for substituted phosphines^a

Phosphine	k_3 (L mol ⁻¹ s ⁻¹)	σ_p
P(<i>p</i> -CH ₃ C ₆ H ₄) ₃	(9.4 ± 0.6) × 10 ⁵	-0.17
P(C ₆ H ₅) ₃	(7.4 ± 0.5) × 10 ⁵	0.00
P(<i>p</i> -ClC ₆ H ₄) ₃	(4.8 ± 0.2) × 10 ⁵	0.23
P(<i>p</i> -CF ₃ C ₆ H ₄) ₃	(3.2 ± 0.2) × 10 ⁵	0.54

^a In 1:1 CH₃CN–H₂O at 0.10 M HClO₄ and 25 °C.

The kinetic trend for the Group 15 compounds (EPh₃) deserves comment. The rate constants for A follow the order P > Sb > As. It has been known for some time that aryl stibines are oxidized by alkaline hydrogen peroxide more readily (surprisingly) than aryl arsines.²³ Relative nucleophilic reactivity parameters (n_{Pt}) for a variety of nucleophiles were determined from the rates of their reactions toward the electrophile *trans*-[Pt(py)₂Cl₂].²⁴ The second-order rate constants for the reactions of Ph₃As and Ph₃Sb with *trans*-[Pt(py)₂Cl₂] are 2.3 and 1.8 L mol⁻¹ s⁻¹, respectively. These rate constants are close, although in opposite order than those with A.

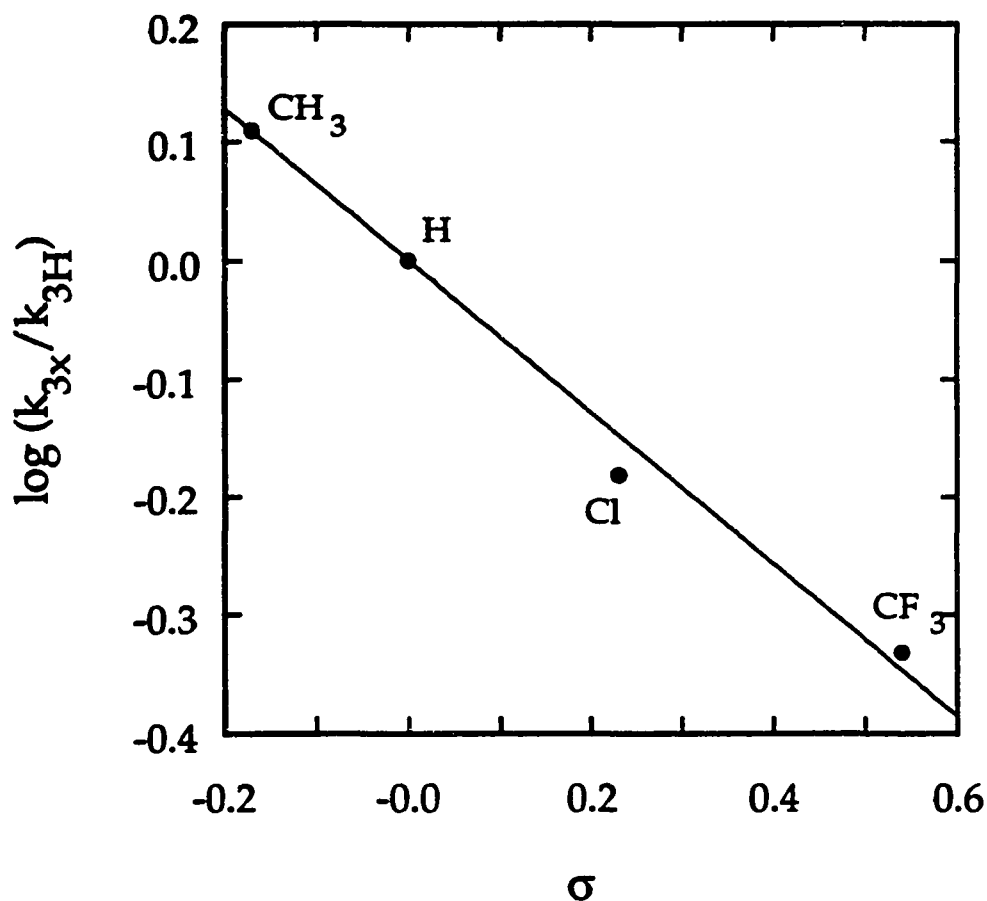
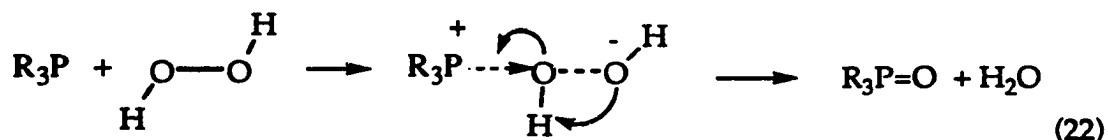


Figure 12. The Hammett correlation between the rate constants for the reactions of substituted phosphines with A. The linear fit yields the reaction constant ρ of -0.63 ± 0.05 .

This still does not account for the small difference in the reactivities of Ph_3P and its arsine and stibine analogs. Such a resemblance in reactivities is not unprecedented. In fact some metal-peroxo catalysts have been used to oxidize arsines as well as phosphines (proving to be somewhat slower for arsines).²⁵ Some materials were found to be ineffective in catalyzing Ph_3P oxidation but very effective

for catalytic oxidation of Ph_3As .²⁶ For example, $\text{Ru}(\eta^2\text{-O}_2)(\text{NO})(\text{PPh}_3)_2(\text{CO})(\text{SCN})$ ²⁷ oxidizes Ph_3As 3–4 times faster than Ph_3P under the same conditions. The relative rates of reaction of PhNEt_2 , PhPEt_2 , and PhAsEt_2 with EtI was found to be 1:500:70.²⁸ The difference here in reactivity between PhPEt_2 and PhAsEt_2 amounts to only a factor of 7. We thus conclude that the rhenium-peroxide catalyst **A** (and possibly **B** also) shows relatively little discrimination with respect to changing from phosphine to arsine or stibine. This might be a consequence of the high electrophilic activation of the η^2 -coordinated peroxide ion (O_2)⁻² upon binding to Re(VII) .

Hydrogen peroxide is generally thought to react with reducing nucleophiles by an $\text{S}_{\text{N}}2$ mechanism.²⁹ Since phosphines are nucleophilic in their chemistry,^{12b} the mechanism of their oxidation by H_2O_2 is assumed to be nucleophilic attack by the phosphine on the O-O peroxide bond,³⁰ as depicted in eq 22:

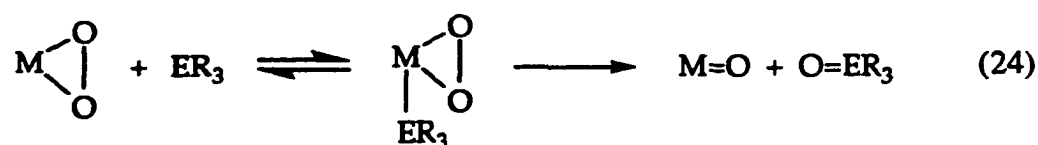
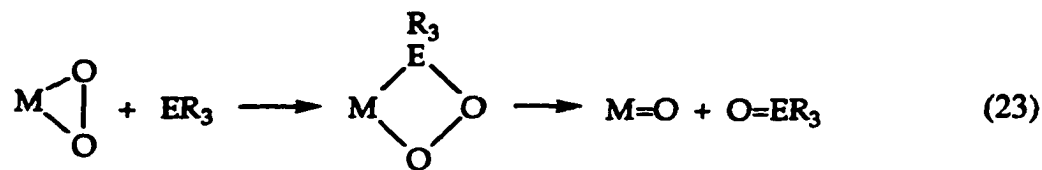


It is reasonable to assume that the same type of nucleophilic attack by ER_3 occurs in the MTO-catalyzed reaction. That is, the phosphorus, arsenic, or antimony atom attacks the oxygen of the coordinated peroxide ion of **A**.

Our proposed mechanism involves the formation of 1:1 and 2:1 peroxides **A** and **B**, that then react with the substrate ER_3 . The electron-poor rhenium makes the peroxide more electrophilic, and, hence, more susceptible to nucleophilic attack, and a better source of an oxygen atom. The activation of hydrogen peroxide upon coordination to Re(VII) is remarkable, $k_{\text{cat}}/k_{\text{uncat}} = (0.2\text{--}4.0) \times 10^6$. Such a large activation indicates major electronic changes in the peroxide upon coordination.

The possibility of coordination of the substrate prior to oxygen transfer should be considered at this stage. Such a mechanism would involve a four

membered ring peroxo-metalacycle as shown in eq 23. Mimoun proposed such a mechanism for reactive substrates, such as phosphines, sulfides, and amines with molybdenum peroxo complexes.⁶ A different, but closely related mechanism, would be direct coordination as the first step, eq 24.

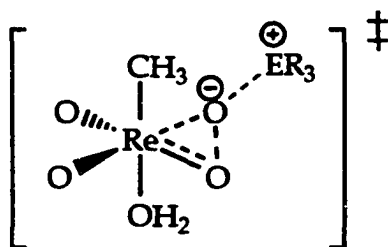


We sought evidence from the kinetic studies to support or reject such a mechanism as the major pathway for oxidation under the conditions of our investigations. But first let us consider some of the chemical and structural properties of the active peroxides **A** and **B**. From a structural point of view, **B**, the diperoxide, is seven-coordinate, with a coordinated water molecule that has been shown by ¹⁷O NMR to be bound in solution.¹⁴ Then **B** is unlikely to coordinate a substrate molecule (ER₃) prior to oxygen transfer. Since **B** contains a tightly bound water molecule in its coordination sphere, it is not at all unreasonable to assume that **A** also contains a tightly bound water molecule, making the rhenium atom in **A** six-coordinate. Nevertheless, an argument (based on the ability of **B** to be seven-coordinate) in favor of substrate coordination prior to oxidation might still be made in the case of **A**. In so doing, however, one would be assigning different mechanisms to the pair of peroxides, which seems implausible.

Addition of excess OPPh₃ (5 × [ER₃]), which would compete with substrate for a coordination site on **A** were such involved, caused no retardation in the rate of oxidation. Another general tool for establishing substrate coordination in the

catalytic oxidation process is the effect of steric hindrance on oxidation rates.³¹ Whereas steric factors are known to be rather unimportant in typical electrophilic oxidations, such as the acid-catalyzed oxidation of sulfides with hydrogen peroxide,³² they should play a major role in processes that involve the coordination of two reactants (catalyst and substrate here). For example, in the metal-catalyzed homogeneous hydrogenations of olefins where coordination of the olefin to the metal complex occurs, the retardation caused by the steric hindrance of the olefin is remarkable;³³ the reactivity ratio of cyclohexene:1-methylcyclohexene with certain Rh complexes is > 40 .³³

Since (*p*-tolyl)₃P and (*o*-tolyl)₃P are electronically the same (Tolman's electronic parameter, ν ,³⁴ for both of them is 2066.7 cm⁻¹) but sterically very different (cone angle, θ ,³⁴ of 145° for the *para*-substituted methyl and 194° for the *ortho*-substituted one), we compared their reaction rates with A. The rate constants for the reactions of (*p*-tolyl)₃P and (*o*-tolyl)₃P with A (Table 1) are 9.4×10^5 and 1.9×10^5 L mol⁻¹ s⁻¹, respectively. This small difference in rate, less than that observed in the uncatalyzed oxidations by H₂O₂, gives further support to the general validity of the 'electrophilic' mechanism. That is, direct attack of the nucleophilic substrate on the electrophilic bound-peroxide oxygen is the major pathway accounting for the oxidations of ER₃. Therefore, we suggest the following structure for the transition state (a similar transition state could be drawn for B and ER₃):



The oxidation of Ph_3P by many peroxy and oxo metal complexes is well known.³⁵⁻³⁸ Some of these results are compared with the work reported here in Table 3. The $\text{MTO-H}_2\text{O}_2$ system is more reactive than most systems we are aware of that utilize O_2 in the formation of the $(\text{O}_2)^{2-}$ ion to bind in an η^2 fashion to the metal, such as $\text{Ru}(\eta^2\text{-O}_2)(\text{NO})(\text{PPh}_3)_2(\text{CO})(\text{SCN})$.²⁷ Also, as evident from Table 3, $\text{CH}_3\text{ReO}_3\text{-H}_2\text{O}_2$ adducts seem to be more effective than other metal complexes that activate H_2O_2 , such as Cr-OOH^{2+} .

Conditions in this study were adjusted in order to obtain optimal kinetic parameters. We specially sought to make $V_{\text{cat}} \gg V_{\text{uncat}}$ so that the correction for the uncatalyzed reaction need not be made. Therefore, it was sometimes desirable to use CH_3ReO_3 concentrations that are not much lower than those of substrate. However, the stability and catalytic ability of CH_3ReO_3 were tested by using substrate and H_2O_2 concentrations that were > 100 times that of CH_3ReO_3 . As best we could tell, most of the CH_3ReO_3 remained at the end, capable of performing many further catalytic cycles.

Conclusion. The following diagram presents the chemical transformations in diagrammatic form.

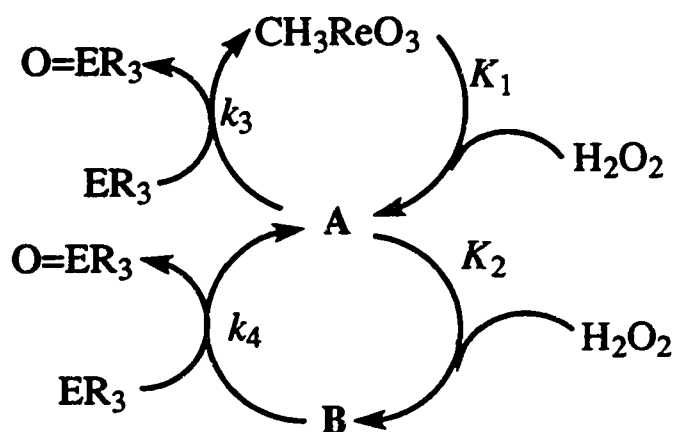


Table 3. Summary of Rate Constants (25.0 °C) for the Oxidation of PPh₃.

Oxidant	Rate Constant/ L mol ⁻¹ s ⁻¹	Reference
H ₂ O ₂	3.0 (2.94)	This work (34)
CH ₃ Re(η ² -O ₂)(O) ₂ (H ₂ O)	7.3 x 10 ⁵	This work
CH ₃ Re(η ² -O ₂) ₂ (O)(H ₂ O)	2.1 x 10 ⁶	This work
[Ru(EDTA)(H ₂ O)] ⁻ /O ₂	(1.4 x 10 ⁻⁴ s ⁻¹)	35
(H ₂ O) ₅ CrO ²⁺	2.1 x 10 ³	36
(H ₂ O) ₅ CrOOH ²⁺	75	34
[MoO ₂ (S ₂ CNEt ₂) ₂] ⁺	1.1	37

Acknowledgment. We thank Professor D. J. Darensbourg for a gift of PTA. This research was supported by the U. S. Department of Energy, Office of Basic Energy Sciences, Chemical Sciences Division, under contract W-7405-Eng-82.

References

- (1) Strukul, G. in *Catalytic Oxidations with Hydrogen Peroxide as Oxidant*; G. Strukul, Ed.; Kluwer Academic Publishers, Dordrecht 1992.
- (2) Herrmann, W. A.; Fischer, R. W.; Marz, D. W. *Angew. Chem. Int. Ed. Engl.* 1991, 30, 1638.
- (3) Huston, P.; Espenson, J. H.; Bakac, A. *Inorg. Chem.* 1993, 32, 4517.
- (4) Espenson, J. H.; Pestovsky, O.; Huston, P.; Staudt, S. J. *Am. Chem. Soc.* 1994, 116, 2869.
- (5) Arzoumanian, H.; Pétrignani, J. F.; Pierrot, M.; Ridonane, F.; Sanchez, J. *Inorg. Chem.* 1988, 27, 3377.
- (6) Mimoun, H. *J. Mol. Catal.* 1980, 7, 1.
- (7) Diagle, D. J.; Peppermann, A. B., Jr.; Vail, S. L. *J. Heterocycl. Chem.* 1974, 17, 407.
- (8) Herrmann, W. A.; Kuhn, F. E.; Fischer, R. W.; Thiel, W. R.; Ramao, C.C. *Inorg. Chem.* 1992, 31, 4431.
- (9) Herrmann, W. A.; Kiprof, P.; Rydpal, K.; Tremmel, J.; Blom, R.; Alberto, R.; Behm, J.; Albach, R. W.; Bock, H.; Solouki, B.; Mink, J.; Lichtenberger, D.; Gruhn, N. E. *J. Am. Chem. Soc.* 1991, 113, 6527.
- (10) Beattie, I. R.; Jones, P. J. *Inorg. Chem.* 1979, 18, 2318.
- (11) Kunkely, H.; Turk, T.; Teixeira, C.; deMeric de Bellefon, C.; Herrmann, W. A.; Volger, A. *Organometallics*, 1991, 10, 2090.
- (12) (a) Jaffé, H. H. *J. Chem. Phys.* 1954, 22, 1430; (b) Hudson, R. F., *Structure and Mechanism in Organophosphorus Chemistry*, Academic Press, New York (1965).
- (13) Yamazaki, S.; Espenson, J. H.; Huston, P. L. *Inorg. Chem.* 1993, 32, 4368.
- (14) Herrmann, W. A.; Fischer, R. W.; Schere, W.; Rauch, M. H. *Angew. Chem. Int. Ed. Engl.* 1993, 32, 1157.

- (15) Pestovsky, O.; van Eldik, R.; Huston, P.; Espenson, J. H. submitted for publication.
- (16) Felixberger, J.K.; Kuchler, J.G.; Herdtweck, E.; Paciello, R.A.; Hermann, W.A. *Angew.Chem.Int.Ed.Engl.* **1988**, *27*, 946.
- (17) The data sets employed to determine values for k_{-1} and k_3 were fit iteratively to determine the best values for these rate constants.
- (18) Barshop, B. A.; Wrenn, C.F.; Frieden, C. *Anal. Biochem.* **1983**, *130*, 134.
- (19) Vassell, K.; Espenson, J. H. unpublished observations.
- (20) Hammett, L. P. , *Physical Organic Chemistry*, McGraw-Hill Book Co. 1970.
- (21) Hammett, L. P. *Chem. Rev.* **1935**, *17*, 131.
- (22) Brown, H. C.; Okamoto, Y. *J. Am. Chem. Soc.* **1958**, *80*, 4979.
- (23) Sidgwick, N. V. *The Chemical Elements and their Compounds: vol. I*, Oxford University Press, London (1962).
- (24) Pearson, R. G.; Sobel, H.; Songstad, J. *J. Am. Chem. Soc.* **1968**, *90*, 319.
- (25) (a) Cenini, S.; Fusi, A.; Capparella, G. L.J. *Inorg. Nucl. Chem.* **1971**, *33*, 3576; (b) Sutin, N.; Yandell, J. K. *J. Am. Chem. Soc.* **1973**, *95*, 4847.
- (26) Chaloner, P.A., *Handbook of Coordination Catalysis in Organic Chemistry*, Butterworth & Co., Boston (1986).
- (27) Graham, B. W.; Laing, K. R.; O'Connor, C. J.; Roper, W. R. *J. Chem. Soc. Dalton Trans.* **1972**, 1237.
- (28) Davies, W. C.; Lewis, W. P. *J. Chem. Soc.* **1934**, 1599.
- (29) Hoffman, M.; Edwards, J. O. *Inorg. Chem.* **1977**, *16*, 3333 and references therein.
- (30) Denney, D. B.; Goodyear, W. F.; Godstein, B. *J. Am. Chem. Soc.* **1960**, *82*, 1393.
- (31) Bortolini, O.; Campello, E.; DiFuria, F.; Modena, G. *J. Mol. Catal.* **1982**, *14*, 63.
- (32) Modena, G. *Gazz. Chim. Ital.* **1959**, *89*, 834.

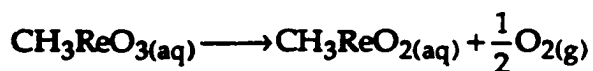
- (33) James, B. R. *Homogeneous Hydrogenation*, Wiley-Interscience, New York (1973).
- (34) Tolman, C.A. *Chem. Rev.* **1977**, *77*, 313.
- (35) Wang, W-D.; Bakac, A.; Espenson, J. H. *Inorg. Chem.* **1993**, *32*, 5034.
- (36) Taqui Khan, M. M.; Chatterjee, D.; Siddiqui, M. R. H.; Bhatt, S. D; Bajaj, H. C.; Venkatasubramanian, K.; Moiz, M. A. *Polyhedron* **1993**, *12*, 1443.
- (37) Scott, S. L.; Bakac, A.; Espenson, J.H. *J. Am. Chem. Soc.* **1992**, *114*, 4205.
- (38) Durant, R.; Garner, C. D.; Hyde, M. R.; Mabbs, F. E. *J. Chem. Soc. Dalton Trans.* **1977**, 955.

GENERAL CONCLUSIONS

Methylrhenium trioxide (MTO) is reduced by hypophosphorous acid to give the strongly reducing methylrhenium dioxide (MDO) and phosphorous acid. In the absence of a complexing ligand, MDO undergoes oligomerization leading to a black polymeric precipitate. The methyl-rhenium bond is retained in this polymeric species as evidenced by the solvation and reformation of the peroxide complexes of MTO upon addition of H_2O_2 to the precipitate. At low $[\text{Re}]$ (≤ 0.5 mM) the polymerization process is greatly retarded; therefore, MDO could be generated *in situ* and its subsequent reactions with $\text{X}=\text{O}$ oxygen donors studied. The oxo donor compounds that react with MDO include inorganic oxoanions (XO_n^- : $\text{X} = \text{Cl}, \text{Br}, \text{I},$ or N and $n = 3$ or 4), sulfoxides, pyridine N-oxides, triphenylarsine oxide, triphenylstibine oxide, and some oxo metal complexes. MDO is a very effective oxygen abstractor when the oxidant has an available oxygen atom. For example the rate constant for the reduction of ClO_4^- by MDO is a record high rate of $7.3 \text{ L mol}^{-1} \text{ s}^{-1}$, but phenols are not able to oxidize MDO.

An attempt to correlate reaction rates with the overall driving force was not successful, presumably because the overall driving force does not represent the species that emerge from the transition state. Also the self-exchange O-transfer rates in general are not known. On the other hand, we were able with some limitations to relate the kinetic rates to the element-oxygen ($\text{X}=\text{O}$) force constants, which are a more accurate measure of what controls O-atom transfer in the transition state.

Since the reaction between V^{2+} , VO^{2+} , MTO and MDO comes to a finite equilibrium (eq 1), the value of its equilibrium constant allows the calculation of $\Delta G^\circ_{\text{ox}}$ of 56 kcal mol^{-1} for the reaction:



The comparison between vanadium and rhenium provides a useful illustration of the lack of correlation of rates with the driving force. Whereas MDO reacts with DMSO and other O-atom donors very rapidly, V^{2+} does not react at all, despite equivalent thermodynamics.

In general the reactivity of MDO could be attributed to the (1) oxophilicity of the high-valent rhenium, (2) the considerable stability of MTO, and (3) the relatively low coordination numbers of MDO.

MTO is also an effective catalyst for oxygen transfer reactions from hydrogen peroxide. The rhenium catalyst activates H_2O_2 electrophilically through binding to form $\text{CH}_3\text{ReO}_2(\eta^2\text{-O}_2)$, A, and $\text{CH}_3\text{ReO}(\eta^2\text{-O}_2)_2(\text{H}_2\text{O})$, B. These rhenium peroxides are formed in equilibrium reactions: $K_1 = 16 \text{ L mol}^{-1}$ and $K_2 = 132 \text{ L mol}^{-1}$ at pH 0 and $\mu = 2.0$ in water. The catalyst's stability depends on $[\text{H}_2\text{O}_2]$, $[\text{H}_3\text{O}^+]$, and the solvent. In organic solvents and at high $[\text{H}_2\text{O}_2]$ ($\geq 0.10 \text{ M}$) the catalyst (mainly in the B form) is stable for many days. On the other hand in aqueous solutions $1.0 \text{ M H}_3\text{O}^+$ is required to stabilize the catalyst. The catalyst decomposes in the presence of H_2O_2 to give methanol and perrhenate as final products. We believe the production of methanol takes place via the reaction of HO_2^- and MTO to give a hydroperoxo rhenium complex analogous to A; then the methyl migrates to a peroxo oxygen eliminating MeOH and leaving behind ReO_4^- . B, on the other hand, evolves oxygen and regenerates the starting MTO.

Both rhenium peroxides are active in catalysis. As a matter of fact both compounds exhibit similar rates with most oxidizable substrates. This is not to

say, however, that both rhenium peroxides give rise to comparable yields of products. The respective contribution of each to product formed is controlled by how much **A** and **B** are present under any particular $[H_2O_2]$ as well as the rates of formation of **A** and **B** relative to rates of substrate oxidation by the respective rhenium peroxides. The kinetic data for the oxidations of a large family of phosphines by **A** and **B** show rate enhancement when the nucleophilicity of the phosphorous is increased. Hence the mechanism of peroxy oxygen transfer from rhenium (**A** or **B**) proceeds via nucleophilic attack of the substrate at the electrophilically activated peroxide ligand.

The oxidations of β -diketones to give cleavage products, organic acids, is catalyzed by MTO. These oxidations involve many steps prior to the formation of final products. The initial oxidation step is the epoxidation of the enolic form (major species in solution) of the diketone. This oxidation features the customary behavior of **A** and **B**, namely, nucleophilic attack of the enol at the electrophilic bound peroxides of **A** and **B**. The subsequent steps being controlled by a Baeyer-Villiger-type oxidation involving oxygen insertion into C-C bond exhibit opposite reactivity trends- more nucleophilic substrates are less reactive towards O-insertion. This clearly points towards a mechanism in which the peroxides of **A** and **B** are behaving as nucleophiles. The ability of **A** and **B** to change reactivity depending on substrate demand speaks to the versatility of this MTO catalyst.

ACKNOWLEDGMENTS

I would like to thank Professor James Espenson for excellent mentorship throughout my graduate career. I am also thankful to the members of my research group for their friendship and many stimulating scientific discussions. I would like to acknowledge financial support from the U.S. Department of Education in the form of a GAANN graduate Fellowship.

I want to particularly acknowledge moral support from my wife, Kristen, who was convinced I could do it. I would also like to thank my children, Jasmine and Moeen, for their grace and unlimited smiles; my graduate school experience wouldn't have been the same without them.

This work was performed at Ames Laboratory under Contract No. W-7405-Eng-82 with the U.S. Department of Energy. The United States government has assigned the DOE report number IS-T1778 to this report.